

CHARLES UNIVERSITY IN PRAGUE, FACULTY OF SCIENCE

Department of Physical Geography and Geoecology



**LONG-TERM VARIABILITY OF HEAT WAVES  
AND COLD SPELLS IN CENTRAL EUROPE**

**DLOUHODOBÁ PROMĚNLIVOST HORKÝCH A  
STUDENÝCH VLN VE STŘEDNÍ EVROPĚ**

Doctoral dissertation

Mgr. Ondřej Lhotka

Supervisor: RNDr. Jan Kyselý, Ph.D.

Prague 2016

I hereby declare that I carried out this doctoral thesis independently and all utilized references are properly cited. This thesis neither its part has been submitted for obtaining other academic degree.

Prohlašuji, že jsem předloženou disertační práci zpracoval samostatně a že jsem řádně odcitoval všechny použité zdroje. Tato práce ani její část nebyla předložena k získání dalšího akademického titulu.

.....  
In Prague, 24.5.2016

**Title:** Long-term variability of heat waves and cold spells in Central Europe

**Author:** Mgr. Ondřej Lhotka

**Department:** Department of Physical Geography and Geocology, Faculty of Science, Charles University in Prague

**Supervisor:** RNDr. Jan Kyselý, Ph.D., Institute of Atmospheric Physics, Czech Academy of Sciences

**Abstract:** Heat waves and cold spells have serious impacts on natural environment and society. The main aims of this thesis are to examine past variability of Central European heat waves and cold spells, to assess severity of recent events in a long-term context, to evaluate simulation of heat waves in climate models, and to construct their scenarios for a possible future climate. Heat waves and cold spells were primarily investigated as spatial events, using gridded data sets. E-OBS gridded data was utilized to assess past variability of heat waves and cold spells and to evaluate regional climate model (RCM) simulations from the ENSEMBLES and EURO-CORDEX projects. An extremity index that captures joint effects of temperature, duration, and spatial extent of individual heat waves and cold spells was proposed and tested. The persistent 1994 heat wave was found to be the most extreme over Central Europe in the 1950–2012 period, and the summer of 2013 was unprecedented at several Central European stations according to seasonal heat wave characteristics. The severity of cold spells was largest in the winters of 1955/1956 and 1962/1963, and the winter of 2011/2012 was ranked as the 6<sup>th</sup> most severe since the mid-20<sup>th</sup> century according to seasonal sums of the extremity index. Reproduction of heat waves in Central Europe was examined in an ensemble of RCMs driven by the ERA-40 reanalysis. The multi-model mean reflected the characteristics of heat waves quite well, but considerable differences were found among the individual RCMs and deficiencies were identified also in reproducing interannual and interdecadal variability of heat waves. Magnitude of the 1994 heat wave was underestimated in all RCMs and this bias was linked to overestimation of precipitation during and before the heat wave. Projections of heat waves for a possible future climate were studied using RCM simulations driven by global climate models forced by three different concentration scenarios. In the near future (2020–2049), heat waves are projected to be twice as frequent compared to the historical period and a similar increase was found under all concentration pathways. By contrast, the projected frequency of heat waves in the late 21<sup>st</sup> century (2070–2099) depends largely upon concentration scenarios. Three to four heat waves per summer are projected in this period (compared to less than one in the recent climate) and severe heat waves are likely to become a regular phenomenon. These projections may be potentially useful for stakeholders and policymakers, however, an interpretation has to be carried out with caution due to substantial uncertainties originating mainly from concentration scenarios and different responses of climate models to altered radiative forcing. The thesis contributed also to better understanding of RCMs' strengths and weaknesses with respect to simulation of heat waves that might eventually lead to improvements of climate models.

**Keywords:** heat waves; cold spells; climate change; climate models; Central Europe

**Název:** Dlouhodobá proměnlivost horkých a studených vln ve střední Evropě

**Autor:** Mgr. Ondřej Lhotka

**Katedra:** Katedra fyzické geografie a geoekologie, Přírodovědecká fakulta Univerzity Karlovy v Praze

**Školitel:** RNDr. Jan Kyselý, Ph.D., Ústav fyziky atmosféry Akademie věd České republiky

**Abstrakt:** Horké a studené vlny mají závažné dopady na přírodní prostředí i lidskou společnost. Hlavními cíli této práce je zhodnotit proměnlivost horkých a studených vln v minulosti, analyzovat extremitu nedávných událostí v dlouhodobém kontextu, vyhodnotit simulace horkých vln v klimatických modelech a vytvořit scénáře jejich změn v možném budoucím klimatu. Horké a studené vlny byly posuzovány převážně jako prostorové události za pomoci dat v pravidelné síti uzlových bodů (gridu). Analýza proměnlivosti horkých a studených vln v minulosti a validace regionálních klimatických modelů (RCM) z projektů ENSEMBLES a EURO-CORDEX byly provedeny na základě gridové databáze E-OBS. Byl navržen a otestován index extremity, který zohledňuje teplotu, délku a plošný rozsah jednotlivých horkých a studených vln. Dlouhotrvající horká vlna z roku 1994 byla ve střední Evropě v období 1950–2012 nejvýraznější a léto 2013 bylo nejextrémnější na několika středoevropských stanicích, pokud jde o celkové charakteristiky horkých vln. Nejsilnější studené vlny se vyskytly v letech 1955/1956 a 1962/1963 a zima 2011/2012 byla šestá nejchladnější na základě sumy indexu extremity. Zachycení vlastností horkých vln bylo studováno pomocí ensemblu RCM řízených reanalýzou ERA-40. Modelový průměr odrážel charakteristiky horkých vln poměrně dobře, nicméně byly zjištěny velké rozdíly mezi jednotlivými modely a nesprávné bylo rovněž zachycení meziroční i dlouhodobé proměnlivosti horkých vln. Všechny RCM podcenily intenzitu horké vlny z roku 1994, přičemž tato chyba byla způsobena příliš vydatnými srážkami během horké vlny a před ní. Projekce horkých vln pro možné budoucí klima byly vytvořeny na základě simulací RCM řízených globálními klimatickými modely za použití tří scénářů socio-ekonomického vývoje. V blízké budoucnosti (2020–2049) modely simulují dvojnásobnou četnost horkých vln v porovnání s historickým obdobím, přičemž tento nárůst je podobný pro všechny scénáře koncentrací skleníkových plynů. Na druhou stranu, na konci 21. století (2070–2099) je četnost horkých vln silně závislá právě na výše zmíněných scénářích. V tomto období modely simulují 3–4 horké vlny za sezónu v porovnání s méně než jednou v historickém období a intenzivní horké vlny se objevují pravidelně. Tyto projekce by mohly být potenciálně užitečné pro politické činitele i další zúčastněné strany, nicméně je nutná opatrná interpretace z důvodu velkých nejistot plynoucích ze scénářů koncentrací skleníkových plynů a různého chování klimatických modelů při změně radiačního působení. Tato práce rovněž přispěla k lepšímu pochopení silných a slabých stránek RCM s ohledem na simulaci horkých vln, což může být použito i ke zlepšování klimatických modelů.

**Klíčová slova:** horké vlny; studené vlny; změna klimatu; klimatické modely; střední Evropa



## TABLE OF CONTENTS

1	Introduction and motivation .....	8
2	Literature review .....	9
2.1	Definition of heat waves and cold spells .....	9
2.2	Temporal and spatial variability of heat waves and cold spells in Europe.....	10
2.3	Driving mechanisms of heat waves and cold spells .....	12
2.3.1	Heat waves.....	12
2.3.2	Cold spells .....	13
2.4	Simulation of heat waves and cold spells in climate models.....	14
2.5	Projections of future heat waves and cold spells .....	16
3	Work objectives.....	18
4	Study area, data and methods.....	19
5	Overview of research articles used in the thesis .....	22
6	Article I: ‘Characterizing joint effects of spatial extent, temperature magnitude and duration of heat waves and cold spells over Central Europe’ .....	26
6.1	Introduction.....	26
6.2	Data and methods.....	28
6.2.1	Data and area of interest .....	28
6.2.2	Definition of heat waves.....	30
6.2.3	Definition of cold spells .....	31
6.2.4	Characteristics of heat waves and cold spells.....	32
6.2.5	Cluster analysis of heat waves and cold spells .....	33
6.2.6	Statistical testing of heat wave and cold spells characteristics.....	33
6.3	Heat waves .....	33
6.3.1	Characteristics and interannual variability .....	33
6.3.2	Cluster analysis.....	37
6.4	Cold spells.....	38
6.4.1	Characteristics and interannual variability .....	38
6.4.2	Cluster analysis.....	42
6.5	Discussion .....	43
6.5.1	Comparison of characteristics of heat waves and cold spells.....	43
6.5.2	Interannual variability of heat waves.....	44

6.5.3	Interannual variability of cold spells .....	45
6.6	Conclusions.....	45
7	Article II: ‘Hot Central-European summer of 2013 in a long-term context’ .....	51
7.1	Introduction.....	51
7.2	Data and methods.....	52
7.3	European mean and extreme summer temperatures .....	55
7.4	Long-term variability of Central European heat waves.....	58
7.5	Description of the 2013 heat waves and driving mechanisms.....	59
7.6	Discussion and conclusions .....	62
8	Article III: ‘Spatial and temporal characteristics of heat waves over Central Europe in an ensemble of regional climate model simulations’ .....	67
8.1	Introduction.....	67
8.2	Data and methods.....	70
8.2.1	Regional climate model simulations.....	70
8.2.2	Area of interest .....	71
8.2.3	Datasets utilized.....	72
8.2.4	Definition of heat wave .....	72
8.2.5	Heat wave characteristics .....	73
8.2.6	Temporal autocorrelation .....	74
8.3	Evaluation of heat wave characteristics and temporal variability in RCMs.....	74
8.4	Reproduction of the 1994 heat wave in RCMs.....	79
8.5	‘Erroneous’ 1967 heat wave in RCM simulations.....	83
8.6	Discussion.....	86
8.6.1	Evaluation of spatial and temporal characteristics of simulated heat waves.....	86
8.6.2	Reproduction of the 1994 heat wave .....	87
8.6.3	‘Erroneous’ 1967 heat wave in RCM simulations.....	88
8.6.4	Evaporative fraction during the 1967 and 1994 heat waves.....	89
8.6.5	Performance of individual RCMs.....	90
8.7	Conclusions.....	91
9	Article IV: ‘Climate change scenarios of heat waves in Central Europe and their uncertainties’ .....	97
9.1	Introduction.....	97
9.2	Data and methods.....	100

9.2.1	Area of interest and observed data .....	100
9.2.2	Climate model simulations .....	101
9.2.3	Definition of heat wave .....	103
9.2.4	Heat wave characteristics .....	104
9.2.5	Temporal autocorrelation and statistical testing.....	105
9.3	Observed heat waves and evaluation of historical RCM simulations .....	105
9.4	Heat wave scenarios and uncertainties for near future and late 21 <sup>st</sup> century .....	109
9.5	Discussion.....	113
9.5.1	Observed heat waves and selection of severe events .....	113
9.5.2	Historical simulations of heat waves .....	114
9.5.3	Scenarios of heat waves in the near future (2020–2049).....	115
9.5.4	Scenarios of heat waves in the late 21 <sup>st</sup> century (2070–2099) .....	115
9.6	Summary and conclusions .....	116
10	Article V: ‘Long-term variability of heat waves in Argentina and recurrence probability of the severe 2008 heat wave in Buenos Aires’ .....	122
10.1	Introduction .....	122
10.2	Data and methodology .....	124
10.2.1	Data.....	124
10.2.2	Heat wave definition.....	127
10.2.3	Stochastic time series model for daily temperatures .....	128
10.3	Long-term variability of heat waves in Argentina north of 40° S.....	129
10.4	Recurrence probability of the extreme heat wave of November 2008 in BA.....	133
10.5	Discussion and concluding remarks.....	135
11	Conclusions and future perspectives .....	139
12	Acknowledgments.....	141
13	References (excluding chapters 6–10) .....	142
14	Appendices.....	149

## **1 Introduction and motivation**

Heat waves and cold spells are important phenomena of the European climate. These events are traditionally regarded as summer (winter) periods that last several days with weather conditions excessively hotter (colder) than normal. Severe heat waves that occurred in the past two decades and the very cold 2009/2010 winter in Europe prompted broad investigation of these events.

Heat waves have major consequences for the natural environment and society. Beniston et al. (2007) pointed to excess illness and mortality, livestock and wildlife stress, crop damage, spread of pests and increased energy demand for cooling. More specifically, the hot summer of 2003 in France resulted in tens of thousands excess deaths (Robine et al. 2008), reduced crop yields, decreased plant productivity (Bastos et al. 2014) and record-breaking loss of Alpine glaciers mass (De Bono et al. 2004). Analogous impacts were observed during the 2010 Russian heat wave (Barriopedro et al. 2011) and numerous wildfires triggered by this event caused prolonged episodes of extreme air pollution in several Russian cities (Konovalov et al. 2011). Among other impacts, cold spells affect human health, infrastructure, and vegetation (Vavrus et al. 2006; Barnett et al. 2012).

Due to an expected rise in global mean air temperature (IPCC 2013), there are concerns that losses caused by heat waves will be increasing. Although cold spells are expected to become less pronounced in the warming climate, Francis and Vavrus (2012) pointed out that possible future strengthening of atmospheric blocking over the Euro-Atlantic region due to Arctic Amplification may result in an intensification of cold spells. In addition, cold spells may be intensified due to modified wintertime atmospheric circulation (Barriopedro et al. 2008) triggered by a possible decrease of solar activity in coming decades (Abreu et al. 2008). Inasmuch as these extreme events are expected to be more severe and dangerous in a future climate, it is vitally important to understand all their aspects in order to establish suitable adaptation and mitigation strategies.

## 2 Literature review

This chapter reviews current scientific literature related to European heat waves and cold spells. It contains five sections that summarize: i) common approaches to defining heat waves and cold spells, ii) temporal and spatial variability of these events in Europe, iii) driving mechanisms of heat waves and cold spells, iv) capability of climate models to simulate these events, and v) projections of heat waves and cold spells in a future climate.

### 2.1 Definition of heat waves and cold spells

The creation of universal and collective measures of any meteorological extreme, including heat waves and cold spells, is difficult (Perkins and Alexander 2013). Both heat waves and cold spells can be analysed by means of several meteorological variables. Although heat waves are predominantly defined based on daily maximum temperature ( $T_{\max}$ ), daily minimum temperature ( $T_{\min}$ ) is also used because high night-time temperatures are important with respect to heat waves' impacts on human health (e.g. Fischer and Schär 2010). Another suitable variable is apparent temperature, which combines temperature and relative humidity and is also known as a heat index. This discomfort index is mostly used when assessing health risk and mortality during heat waves (e.g. D'Ippoliti et al. 2010), but its usage is limited due to less available relative humidity data. In contrast to heat waves, cold spells have predominantly been defined using temperature-based variables only (mainly  $T_{\min}$ ).

The severity of individual heat waves and cold spells has traditionally been viewed in terms of combined temperature and length. Various criteria have been applied on temperature series to estimate if weather conditions are exceptionally hot or cold. One method is based on the excess of absolute temperature thresholds. This approach was used by Colombo et al. (1999), Gershunov et al. (2009), or Kysely (2010), and it is suitable when delimiting heat waves or cold spells from a single station or from a region with reasonably homogeneous climate. Another method applied by Shevchenko et al. (2013) utilizes temperature deviations from the climatology at individual stations. This approach respects a local climate and is more suitable for regional analyses. Many authors use quantile-based methods to define a heat wave or cold spell. The value of the quantile from a temperature distribution depends upon the focus of the study. For example, an analysis of major events demands higher quantiles (e.g. Meehl and Tebaldi 2004), while statistical and trend analyses (e.g. Della Marta et al. 2007a) need larger data samples and thus lower quantiles. Although a wide range of quantiles have been used, the majority of studies utilize the 5%/95% (e.g. Della Marta et al. 2007b; Kysely

2008; Stefanon et al. 2012) or 10%/90% (e.g. Fischer and Schär 2010; Peings et al. 2013) quantile. The minimum length criterion of a heat wave or cold spell usually varies from 2 days (Barnett et al. 2012) to 5 or more days (Ballester et al. 2010; Fischer and Schär 2010).

Due to a relatively recent development and improvement of gridded data, spatial extent of heat waves and cold spells was not taken into account in the majority of past studies. The spatial extent can be described as a simple fraction of a defined area (Peings et al. 2013) or by performing a search in a domain and then distinguishing within which area the extremity of an event is largest (Müller and Kašpar 2014). Alongside analysing spatial extent, Stefanon et al. (2012) used gridded data to classify European heat waves based on a region of occurrence.

## **2.2 Temporal and spatial variability of heat waves and cold spells in Europe**

Since the beginning of the 20<sup>th</sup> century, two major episodes of heightened heat wave severity were observed in Europe. The first one occurred in the 1940s and 1950s and was especially pronounced over Western Europe (Della-Marta et al. 2007a; Kysely 2008) and the second, ongoing period began in the 1990s. The most notable European events since the 1990s are listed below:

- 1992: Central European heat wave mainly in July (Kysely 2002), absolutely highest temperature measured in Estonia (35.6°C)
- 1994: persistent Central European and Baltic heat wave in the transition of July and August (Tomczyk and Bednorz 2015), record-breaking temperature observed in Lithuania (37.5°C)
- 2003: extraordinary heat wave in Western Europe often referred to as a ‘mega heat wave’ (Barriopedro et al. 2011); temperatures were above their mean climatology during almost the entire summer (Black et al. 2004), and absolutely highest temperatures were measured in France (44.1°C), Portugal (47.4°C), Switzerland (41.5°C), and the United Kingdom (38.5°C)
- 2006: Western and Central European heat wave (Kysely 2010)
- 2007: heat wave mainly over the Balkan Peninsula (Unkašević and Tošić 2011), record-breaking temperatures observed in Hungary (41.9°C), Macedonia (45.7°C), Montenegro (44.8°C), Serbia (44.9°C), and Slovakia (40.3°C)

- 2010: Russian and Eastern European ‘mega heat wave’ (Barriopedro et al. 2011) that lasted almost the whole summer, absolutely highest temperature measured in Belarus (38.9°C), Russia (45.4°C), and Ukraine (42.0°C)
- 2012: record-breaking temperature (40.4°C) was observed in the Czech Republic during a relatively short heat wave (Holtanová et al. 2015), absolutely highest temperature measured also in Moldova (42.4°C) during this summer
- 2013: Central European heat wave, record-breaking temperatures observed in Austria (40.5°C) and Slovenia (40.8°C)
- 2014: heat wave in Scandinavia and Baltic countries, absolutely highest temperature measured in Latvia (37.8°C)
- 2015: persistent Central European heat wave (Russo et al. 2015), record-breaking temperature observed in Germany (40.3°C)

The past 25 years are exceptional also in the long-term context. Kyselý (2010) analysed a temperature series from Prague-Klementinum (1775–2006) and the turn of the 20<sup>th</sup> century was found to be the most extreme according to the severity of heat waves. In addition to the two aforementioned episodes in the mid-20<sup>th</sup> century and since the 1990s, other historical periods with unusually severe heat waves in Prague-Klementinum were observed at the turn of the 18<sup>th</sup> century and in the mid-19<sup>th</sup> century. Similar results were obtained from the Swiss station Basel (Fink et al. 2004). However, the severity of heat waves during 18<sup>th</sup> and 19<sup>th</sup> centuries may be overestimated due to a so-called early instrumental warm bias and inhomogeneities, which are often reported at European stations (Winkler 2009; Böhm et al. 2010). In addition, measurements may be affected also by an urban heat island, but its effect on summer  $T_{\max}$  is relatively small (Wilby 2003). Brázdil and Budíková (1999), for example, found no significant influence of the urban heat island on summer temperatures in Prague.

Using proxy data, Luterbacher et al. (2004) reconstructed mean European summer temperature for the past 500 years and concluded that the summer of 2003 was the warmest one within the entire period. Based on the same reconstructed dataset, Barriopedro et al. (2011) showed that the summer of 2010 was even warmer than the 2003 summer. These two summers markedly surpass others regarding temperature anomaly on the continental scale.

Research articles dealing with temporal variability of cold spells are considerably less frequent compared to those concerning heat waves. According to Kyselý (2008), the most severe cold spells since the beginning of the 20<sup>th</sup> century occurred in the 1940s over most

European areas. Other notable events were observed in winter 1962/1963 (Cattiaux et al. 2010), in February 1956, in January 1987 (Walsh and Phillips 2001) and in winter 2009/2010 (Cattiaux et al. 2010). Although severity of cold spells shows negative trend since the 1940s, this decline is smaller compared to the increase of heat wave severity (Kyselý 2008).

### **2.3 Driving mechanisms of heat waves and cold spells**

The development of both heat waves and cold spells in Europe is related to an interruption of prevailing zonal flow (Cattiaux et al. 2012) which is linked to atmospheric blocking (Barriopedro et al. 2006). Atmospheric blocks are formed by quasi-stationary anticyclones lasting one week or more (Buehler et al. 2011). An occurrence of these blocks is linked to Rossby wave breaking events (Altenhoff et al. 2008), driven by large-scale meanders in the upper troposphere jet stream. According to Shubert et al. (2011), Rossby waves account for roughly 60% of temperature variability on monthly sub-seasonal time scales over middle latitudes in the northern hemisphere.

#### **2.3.1 Heat waves**

Blocking anticyclones trigger extremely high summer temperatures based on two basic mechanisms: i) creating positive anomalies in surface radiation budget through clear-sky conditions associated with subsiding motions (mainly in the central part of an anticyclone), and ii) causing a meridional advection of warm air masses (mainly in outer regions of an anticyclone, Pfahl and Wernli 2012). Shubert et al. (2011) demonstrated a key role of atmospheric blocking in development of the 2003 and 2010 heat waves, and Schneidereit et al. (2012) concluded that the blocking high over western Russia lasted more than twice as long as the mean blocking duration for summer.

Kyselý (2008) analysed large-scale flow during European heat waves using Hess-Brezowsky synoptic catalogue (Werner and Gerstengarbe 2010) and found four major circulation types conducive to heat waves. The anticyclone was located over Central Europe (types HM and BM) or over Scandinavia (type HFA). In the fourth type (SWZ), south-western cyclonal flow was dominant. Cassou et al. (2005) showed that the occurrence of blocking anticyclone over central Europe or Scandinavia may be favoured by the anomalous tropical Atlantic heating. These changes of sea surface temperature in the Northern Atlantic are quasi-periodic and are referred as Atlantic Multidecadal Oscillation (Sutton and Hodson



2005). This oscillation is probably linked to oceanic thermohaline circulation (Knight et al. 2005) and is well correlated with the duration of heat waves in Europe (Della Marta 2007b).

Heat waves can be amplified by a soil moisture deficit that results in a reduced latent cooling and therefore increased summer  $T_{\max}$ . The majority of severe European heat waves were preceded by spring precipitation deficit (Fischer et al. 2007; Barriopedro et al. 2011). This finding was supported by model simulations performed by Jaeger and Seneviratne (2010), who showed that a soil moisture deficit is able to considerably amplify summer  $T_{\max}$ . Haarsma et al. (2009) pointed out possible distant connections between soil moisture deficit in Southern Europe and heat waves over Central and Western Europe. Intense surface heating due to lack of soil moisture may trigger a large-scale Mediterranean heat low, bringing easterly winds over these regions. In addition, the switch from a global dimming to global brightening phase in the 1980s due to decline of aerosol emissions may be also reflected in increased severity of heat waves (Tang et al. 2012).

### 2.3.2 Cold spells

Euro-Atlantic atmospheric blocking occurs most frequently in winter (Crocchi-Maspoli et al. 2007), and the relationship between atmospheric circulation and European temperature is strongest also during this season (Cattiaux et al. 2012). The severity of cold spells is well correlated with the North Atlantic Oscillation index (NAO) that expresses the strength of a zonal flow (Scaife et al. 2005). More specifically, winter conditions can be described using four ‘weather regimes’ (e.g. Hurrell and Deser 2010), which are derived from pressure patterns over the Euro-Atlantic domain. These are i) positive NAO phase, ii) negative NAO phase, iii) Scandinavian blocking, and iv) Atlantic ridge of high pressure. In addition, occurrence of these regimes and winter atmospheric circulation generally is modulated by quasi-periodical changes in solar activity (Barriopedro et al. 2008; Huth et al. 2008).

The aforementioned cold winter of 2009/2010 was related to an exceptionally persistent negative NAO phase (Cattiaux et al. 2010). The second most abundant weather regime during the 2009/2010 winter was Scandinavian blocking, which is also conducive to cold spells over Europe (Kyselý 2008). By contrast, the frequency of positive NAO phase was extremely low (5 of 90 days) during the winter of 2009/2010 (Cattiaux et al. 2010).

Beside atmospheric circulation, the severity of cold spells may be amplified by snow cover albedo feedback. Plavcová and Kyselý (2016) showed that the frequency of north-

eastern cyclonic synoptic types, which are linked to snowfall in Europe (Bednorz 2011), is significantly increased before the onset of cold spells in Central Europe.

A shift to positive NAO phase since the 1970s is likely to be responsible for the majority of the aforementioned decline in cold spell occurrence at the end of the 20<sup>th</sup> century (Scaife et al. 2008). Cattiaux et al. (2010), however, concluded using flow analogues method that the winter of 2009/2010 was warmer than expected based on its record-breaking seasonal circulation characteristics and attributed this inconsistency to a ‘background warming’. It is possible that multidecadal variability of NAO may be also influenced by global climate change. Therefore, the higher winter temperatures may be partly either consequence or cause of the increased NAO index.

#### **2.4 Simulation of heat waves and cold spells in climate models**

Climate models have become a powerful tool for studying possible climate change scenarios. There has been a continuous increase of their horizontal and vertical resolution. Present CMIP5 global climate models (GCMs) have the horizontal grid spacing of an atmospheric component roughly 0.5–4°, and more than half of them have grids finer than 1.3° (Taylor et al. 2012). This resolution is nevertheless still not sufficient to resolve smaller-scale processes and thus additional downscaling is needed, especially for regional analyses. There are two main branches of downscaling methods: statistical, and dynamical (e.g. Haylock et al. 2006).

Statistical downscaling involves deriving empirical relationships that transform large-scale features of the GCMs to regional scale variables and includes three categories: i) weather generators, ii) weather typing and iii) transfer functions (Ghosh and Mujumdar 2007). A weather generator creates a large number (thousands) of time series for any meteorological variable based on its statistical characteristics (e.g. mean, variance, autocorrelation coefficient) and it was used by Kysely (2010) to estimate future characteristics of heat waves in Prague. Although many different statistical downscaling methods are available, allowing flexible and computationally inexpensive process, their largest drawback is that empirical relationships valid in the present climate may be altered under climate change conditions.

Dynamical downscaling is represented by regional climate models (RCMs). RCMs are nested into coarser-grid driving GCMs that provide boundary conditions and work within limited domains (e.g. Europe), thereby allowing the use of a denser grid while preserving reasonable computation time. RCMs may also be driven by a reanalysis (i.e. perfect boundary

conditions), and these outputs are used for model evaluation. Present RCMs from the EURO-CORDEX project have a horizontal grid spacing of 12.5 km (Jacob et al. 2014) and very high-resolution (1–2 km grid) RCMs were recently introduced. These very high-resolution models are able to resolve small-scale processes (e.g. atmospheric convection) which mainly improve simulation of a diurnal cycle of precipitation. A better representation of orography further improves simulation of heavy precipitation, local wind patterns, or urban canopy effects (Rummukainen et al. 2015).

Before analysing climate change projections, model simulations should be evaluated against observed data. Realistic simulation of temperature extremes is related to credible representation of their driving mechanisms, i.e. atmospheric blocking, soil moisture, or snow cover albedo feedback (Section 2.3). Although GCMs are able to simulate a geographical location of blocking anticyclones, the frequency of blocks is generally underestimated (Scaife et al. 2010). Biases were also found in simulations of snow cover (Peings 2013) and soil moisture (Boé and Terray 2008), which may alter future projections. It should be noted that successful simulation of heat waves in climate models may originate from compensating effect of underestimated blocking condition and overestimated intensity of drought. Analogously, successful simulation of cold spells may be based on less frequent blocks and overestimated snow-albedo feedback.

The evaluation of RCMs from the PRUDENCE project was performed by Kjellström et al. (2007). RCMs overestimated the 95% quantile of summer  $T_{\max}$  over Mediterranean and Balkan Peninsula while underestimation was found mainly in Scandinavia and the British Isles. A similar bias pattern is present in RCMs from the ENSEMBLES project (Dosio and Parulo 2011). Kjellström et al. (2011) attributed the negative temperature bias in the northern parts of the European domain to improper simulation of sea surface temperature and ice condition in the North Atlantic, while the positive temperature bias in the south is triggered by too-dry model climate in spring and summer in the Mediterranean. These model deficiencies and analogous temperature bias patterns are also present in the EURO-CORDEX project (Kotlarski et al. 2014), despite the fact that RCMs were driven by the perfect boundary conditions. Relatively good simulation of summer  $T_{\max}$  is achieved over Central Europe, where Kjellström et al. (2010) found the highest skill scores and only small negative temperature bias is usually reported (Nikulin et al. 2011; Plavcová and Kyselý 2011).

Analogously to summer  $T_{\max}$ , Kjellström et al. (2007) evaluated winter  $T_{\min}$  in PRUDENCE RCMs. The bias was positive in Western and Northern Europe (especially in

Scandinavia) and negative in the south-eastern regions. The mild winters were attributed to overestimated zonal flow in the HadGEM GCM. This is in accordance with Dosio and Parulo (2011), who showed that the winter  $T_{\min}$  bias in ENSEMBLES RCMs is strongly related to atmospheric circulation provided by driving GCMs. This fundamental dependence on driving data resulted in a different bias pattern in EURO-CORDEX RCMs driven by the reanalysis compared to ENSEMBLES RCMs driven by GCMs (Kotlarski et al. 2014).

Reproduction of heat waves (cold spells) requires not only good simulation of the right (left) tail of a temperature distribution but also of the persistence of high (low) temperatures. Many studies (e.g. Ballester et al. 2010; Fischer et al. 2010; Peigns et al. 2013) define heat waves and cold spells based on quantiles calculated for each climate model individually, in order to remove temperature bias. The capability of CORDEX RCMs to simulate heat waves over Europe was evaluated by Vautard et al. (2013). Even though the RCMs were driven by the reanalysis and quantiles were calculated individually for each RCM, the simulated heat waves were too persistent and severe, probably due to improper simulation of surface energy fluxes. In addition, Plavcová and Kyselý (2015) concluded that the overly persistent circulation in ENSEMBLES RCMs driven by the reanalysis contributed to the overestimated frequency of long heat waves and cold spells. Overestimated severity of cold spells was found also by Peigns et al. (2013), mainly due to too-long left tail of the temperature distribution. Most of the utilized CMIP5 GCMs overestimated the duration of cold spells, while their spatial extent was generally underestimated (Peigns et al. 2013).

## **2.5 Projections of future heat waves and cold spells**

Projections of a possible future climate are based on concentration scenarios, which are used to provide a description of possible future evolution with respect to socio-economic change, technological change, energy and land use, and emissions of greenhouse gases and air pollutants (van Vuuren et al. 2011). Depending on the choice of concentration scenarios, simulations of GCMs project increase of temperatures over Europe by 2–3°C in the 2046–2065 period and by 2–6°C in the late 21<sup>st</sup> century (IPCC 2013).

In addition to the shift in mean value of the temperature distribution, heat waves and cold spells are also influenced by changes in its variance. In summer, GCMs simulate a widening of temperature distribution (Cattiaux et al. 2012) that may be caused by increased blocking frequency or enhanced soil-moisture feedback. Therefore, in combination with higher mean temperatures, heat waves are expected to become more frequent, more intense, and longer

lasting in a future climate (e.g. Meehl et al. 2004). According to Fischer and Schär (2010), the frequency of Central European heat waves is projected to be four heat waves per decade in the 2021–2050 period and 13 heat waves per decade in the late 21<sup>st</sup> century under the SRES A1B scenario, while only one heat wave per decade is simulated in a historical period. Although these expected changes are usually reported to be driven mainly by higher mean temperature (Ballester et al. 2010), Seneviratne et al. (2006) also emphasize the role of increasing temperature variance. Increased frequency of heat waves is projected also under the RCP 4.5 ‘low’ concentration scenario (Lau and Nath, 2014).

Changes in wintertime temperature variance mainly depend on atmospheric circulation. CMIP3 GCMs project decreased temperature variance in winter (Cattiaux et al. 2012), which is attributable to the increased zonal flow. These results are in accordance with Peings et al. (2013), who projected a higher frequency of positive NAO phase in a future climate. By contrast, CMIP5 GCMs simulate increased occurrence of negative NAO phase in a future climate (Cattiaux et al. 2013) and Francis and Vavrus (2012) suggest that the occurrence of wintertime blocking anticyclones may be enhanced due to rapid warming over the Arctic. Inasmuch as projections of cold spells are related to many uncertainties, it is difficult to conclude possible future scenarios for these events.

### 3 Work objectives

A general aim of this thesis is to study variability of heat waves and cold spells in the past, present, and possible future climate. The study is conducted over Central Europe, which was affected by several extraordinary events in recent years. Based on the literature review (Section 2.2), an analysis of heat waves and cold spells is carried out with emphasis on their spatial extent using gridded data sets, because this characteristic was not often considered in previous studies. In addition, use of gridded data sets is suitable for evaluating climate models that provide spatial fields of meteorological variables. Nevertheless, ‘point’ station data is also utilised in order to assess the magnitude of recent severe heat waves on a centennial scale, because no high-quality gridded data is available for these long-term analyses.

Changes in these events in a possible future climate are analysed with respect to related uncertainties originating from the selection of concentration scenarios, combinations of RCM  $\times$  GCM, and climate models’ spatial resolution. Previous studies that analysed heat waves or cold spells in a possible future climate did not evaluate these uncertainties in detail. An emphasis is given to heat waves as these are regarded as a larger threat in the context of climate change compared to cold spells, and partly because the occurrence of cold spells is also related to extraterrestrial effects (Section 2.5), which are not taken into account in present climate models. Before assessing changes of heat waves under climate change scenarios, the capability of climate models to simulate these events is evaluated. Identifying strengths and weaknesses of climate models is vital for credible interpretation of simulated heat waves in a possible future climate. The aim of the thesis is achieved through completing four work packages (WPs) listed below:

- WP1: Analysing temporal variability of heat waves and cold spells using (i) meteorological stations with long-term measurements and (ii) gridded data that allow investigating the spatial extent of these events
- WP2: Describing the most prominent heat waves and cold spells and assessing the extremity of recent events in a long-term context
- WP3: Evaluating the capability of RCMs to simulate heat waves in a historical climate and identifying possible sources of errors
- WP4: Investigating possible changes of frequency and characteristics of heat waves in a future climate under various concentration scenarios

#### 4 Study area, data and methods

Heat waves and cold spells are analysed over Central Europe, which is defined to encompass more than 600,000 km<sup>2</sup> approximately between 47–53°N and 8–22°E. This area includes Germany (excluding its northern areas and the Rhineland), the south-western part of Poland, the Czech Republic, northern Austria (bordered by the northern slope of the Alps), Slovakia (excluding its eastern part) and northern Hungary (Figure 4.1). The majority (75%) of this area has an elevation below 500 m a.s.l., while the rest is formed by highlands and mountains. According to Köppen-Geiger climate classification, almost entire Central Europe has warm temperate and fully humid climate with warm summers (Cfb), while the rest of the region exhibits snow and fully humid climates (Df) in mountainous areas (Kottek et al. 2006). The definition of Central Europe varies slightly among research articles included into the thesis, mainly due to the use of different data sets.

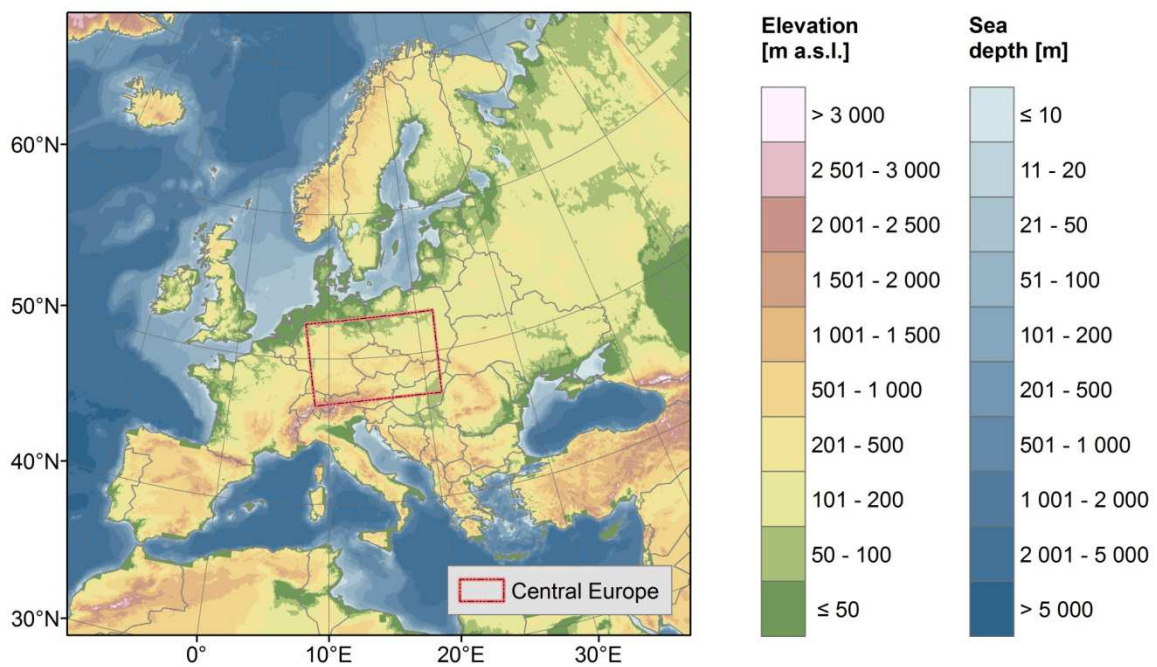


Figure 4.1. Definition of Central Europe and World digital elevation model (ETOPO5).

The data sets and meteorological variables utilized in the thesis are listed below. The data were used for assessing temporal variability and characteristics of observed heat waves and cold spells, evaluating RCMs' simulations of heat waves, projecting their future changes, and performing additional analyses.

- European Climate Assessment & Dataset (ECA&D) project (Klein Tank et al. 2002) – This data set is receiving daily data from 62 countries (10455 meteorological stations) over Europe, Northern Africa, and Western Asia. The majority of these series can be downloaded online (<http://www.ecad.eu/>). Although many stations exhibit some inhomogeneities (Wijngaard et al. 2003), this data set nevertheless represents the best source of long-term station data over Central Europe and has been used in a variety of analyses (e.g. Beniston 2013; Simolo et al. 2014). Daily maximum temperature from this data set was used to assess the severity of heat waves at Central European stations with long-term measurements.
- E-OBS gridded data set (Haylock et al. 2008) – These data are based on the aforementioned ECA&D station data and are available over most European regions. Its grid has a horizontal resolution of 25 or 50 km and data are available from 1950 to the present. The data set is still being developed by adding new observations and correcting previous errors. Current and previous versions are available online via project webpage (<http://www.ecad.eu/download/ensembles/download.php>). Gridded daily maximum (minimum) temperature from this data set was used to delimit heat waves (cold spells) with respect to their spatial extent. Links between soil-moisture deficit and severity of heat waves were studied through precipitation data, and daily mean temperature was utilized to identify hot summers.
- RCMs from the ENSEMBLES project (van der Linden and Mitchell 2009) – These simulations are available in 25 or 50 km grid, covering whole Europe. RCMs are driven either by the ERA-40 reanalysis (perfect boundary conditions experiments) or by GCMs (historical and A1B scenario runs). RCMs driven by the reanalysis and historical runs are available from the mid-20<sup>th</sup> century to 2000, while scenario runs cover the 2001–2100 period. Data can be downloaded from the project website (<http://ensemblesrt3.dmi.dk/>). A capability of RCMs to reproduce severe Central European heat waves was evaluated using these simulations driven by the reanalysis. Besides daily maximum temperature utilized for identifying and describing severity of heat waves, additional analyses were carried out using simulated precipitation and surface fluxes data. In addition, GCMs-driven simulations were analysed to examine changes in heat wave frequency in a possible future climate.
- RCMs from the EURO-CORDEX (Jacob et al. 2014) – This project is a successor to the ENSEMBLES project. Individual RCMs were subjected to various upgrades,



including an improvement of their respective sets of physical parameterizations, while keeping their basic principles from the ENSEMBLES stage. The EURO-CORDEX project consists of simulations in high resolution (12.5 km grid) and in coarser 50 km grid. RCMs are driven either by the reanalysis (ERA-Interim, Dee et al. 2011) or GCMs. Scenario runs are forced mostly by RCP 4.5 or RCP 8.5 concentration scenarios. Changes in heat wave frequency in a possible future climate were analysed also using this data set.

- NCEP/NCAR reanalysis (Kalnay et al. 1996) – This data set is available from 1948 to present with global coverage and a horizontal resolution of  $2.5 \times 2.5^\circ$ . Mean sea level pressure and 500 mb geopotential height were obtained from this data set in order to analyse a large-scale flow during the 2013 heat wave.
- CLARIS LPB dataset – These data were provided by the Argentine National Weather Service and their quality was analysed through the European project CLARIS LPB (Penalba et al. 2014). Maximum and minimum daily temperature from 58 stations were used to describe temporal variability of heat waves over Argentina.

Due to relatively complex climate of Central Europe, heat waves and cold spells were defined in this thesis based on relative thresholds. The 90% or 95% quantiles were applied on both station and gridded data. Due to considerable temperature biases in modelled data, these quantiles were calculated separately for each simulation, in order to focus rather on the behaviour of the right tail of temperature distributions than on the bias itself. This approach was widely used in previous studies that analysed heat waves and cold spells in climate model simulations (Ballester et al. 2010; Peigns et al. 2013; Vautard et al. 2013). The magnitude of heat waves and cold spells in gridded data was assessed using the extremity index that takes into account temperature anomaly, length, and spatial extent of the events, while the magnitude of heat waves in station data was calculated through combination of temperature anomaly and length only. Detailed descriptions of other methods, including cluster analysis, calculation of effective precipitation, evaporative fraction and temporal autocorrelation of temperature are given in individual research articles in Sections 6–10.

## 5 Overview of research articles used in the thesis

The thesis is based on five research articles focused on temperature extremes and published or submitted to impact factor rated international journals:

Lhotka O, Kyselý J (2015): Characterizing joint effects of spatial extent, temperature magnitude and duration of heat waves and cold spells over Central Europe, *International Journal of Climatology*, 35, 1232-1244, DOI: 10.1002/joc.4050

Lhotka O, Kyselý J (2015): Hot Central-European summer of 2013 in a long-term context, *International Journal of Climatology*, 35, 4399-4407, DOI: 10.1002/joc.4277

Lhotka O, Kyselý J (2015): Spatial and temporal characteristics of heat waves over Central Europe in an ensemble of regional climate model simulations, *Climate Dynamics*, 45, 2351-2366, DOI: 10.1007/s00382-015-2475-7

Lhotka O, Kyselý J (2016): Climate change scenarios of heat waves in Central Europe and their uncertainties, *Theoretical and Applied Climatology* [under review]

Rusticucci M, Kyselý J, Almeida G, Lhotka O (2016): Long-term variability of heat waves in Argentina and recurrence probability of the severe 2008 heat wave in Buenos Aires, *Theoretical and Applied Climatology*, 124, 679-689, DOI: 10.1007/s00704-015-1445-7

The first four papers resulted from collaboration with my supervisor, J. Kyselý. I prepared the data sets, performed all analyses and was primarily responsible for the manuscripts' preparation. J. Kyselý assisted me with interpretation of results, publication of research articles, and he supervised my work. The last study, of which I am not the first author, broadens and supplements the topic of the thesis. The specification of my contribution to this research article, confirmed by the leading author, is in the appendices (Section 14).

The first article is entitled 'Characterizing joint effects of spatial extent, temperature magnitude and duration of heat waves and cold spells over Central Europe' and was published in *International Journal of Climatology*. In this paper, heat waves and cold spells over Central Europe were analysed using the E-OBS gridded data set. An extremity index was proposed which combines spatial extent, temperature, and duration of heat waves and cold spells. The most severe heat waves in the 1950–2012 period occurred in the summers of 1994 and 2006, while the most extreme cold spells were observed in winters 1955/56 and 1962/63. The well-known European heat waves in 2003 and 2010 were not that pronounced over Central Europe,

since largest temperature anomalies were observed in France and Russia, respectively. Both heat waves and cold spells were classified through a hierarchical cluster analysis of temperature amplitude, spatial extent, and duration into four basic types and the list of major Central European events was established. This article contains the results from WP1 – analysis of temporal variability of heat waves and cold spells in gridded data and WP2 – description of the most prominent heat waves and cold spells.

The second article ‘Hot Central-European summer of 2013 in a long-term context’ was also published in *International Journal of Climatology*. The paper was focused on the anomalously hot summer of 2013, and its extremity was analysed using both station and gridded data. This summer was ranked as the fifth warmest since 1951 on the European scale, with high positive temperature anomalies over Central Europe. In Kremsmuenster and Graz (Austria), the 2013 summer was unprecedented according to heat wave characteristics since the end of the 19<sup>th</sup> century and it was extreme also at other Central European stations with long-term measurements. The most intense heat wave over Central Europe in early August 2013 was driven primarily by anticyclonic conditions and was probably amplified by the preceding precipitation deficit. The paper contributed to WP1 – analysis of temporal variability of heat waves and cold spells using meteorological stations with long-term measurements and WP2 – assessment of the extremity of recent events in a long-term context.

The third article is entitled ‘Spatial and temporal characteristics of heat waves over Central Europe in an ensemble of regional climate model simulations’ and was published in *Climate Dynamics*. The study examines the capability of RCMs driven by the reanalysis to reproduce spatial and temporal characteristics of severe Central European heat waves, and it benefits from the methodology developed and tested in the first article. The multi-model mean reflected the observed characteristics of heat waves quite well, but considerable differences were found among the individual RCMs. Deficiencies were found also in reproducing interannual and interdecadal variability of heat waves. The magnitude of the most severe Central European heat wave that occurred in 1994 was underestimated in all RCMs and this error was related to overestimated precipitation during and before this event. By contrast, a simulated precipitation deficit during summer 1967 in the majority of RCMs contributed to an ‘erroneous’ heat wave. The results suggest that land–atmosphere interactions are crucial for developing severe heat waves, and their proper reproduction in climate models is essential for obtaining credible scenarios of future events. This article contributed to WP3 – evaluation of

the capability of RCMs to simulate heat waves in a historical climate and the identification of possible sources of errors.

The fourth article ‘Climate change scenarios of heat waves in Central Europe and their uncertainties’ was submitted to *Theoretical and Applied Climatology*. The study examines climate change scenarios of Central European heat waves with a focus on related uncertainties. A methodology was partly based on the first article and some of the RCMs utilized (driven by the reanalysis) were evaluated in the third article. In the fourth article, a large ensemble of RCM simulations (62) was analysed in order to calculate several possible scenarios. Although the RCMs were found to reproduce the frequency of heat waves quite well, those RCMs with the coarser grid considerably overestimated the frequency of severe heat waves. This deficiency was overcome in the higher-resolution EURO-CORDEX RCMs. In the near future (2020–2049), heat waves are projected to be nearly twice as frequent in comparison to the modelled historical period, and the increase is even larger for severe heat waves. Uncertainty originates mainly from the selection of RCMs and GCMs, because the increase is similar for all concentration scenarios. For the late 21<sup>st</sup> century (2070–2099), a substantial increase in heat wave frequencies is projected, the magnitude of which depends mainly upon concentration scenario. Two to four heat waves per summer are projected in this period, depending on concentration scenario (compared to less than one in the recent climate), and severe heat waves are likely to become a regular phenomenon. The paper contains the results from WP4 – investigation of possible changes of frequency and characteristics of heat waves in a future climate under various concentration scenarios and partly contributed to WP3 – evaluation of the capability of RCMs to simulate heat waves in a historical climate and the identification of possible sources of errors.

Some methodological approaches based on analysis of Central European heat waves were applied in the fifth article entitled ‘Long-term variability of heat waves in Argentina and recurrence probability of the severe 2008 heat wave in Buenos Aires’, which resulted from a joint project with the University of Buenos Aires and was published in *Theoretical and Applied Climatology*. The objectives of this work were to study the long-term variability of heat waves over Argentina and to estimate recurrence probability of the most severe 2008 heat wave in Buenos Aires using long artificial time series of  $T_{\max}$  simulated by a first-order autoregressive model. A positive trend of heat wave days was found in Buenos Aires, while some stations exhibited a decrease of heat wave days. The recurrence probability of the major

2008 heat wave was found to be small in the present climate but it is likely to increase substantially in the near future even under a moderate warming trend.

## 6 Article I: ‘Characterizing joint effects of spatial extent, temperature magnitude and duration of heat waves and cold spells over Central Europe’

Ondřej Lhotka<sup>a,b</sup> and Jan Kyselý<sup>a</sup>

<sup>a</sup> Institute of Atmospheric Physics, Academy of Sciences of the Czech Republic, Prague, Czech Republic

<sup>b</sup> Faculty of Science, Charles University, Prague, Czech Republic

International Journal of Climatology, 35, 1232-1244, DOI: 10.1002/joc.4050

**Abstract:** Heat waves and cold spells have pronounced impacts on the natural environment and society. The main aim of this study was to identify major Central European heat waves and cold spells since 1950 and assess their severity not only from the viewpoint of temperature and duration but also as to the affected area. The heat waves and cold spells were delimited from the E-OBS gridded data set. An extremity index was proposed that captures joint effects of spatial extent, temperature and duration of heat waves and cold spells. During the 1950–2012 period, we identified 18 major heat waves and 24 major cold spells over Central Europe. The most severe heat wave occurred in summer 1994, followed by the 2006 heat wave; both these events were far more extreme over Central Europe than heat waves in the well-known 2003 and 2010 summers. The most severe cold spells occurred in the winters of 1955/56 and 1962/63. The recent winter of 2011/12 was found to be the 6th coldest since 1950/51 according to the seasonal sum of the extremity index. The heat waves and cold spells were classified through a hierarchical cluster analysis of their characteristics (temperature amplitude, spatial extent of the core, and duration) into 4 basic types. The established list of major Central European heat waves and cold spells might be utilized in further analyses. The extremity index may be applied over different areas to perform comparative studies and used also for evaluation of regional climate model simulations.

**Keywords:** heat waves; cold spells; extremity index; interannual variability; cluster analysis; E OBS gridded data set

### 6.1 Introduction

Heat waves and cold spells are important phenomena of the European climate and have major impacts on the natural environment and society. These events are traditionally regarded as several days long summer/winter periods when weather conditions are excessively hotter/colder than normal. Severe heat waves that occurred during the past two decades and the very cold winter of 2009/2010 in Europe have prompted intense investigation of these events. De Bono et al. (2004) reported more than 30,000 deaths during the 2003 western European heat wave along with other economic losses; however, the number of excess deaths

varies across studies and the estimates reach up to 70,000 (Robine et al. 2008). The extreme eastern European summer of 2010 was associated with an estimated death toll of 55,000, substantial crop failures and more than 1 million ha of burned areas (Barriopedro et al. 2011). Heat waves also cause stress for livestock and wildlife, spreading of pests, and increased energy demand for cooling (Beniston et al. 2007). Inasmuch as the relationship between ambient temperature and mortality is U-shaped (increased risks for both low and high temperatures), cold spells also affect public health (Barnett et al. 2012). Harsh conditions during cold spells can harm vegetation, and air temperature might fall below the thresholds for which buildings and other infrastructural components were designed (Vavrus et al. 2006).

European heat waves have been analysed by many authors. The influence of a large scale forcing on heat waves was evaluated by Della Marta et al. (2007a), who showed that heat waves over Europe are related to the Atlantic Multidecadal Oscillation (e.g. Sutton and Hodson 2005). A detailed analysis of synoptic factors during the 2003 heat wave was made by Black et al. (2004), while the large scale flow during the extreme 2010 summer was analysed by Schneidereit et al. (2012). Recurrence probability of recent severe heat waves was estimated using simulations with a stochastic time series model by Kyselý (2002, 2010), including possible changes under future scenarios. The role of anthropogenic climate change was analysed by Stott et al. (2004) for the 2003 European heat wave and by Meehl et al. (2007) for temperature extremes over the United States. Another important factor that contributes to heat wave amplification is land–atmosphere coupling. Many papers emphasize the role of soil moisture deficit during major heat waves (e.g. Fischer et al. 2007; Jaeger and Seneviratne 2010). Interannual variability of European heat waves during 1880–2005 was investigated by Della Marta et al. (2007b). The duration of heat waves was pronounced in the middle of the 20<sup>th</sup> century and at the end of the examined period, and the positive trend in the duration of heat waves was significant at the majority of stations. Analyses of temporal variability of heat waves in Central and Eastern Europe were performed by Kyselý (2010) for the Czech Republic and by Shevchenko et al. (2013) for Ukraine.

Recent studies of cold spells over Europe have been mainly focused on the anomalous winter of 2009/2010. L'Heureux et al. (2010) showed that the Arctic Oscillation (e.g. Thompson and Wallace 1999) contributed greatly to the below-average temperatures over Europe. Cattiaux et al. (2010) ranked the winter of 2009/2010 as the 13th coldest over Europe since 1949, far behind the cold record for the winter of 1962/1963. Using the flow analogue method, authors demonstrated that atmospheric dynamics during the winter of 2009/2010 was

favourable to a temperature anomaly comparable in magnitude to the record-breaking winter of 1962/1963, and attributed this inconsistency to the background warming. An analysis of interannual variability of cold wave days over Europe during 1901–2000 was performed by Kysely (2008) using station data from the ECA data set (Klein Tank et al., 2002). Cold wave days were most pronounced in the mid-20<sup>th</sup> century and almost vanished at the end of the examined period.

Although a lot of work has been done to examine heat waves and cold spells, only several studies have considered their spatial extent (e.g. Stefanon et al. 2012; Peings et al. 2013). There is a need to investigate these events not only regarding the aspects of air temperature and duration but also with a view to the affected area. Therefore, we propose an extremity index that takes into account all these variables, and use it to evaluate heat waves and cold spells over Central Europe. This region was recently affected by exceptionally high temperatures in August 2012, when the new record-breaking air temperature (40.4°C) was measured in the Czech Republic (Němec, 2012). In addition, Central Europe experienced extremely cold conditions in the winter of 2011/2012 which resulted in more than 800 deaths due to hypothermia in Central and Eastern Europe (Aon Benfield, 2012).

The main aim of this study was to identify major Central European heat waves and cold spells since 1950 and to assess their severity using an extremity index proposed for characterizing joint effects of spatial extent, magnitude and duration of heat waves and cold spells.

## **6.2 Data and methods**

### **6.2.1 Data and area of interest**

The daily temperature data was taken from the E-OBS 9.0 gridded data set (Haylock et al. 2008) that has spatial resolution of 25 km (0.22 deg. rotated pole grid) and covers the period from 1 January 1950 to 30 June 2013. Although Kysely and Plavcová (2010) published a critical remark on the applicability of its second version, it represents the best source of high-resolution data covering the whole European land area. The analysis of the spatial characteristics of heat waves and cold spells would not be straightforward from irregularly spaced station data. Another advantage of using E-OBS is that the methodology and the extremity index as proposed in the present study might be utilized for evaluation of regional climate models (RCMs), due to the same grid being used by E-OBS and many RCMs.



Moreover, the E-OBS data set is being developed by increasing the station density and correcting previous errors (more information is available at the project website – <http://www.ecad.eu/download/ensembles/oldversions.php>).

We examined 63 years long series for both seasons (summers of 1950–2012 for heat waves and winters of 1950/1951–2012/2013 for cold spells). Summer was defined as the period between 1 June and 31 August, while winter was regarded as the period between 1 December and 28 February. This is a standard definition of seasons in European climate and it was adopted also to allow a comparison with other studies.

The analysis was performed over Central Europe defined by 1,000 grid points (40×25) and covering an area of 625,000 km<sup>2</sup>. This domain is located approximately between 47–53°N and 8–22°E and includes Germany (excluding its northern areas and the Rhineland), northern Austria, the Czech Republic, the south-western part of Poland, Slovakia (excluding its eastern part) and northern Hungary (Figure 6.1). The geographical demarcation of Central Europe varies across sources, however, we included all countries traditionally regarded as Central European. The location of the centre (50°N, 15°E) is in accordance with previous works for Central Europe (e.g. Plavcová and Kyselý, 2012).

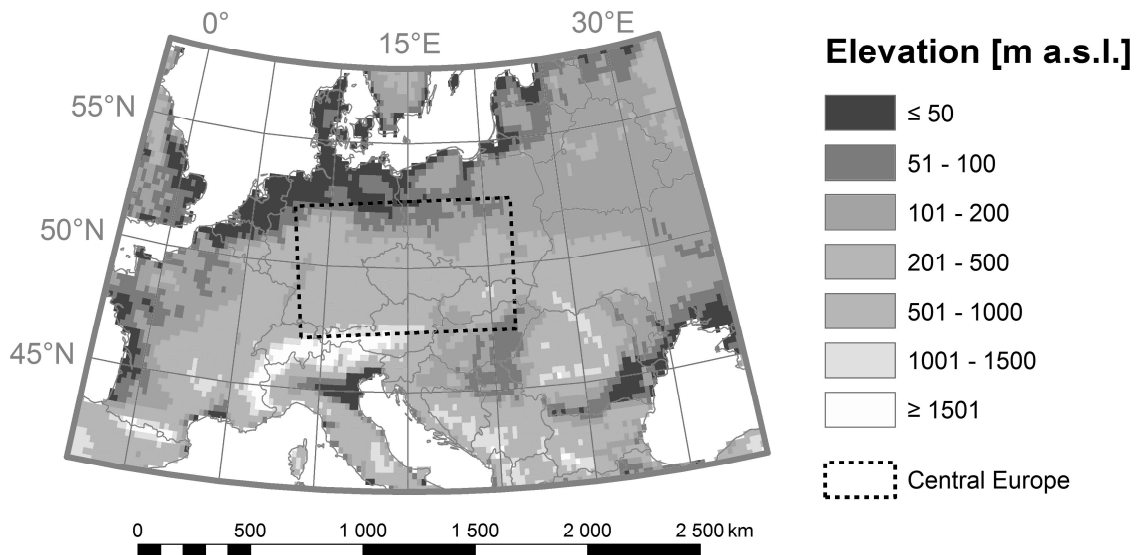


Figure 6.1. Definition of Central Europe (black dashed polygon) and elevation model (GTOPO30) used in E OBS 9.0 gridded data set (grayscale).

### 6.2.2 Definition of heat waves

There is no universal definition of heat waves (HWs). Perkins and Alexander (2013) summarized definitions of these events and concluded that a HW is traditionally regarded as a period of consecutive days when conditions are excessively hotter than normal. Based on this definition, a HW can occur anytime during the year. Despite this, we focused on summer HWs only because of their serious impacts on the natural environment and society.

In previous works, various criteria have been applied to delimit HWs. Two main approaches have been adopted for estimating whether conditions are ‘excessively hotter’. The first one is based on given temperature thresholds (e.g. Colombo et al. 1999; Gershunov et al. 2009; Kysely 2010) and it is suitable when delimiting HWs from single station data or from a region with quite homogeneous climate. The second approach uses a certain quantile for each station/grid point (e.g. Beniston et al. 2007; Cassou et al. 2005; Della-Marta et al. 2007b; Fischer et al. 2007). This approach respects the local climatology across the entire area of interest and thus is useful when performing regional analyses. Since the climate across Central Europe is very diverse (e.g. northern slope of the Alps vs. Pannonian lowlands), we adopted the latter approach.

The definition of a HW was based on the persistence of hot days (HDs). For each day in summer, daily maximum air temperature ( $T_{\max}$ ) in each grid point over Central Europe was transformed into  $T_{\max}$  deviation by subtracting the grid point specific 95% quantile of summer  $T_{\max}$  distribution. The 95% quantile was calculated over the 40 years period 1961–2000. Using this limited period allows updating the list of HWs without the need of recalculating respective quantiles. In addition, this period corresponds to many RCM runs driven by reanalysis, such as those from the ENSEMBLES project (van der Linden and Mitchell, 2009), which can be utilized in further work dealing with evaluation of HWs in RCM simulations.

Any day was considered a HD when the average of the  $T_{\max}$  deviations from the 95% quantile of summer  $T_{\max}$  distribution over Central Europe (Figure 6.1) was greater than zero. Thus, a HD can occur only if a substantial part of Central Europe is affected by  $T_{\max}$  above the 95% quantile. Therefore, it is necessary to design the domain with respect to a typical extent of synoptic features in order to identify HDs appropriately.

A HW over Central Europe was defined as a period of at least 3 consecutive HDs. The minimum duration of a HW in previous works varies from 2 days (e.g. Barnett et al. 2012) to 5 or more days (e.g. Ballester et al. 2010; Fischer and Schär 2010). The commonly used 3-day minimum duration (e.g. Della Marta et al. 2007a; Kysely 2010; Meehl and Tebaldi 2004) was

applied in our analysis. These relatively strict criteria allow identifying only major heat waves that are presumed to have considerable impacts on the natural environment and society. For this period (3 or more days), the daily grid maps of positive  $T_{\max}$  deviations were summed up into a cumulative map. Negative  $T_{\max}$  deviations were not taken into account.

To describe the severity of individual HWs, a heat wave extremity index ( $I_{hw}$ ) was proposed.  $I_{hw}$  is calculated from a cumulative map of positive  $T_{\max}$  deviations, and it is analogous to the station based TS30 index, used by Kyselý (2010) to examine severity of HWs. Values of individual grid points ( $TS_{max}'$ ) are summed up and scaled by the total number of grid points in Central Europe (1,000):

$$I_{hw} = \frac{1}{1000} \sum_{i=1}^n (TS_{max}')_i \text{ [}^{\circ}\text{C]}$$

where  $n$  is the number of grid points with a positive  $T_{\max}$  deviation in a cumulative map. The index uses summed up deviations over the whole period when a HW persists, and hence it captures joint effects of spatial extent, temperature magnitude and duration of a HW over the area of Central Europe.

### 6.2.3 Definition of cold spells

The definition of a cold spell (CS) was made analogous to that of a HW in order to allow direct comparison of these events and their characteristics. The definition was based on the persistence of cold days (CDs) in winter. A CD occurred when the average of daily minimum air temperature ( $T_{\min}$ ) deviations from its 5% quantile over Central Europe was less than zero. Analogously to HWs, we focus on major CSs that were defined as periods of at least 3 consecutive CDs. The description of CS severity was based on a cold spell extremity index ( $I_{cs}$ ) that analogously utilizes accumulated negative  $T_{\min}$  deviations over Central Europe and is given as an absolute value:

$$I_{cs} = \left| \frac{1}{1000} \sum_{i=1}^n (TS_{min}')_i \right| \text{ [}^{\circ}\text{C]}$$

#### 6.2.4 Characteristics of heat waves and cold spells

Besides  $I_{hw}$  and  $I_{cs}$ , we calculated several other characteristics of HWs and CSs. The temperature amplitude ( $T$  [°C]) is the highest daily value of  $T_{max}$  deviations from the 95% quantile of the summer  $T_{max}$  distribution during a HW (at any grid point in Central Europe) and represents the temperature anomaly of its peak. In the case of CSs, temperature amplitude is analogously computed from  $T_{min}$  and its respective 5% quantile and is given as an absolute value. The spatial extent of the HW core ( $A$  [km<sup>2</sup>]) is given by an area in which the sum of  $T_{max}$  deviations is greater than 10°C in a cumulative map. This represents the size of the area where weather conditions are considered extreme. The spatial extent of the CS core is calculated analogously, but the threshold was modified to 20°C. This adjustment was necessary due to differences between summer  $T_{max}$  and winter  $T_{min}$  distributions, as discussed in Section 6.5.1. Although the choice of 10°C and 20°C thresholds is somewhat arbitrary, we found it a reasonable compromise between too-low thresholds (in which case almost the whole area of Central Europe would be considered) and too-high thresholds (in which case many events would have spatial extent equal to zero). The duration of HW/CS ( $D$  [days]) is the number of days when HW/CS persists. A ratio between the total duration of HWs/CSs and the total number of HDs/CDs indicates whether HDs/CDs have a high clustering tendency (the ratio is close to 1), or whether HDs/CDs tend to occur separately throughout summer/winter (the ratio is close to 0).

The identified HWs and CSs were visualized over a larger region than just Central Europe in order to obtain the larger-scale pattern associated with each event. However, grid points outside Central Europe were not taken into account when calculating  $I_{hw}$ ,  $I_{cs}$ ,  $T$ ,  $A$  and  $D$ . The only characteristic calculated from all visualized grid points (including grid points outside Central Europe) was the overall spatial extent of the HW (CS) core ( $OA$  [km<sup>2</sup>]). It was computed analogously to  $A$ , but for the whole domain. The calculated characteristics of HWs and CSs are summarized in Table 6.1.

Table 6.1. Characteristics of heat waves and cold spells.

Abbreviation	Description	Units	Domain
$I_{hw}$	heat wave extremity index	°C	Central Europe
$I_{cs}$	cold spell extremity index	°C	Central Europe
$T$	temperature amplitude	°C	Central Europe
$A$	spatial extent of the HW (CS) core	km <sup>2</sup>	Central Europe
$OA$	overall spatial extent of the HW (CS) core	km <sup>2</sup>	whole domain
$D$	duration	days	Central Europe

### 6.2.5 Cluster analysis of heat waves and cold spells

Cluster analysis is widely used in atmospheric sciences for separating data into groups whose parameters are not known in advance. A broad overview of classification methods is presented in Huth et al. (2008). Cluster analysis of HWs and CSs was performed on the basis of their temperature amplitude (T), overall spatial extent of the HW (CS) core (OA), and duration (D). These variables were centred by subtracting their means and scaled by dividing them by their standard deviations. The input to the hierarchical clustering algorithm is a distance matrix (distances between observations) that was computed using Euclidean metric. It is the most commonly used distance measure in cluster analysis, however, other alternatives such as Mahalanobis metrics are also possible (Wilks 2011). The choice of hierarchical clustering algorithm determines how distances between clusters are measured. In the present study, we used the complete linkage (maximum distance) method in order to prevent the chaining of clusters. This method is based on the largest distance between points in two groups. The complete linkage method was also applied by Stefanon et al. (2012), who classified HWs based on the places of their occurrence over Europe.

Determining the final number of classes usually requires a subjective choice that depends to some degree on the goals of the analysis (Wilks 2011). The final number of HW/CS classes was determined by inspecting the plot of the distances between merged clusters, where a rapid jump indicates the final number of classes.

### 6.2.6 Statistical testing of heat wave and cold spells characteristics

The statistical testing was performed for assessing the significance of differences between HW and CS characteristics. We used the non-parametric two-sample Wilcoxon test (e.g. Hollander and Douglas 1999) since some HW and CS characteristics do not exhibit normal distributions. Statistical significance was assessed at the 0.05 level.

## 6.3 Heat waves

### 6.3.1 Characteristics and interannual variability

Over the 1950–2012 period, the total number of HDs in Central Europe was 188 (3.0 HDs/year on average). These days formed 18 HWs (defined as periods of at least 3 consecutive HDs) with a total duration of 84 days. These HWs occurred in 15 individual

years. The ratio between the total duration of HWs and the total number of HDs was 0.45. The list of observed HWs and their characteristics is given in Table 6.2.

Table 6.2. Major heat waves over Central Europe during 1950–2012.

Start	End	$I_{hw}$	T	A	OA	D
19520702	19520705	7.7	7.4	179.4	511.3	4
19520812	19520815	8.8	6.2	281.9	701.3	4
19570704	19570708	13.9	7.7	432.5	871.9	5
19590709	19590712	9.6	7.6	296.3	612.5	4
19630723	19630725	4.3	6.0	66.9	114.4	3
19640719	19640721	3.1	4.3	0.6	0.6	3
19740815	19740817	5.5	4.7	6.9	19.4	3
19760716	19760719	5.7	5.6	45.0	45.0	4
19830726	19830728	6.7	8.4	145.0	404.4	3
19920806	19920810	13.6	8.3	499.4	740.0	5
19940627	19940629	4.0	4.3	18.1	18.1	3
19940723	19940806	32.0	6.9	593.8	1,713.1	15
20000620	20000622	7.0	5.9	109.4	196.3	3
20030802	20030805	6.1	6.5	155.6	873.8	4
20030808	20030810	6.2	7.5	193.1	917.5	3
20060718	20060728	21.0	7.4	583.1	1,753.1	11
20070715	20070717	10.1	7.2	354.4	455.6	3
20100709	20100712	8.5	6.8	243.1	525.6	4
	Average:	9.7	6.6	233.6	581.9	4.7

$I_{hw}$  – heat wave extremity index [°C], T – temperature amplitude [°C], A – spatial extent of the HW core [thousands km<sup>2</sup>], OA – overall spatial extent of the HW core [thousands km<sup>2</sup>], D – duration [days]. Dates of start and end of HW are in YYYYMMDD format. The spatial extent of the Central European domain is 625.0 thousands km<sup>2</sup>.

The most severe HWs over Central Europe (according to  $I_{hw}$ ) occurred from 23 July to 6 August 1994 (15 days) and during 18–28 July 2006 (11 days). These two HWs were markedly above the others by their extremity index, spatial extent, and duration (no other HW lasted longer than 5 days). On the contrary, the greatest temperature amplitude was found during the 1983 HW that was only 3 days long and had relatively low extremity index and spatial extent. Interannual variability of HWs and HDs is visualised in Figure 6.2.

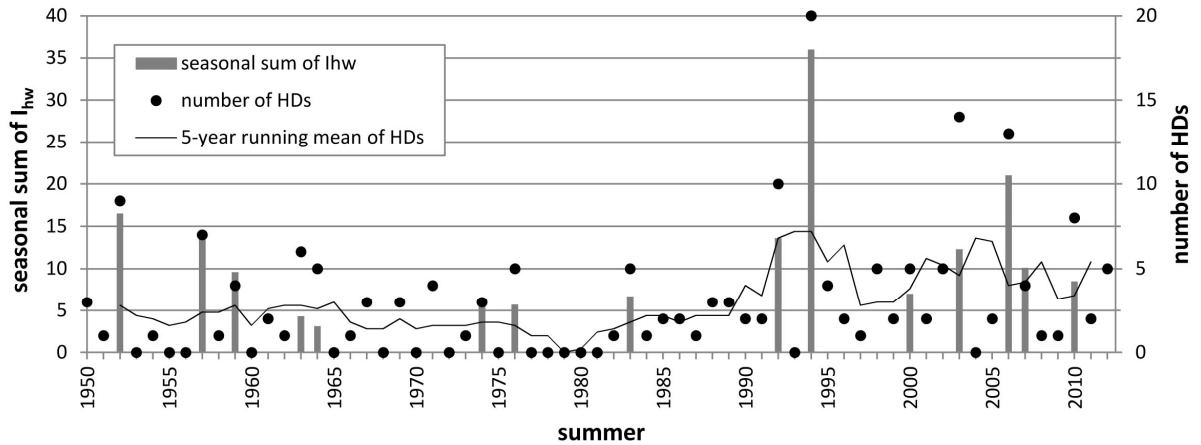


Figure 6.2. Interannual variability of hot days (HDs) and heat waves (HWs) over Central Europe during 1950–2012.

Years with a great seasonal sum of  $I_{hw}$  occurred in two sub-periods at the beginning of the analysed period and since the early 1990s. The summer of 1994 was exceptional in terms of the sum of  $I_{hw}$  and the number of HDs. The 5 year running mean showed a considerably increased annual number of HDs in the last two decades of the examined period while in the 1970s and 1980s, the occurrence of HDs was substantially reduced.

The most-severe 1994 HW (Figure 6.3) is characterized by a large temperature pattern with a centre in Poland and its core (the area where the sum of positive  $T_{max}$  deviations is greater than  $10^{\circ}\text{C}$ ) covered Denmark, southern Sweden, Germany, north-western France, the Czech Republic, Austria, Slovakia, Hungary, Lithuania, Latvia, western Belarus, and western Ukraine. On the contrary, the 2006 HW extended westward, affecting more western European countries. The relatively low severity of the 2003 HWs over Central Europe was related to the position of their temperature patterns (Figure 6.3). In both cases, the eastern part of Central Europe was unaffected by the cores of these HWs, resulting in their small spatial extent over this region and therefore relatively low  $I_{hw}$ . Moreover, the largest sums of temperature deviations for these HWs were located in France, outside of Central Europe.

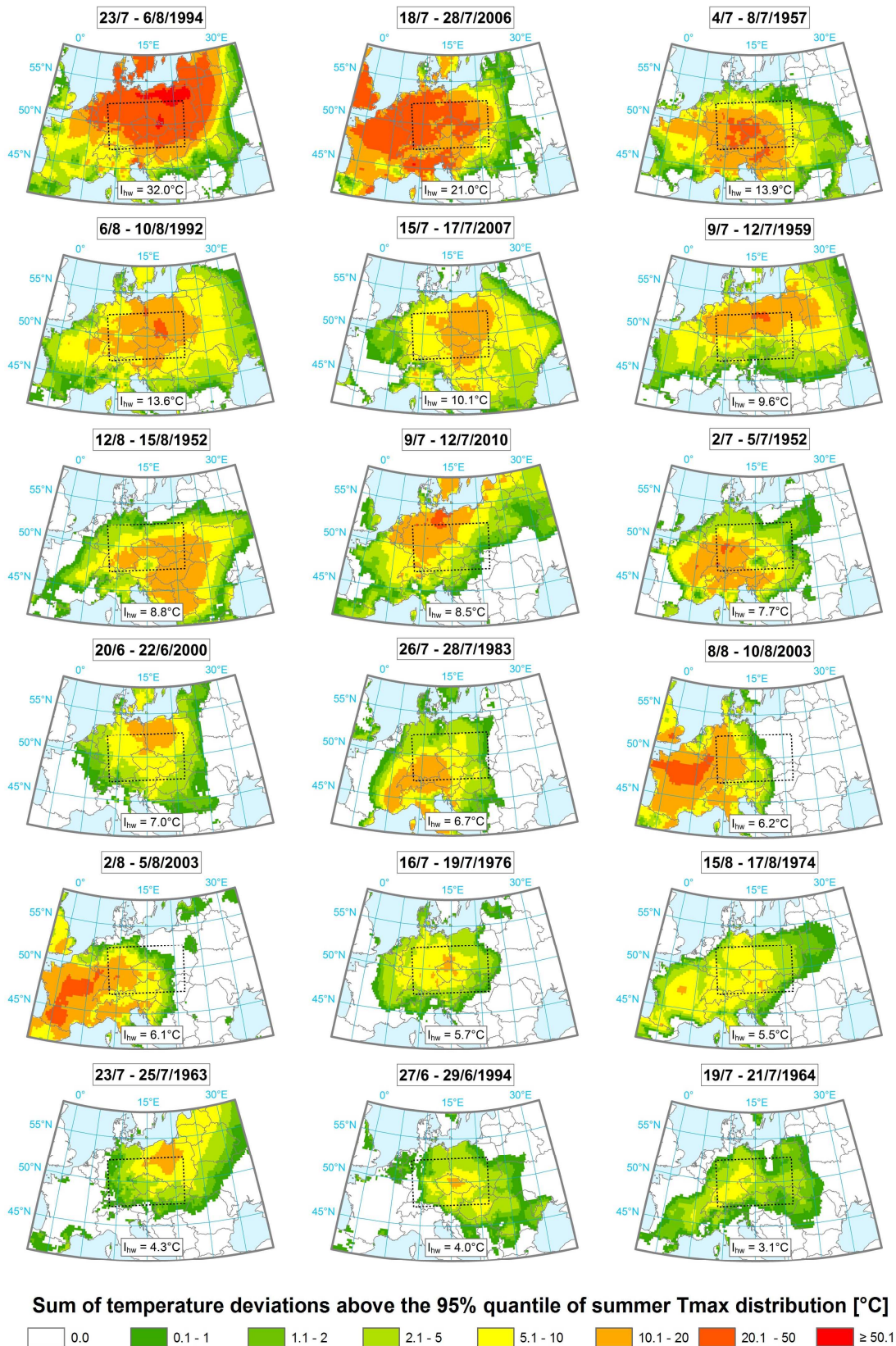


Figure 6.3. Heat waves in Central Europe during 1950–2012. The heat waves are ranked according to  $I_{hw}$  in descending order. Spatial patterns of the sum of positive  $T_{max}$  deviations above the 95% quantile of summer  $T_{max}$  distribution are plotted.



### 6.3.2 Cluster analysis

In order to determine similarities among individual HWs and identify basic types of HWs as to their characteristics, a hierarchical cluster analysis based on temperature amplitude, overall spatial extent of the HW core, and duration was performed. Detailed information is given in Section 6.2.5.

Based upon the cluster analysis, HWs were classified into 4 categories (Figure 6.4). The first category is characterized by exceptional overall spatial extent of the HW core and duration, and it contains the extremely widespread and persistent 1994 and 2006 HWs (their average duration exceeds the average duration in any other heat wave cluster by a factor of 3–4; Table 6.3). Although their extremity index is very pronounced, these do not exhibit the highest temperature amplitude. The second cluster represents weak HWs with the lowest values of their characteristics, especially the temperature amplitude and overall spatial extent, which is reflected in the low extremity index. Moderate HWs are located in the third cluster; these HWs have the extremity index, temperature amplitude and overall spatial extent of the HW core close to the average of all HWs. The fourth cluster is characterized by the highest temperature amplitude. The very intense 1983 HW ( $T = 8.4^{\circ}\text{C}$ ) and the 1992 HW ( $T = 8.3^{\circ}\text{C}$ ) fall into this category.

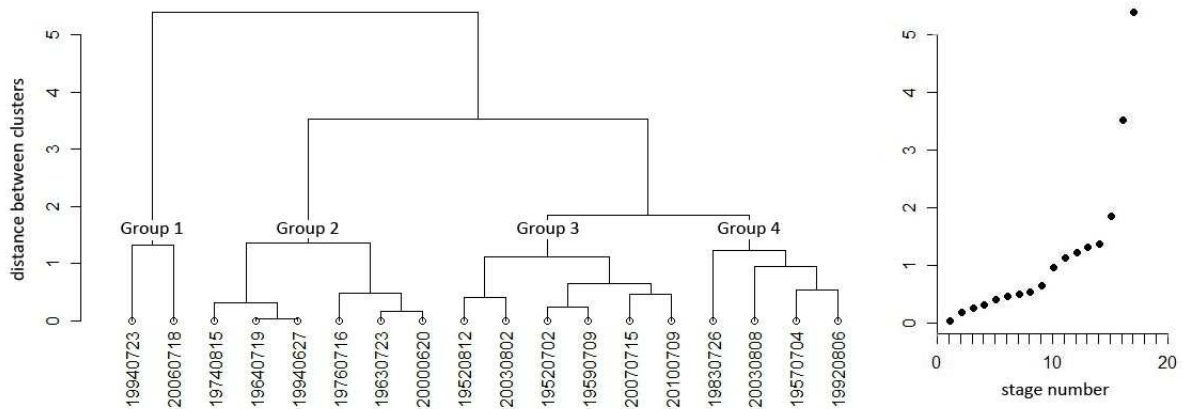


Figure 6.4. Dendrogram and the corresponding plot of the distances between merged heat wave clusters. Heat waves are labelled by the starting date in YYYYMMDD format.

Table 6.3. Mean characteristics of heat waves in individual clusters.

Cluster	Type	Number of HWs	$I_{hw}$	T	OA	D
1	widespread and long	2	26.5	7.2	1,733.1	13.0
2	weak	6	5.2	5.3	120.5	3.3
3	moderate	6	8.5	7.0	613.3	3.8
4	intense	4	10.1	8.0	733.4	4.0
Average of individual HWs:			9.7	6.6	581.9	4.7

$I_{hw}$  – heat wave extremity index [°C], T – temperature amplitude [°C], OA – overall spatial extent of the HW core [thousands km<sup>2</sup>], D – duration [days].

## 6.4 Cold spells

### 6.4.1 Characteristics and interannual variability

Using analogous definition to that for HDs, 201 CDs occurred over Central Europe during the 1950/51–2012/13 period (3.2 CDs/year on average). These days formed 24 CSs with total duration of 131 days. Although the number of CSs is considerably greater than the number of HWs (18), CSs occurred only in 14 individual seasons, which is fewer than in the case of HWs (15). This is related to larger interannual variability of winter temperatures and enhanced clustering tendency of CDs compared to HDs (the ratio between total duration of CSs and the total number of CDs was 0.65, which is substantially greater than in the case of HDs (0.45)). The list of observed CSs and their characteristics is given in Table 6.4.

Table 6.4. Major cold spells over Central Europe during 1950/51–2012/13.

Start	End	$I_{cs}$	T	A	OA	D
19540125	19540203	35.8	13.5	530.0	2,501.3	10
19540205	19540207	5.8	8.6	10.6	152.5	3
19540220	19540222	6.7	9.2	41.3	81.3	3
19560130	19560203	26.8	13.9	545.6	1,666.9	5
19560208	19560218	62.0	17.1	625.0	2,836.3	11
19560224	19560227	11.3	14.1	107.5	151.9	4
19611224	19611226	8.8	11.6	29.4	37.5	3
19621222	19621224	7.3	9.9	0.0	0.0	3
19630111	19630122	41.5	14.6	586.3	2,809.4	12
19630129	19630205	30.4	12.0	539.4	1,415.0	8
19630223	19630225	7.6	10.9	1.3	5.6	3
19680109	19680114	15.3	12.1	171.3	530.6	6
19691220	19691222	11.6	11.5	88.8	88.8	3
19710101	19710107	16.7	11.4	206.3	531.9	7
19790104	19790107	9.2	9.1	55.0	78.1	4
19850105	19850111	34.4	14.1	520.6	1,711.3	7
19850211	19850214	17.8	11.0	255.6	371.3	4
19860224	19860228	13.3	11.1	75.0	79.4	5
19870111	19870115	30.9	14.5	513.8	1,351.3	5
19870130	19870202	14.7	14.3	157.5	203.1	4
19961226	19970102	25.1	11.1	483.1	1,280.6	8
20060123	20060125	10.9	13.8	131.9	420.6	3
20120202	20120207	20.6	10.2	358.1	1,085.6	6
20120209	20120212	11.9	10.0	33.1	369.4	4
	Average:	19.9	12.1	252.8	823.3	5.5

$I_{cs}$  – cold spell extremity index [ $^{\circ}\text{C}$ ], T – temperature amplitude [ $^{\circ}\text{C}$ ], A – spatial extent of the CS core [thousands  $\text{km}^2$ ], OA – overall spatial extent of the CS core [thousands  $\text{km}^2$ ], D – duration [days]. Dates of CS start and end are in YYYYMMDD format. The spatial extent of the Central European domain is 625.0 thousands  $\text{km}^2$ .

By far the most severe CS (according to  $I_{cs}$ ) over Central Europe occurred in February 1956. In addition to its extreme  $I_{cs}$ , this event had the greatest temperature amplitude (17.1 $^{\circ}\text{C}$ ), its core affected the whole of Central Europe, and it persisted for 11 days. In general, CSs exhibited significantly (information about statistical testing is given in Section 6.2.6) greater values of extremity index and temperature amplitude compared to HWs. This issue is discussed in Section 6.5.1. On the contrary, the longest CS persisted for 12 days, which is 3 days less than the longest 1994 HW.

Interannual variability of CSs and CDs is shown in Figure 6.5. The greatest values of seasonal sums of  $I_{cs}$  were identified at the beginning of the examined period. The winters 1955/1956 and 1962/1963 were the most extreme ones. The recent winter 2011/2012 is

ranked as the 6th most pronounced according to the annual sum of  $I_{cs}$  over the 1950/51–2012/13 period. The greatest annual number of CDs occurred in 1962/1963 (29 days). It is noteworthy that this exceptional number of CDs (since 1962/63, in only one season did the number of CDs exceed 10) was not accompanied by the greatest sum of  $I_{cs}$ , mainly due to less pronounced temperature amplitude during the 1962/1963 CSs, compared to the 1955/1956 CSs. The 5 year running mean of CDs revealed their decrease in the mid-1970s and below-average number of cold days was also observed from the 1990s to the end of the examined period.

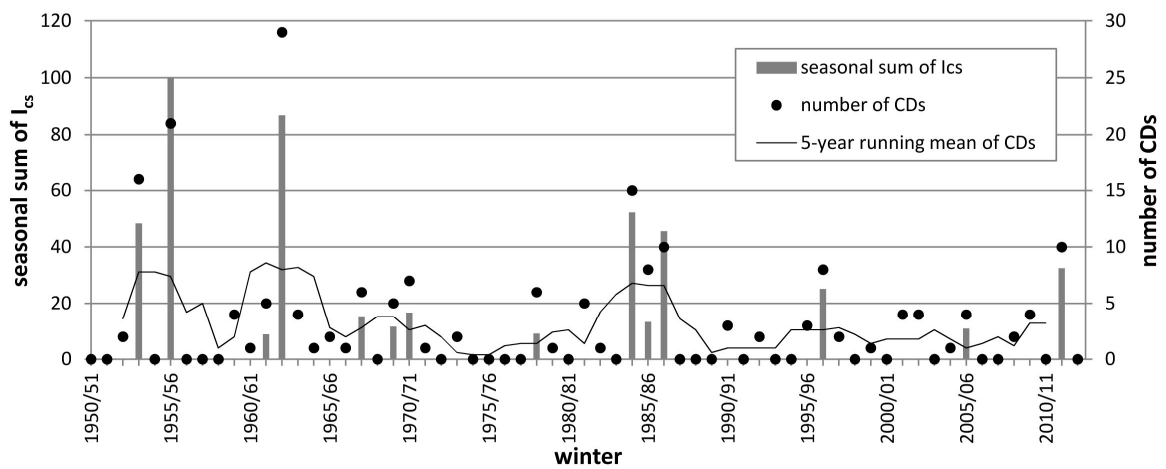
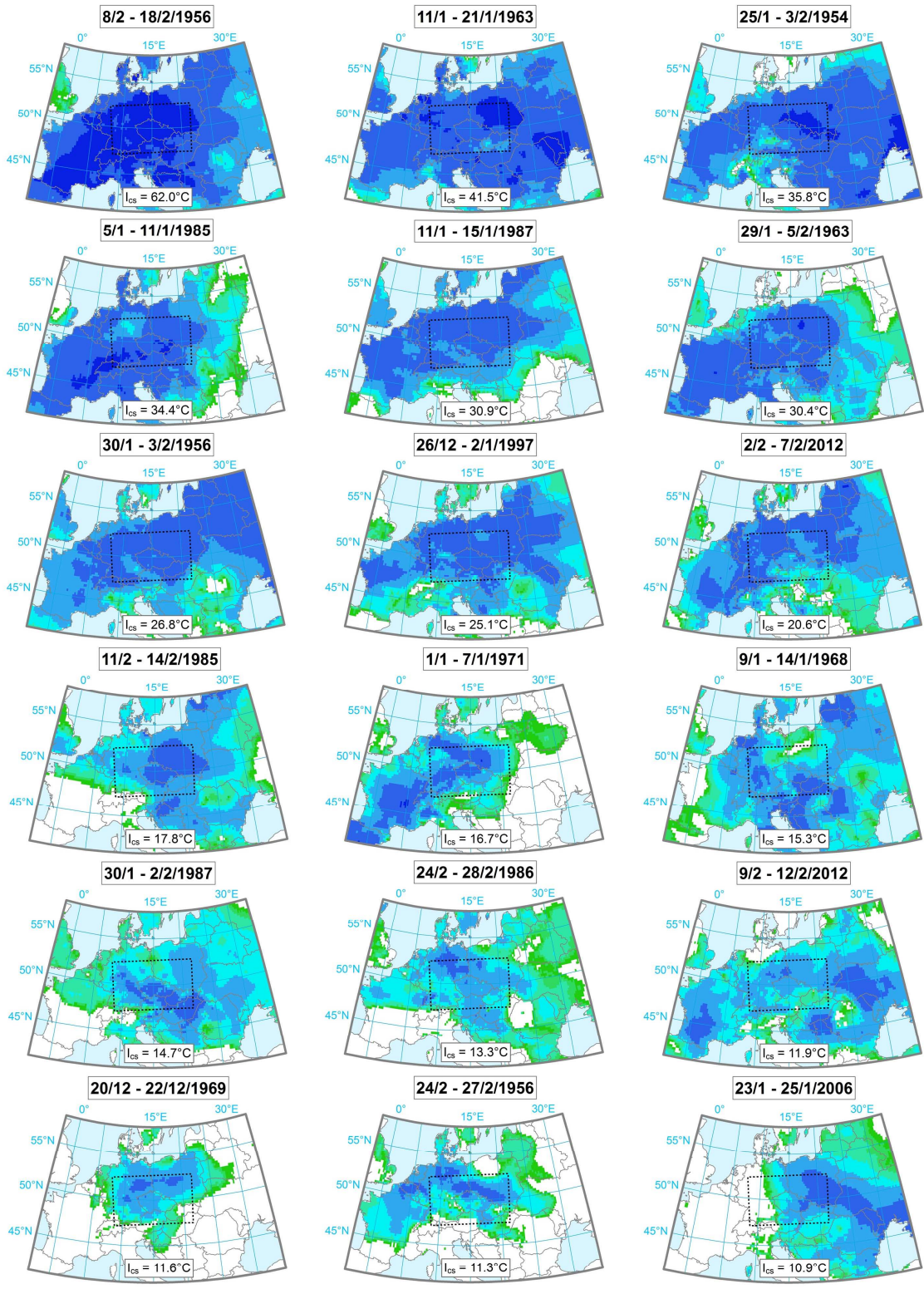


Figure 6.5. Interannual variability of cold spells (CSs) and cold days (CDs) over Central Europe during 1950/1951–2012/2013. Note the different scale of Y-axes compared to Figure 6.2.

The most-severe CS in February 1956 exhibited extreme cold anomalies (sum of temperature deviations below the 5% quantile of winter  $T_{min}$  distribution  $> 50^{\circ}C$ ) over a large area of France, Switzerland, Germany, Austria, the Czech Republic, and Poland (Figure 6.6). Extreme cold anomalies were much smaller during the following extraordinary cold spells.



Sum of temperature deviations below the 5% quantile of winter Tmin distribution [absolute values, °C]



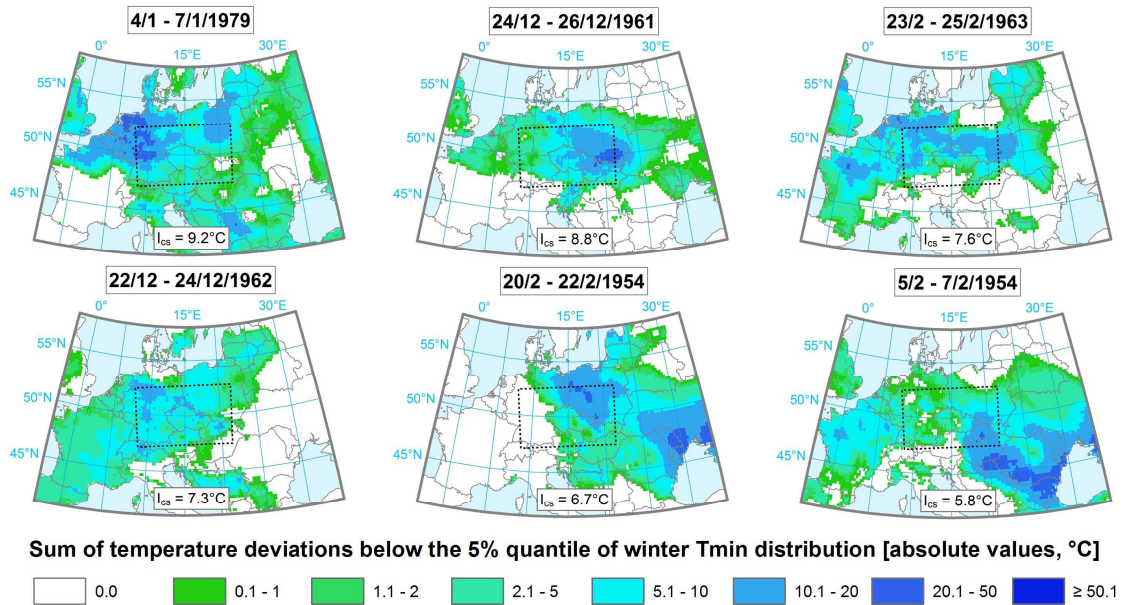


Figure 6.6. Cold spells over Central Europe during 1950/51–2012/13. The cold spells are ranked according to  $I_{cs}$  in descending order. Spatial patterns of absolute values of the sum of negative  $T_{min}$  deviations below the 5% quantile of winter  $T_{min}$  distribution are plotted.

#### 6.4.2 Cluster analysis

Based on the cluster analysis of temperature amplitude, overall spatial extent of the CS core and duration, CSs were also classified into 4 types (Figure 6.7).

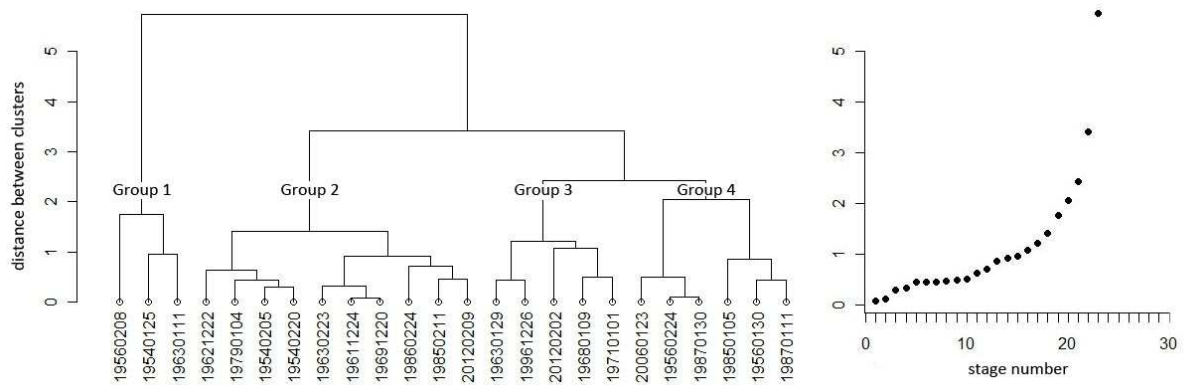


Figure 6.7. Dendrogram and corresponding plot of distances between merged cold spell clusters. Cold spells are labelled by the date of start in YYYYMMDD format.

Similarly to HWs, the first cluster contains CSs with very large overall spatial extent of their cores and long duration (the January 1954, February 1956 and January 1963 CSs). These CSs also exhibit the greatest values of  $I_{cs}$ . The second group associates relatively weak CSs



with low values of their characteristics. Long CSs with below average temperature amplitude are in the third cluster. The fourth category consists of intense CSs (high temperature amplitude) that had relatively short duration. CSs in the third and fourth clusters have similar mean extremity index and overall spatial extent of their cores, but they are clearly distinguished on the basis of temperature amplitude and duration (Table 6.5).

Table 6.5. Mean characteristics of cold spells in individual clusters.

Cluster	Type	Number of CSs	$I_{cs}$	T	OA	D
1	widespread and long	3	46.4	15.1	2,715.6	11.0
2	weak	10	10.0	10.3	126.4	3.5
3	not intense but long	5	21.6	11.4	968.8	7.0
4	intense but short	6	21.5	14.1	917.5	4.7
Average of individual CSs:			19.9	12.1	823.3	5.5

T – temperature amplitude [ $^{\circ}$ C], OA – overall spatial extent of the CS core [thousands  $km^2$ ], D – duration [days].

The final number of classes in the plot of the distances was not clear (suggesting a lower classificability of CSs), so we preserved the same number of classes as in the analysis of HWs. A reduction in the number of classes would result in merging the clearly distinguished third and fourth groups, while a greater number of classes would not provide any additional information.

## 6.5 Discussion

### 6.5.1 Comparison of characteristics of heat waves and cold spells

Despite using an analogous methodology when delimiting HWs and CSs, HWs exhibited significantly lower values of extremity index and temperature amplitude. This relates to the greater temperature variance in winter over Europe (e.g. Cattiaux et al. 2012) and the negatively-skewed winter  $T_{min}$  distribution (e.g. Toth and Szentimrey, 1989). Thus, the left tail of the winter  $T_{min}$  distribution has a greater potential for developing extreme temperatures than does the right tail of the summer  $T_{max}$  distribution. Due to this fact, we modified the threshold for calculating the spatial extent of the CS core. Preserving the original threshold ( $10^{\circ}$ C) would have resulted in too great values of this characteristic, encompassing most of Central Europe for the majority of CSs. The difference in mean duration between HWs and CSs was not statistically significant.

Although the number of HDs and CDs is almost equal, the total duration of CSs was considerably greater than in the case of HWs. This greater clustering tendency of CDs relates to higher persistence of  $T_{\min}$  in winter compared to  $T_{\max}$  in summer. This feature has been studied by, for example, by Kalvová and Nemešová (1998) and Huth et al. (2001), who showed higher autocorrelation of winter  $T_{\min}$  than of summer  $T_{\max}$  in Central Europe. In addition, this difference grew with increasing lag time. The concentration of CSs into a relatively small number of winters might also be caused by high wintertime interannual variability compared to that of summer (e.g. Giorgi et al. 2004).

### 6.5.2 Interannual variability of heat waves

The analysis of interannual variability of HWs shows that the summer of 1994 was more extreme over Central Europe than were the well-known 2003 and 2010 summers. The summer of 2010 was record-breaking on a continental scale (Barriopedro et al. 2011), and the exceptional severity of the 2003 heat waves in Western Europe has been reported by many authors (e.g. Beniston 2004; De Bono et al. 2004), while the summer of 1994 is not listed among the five most extreme European summers (Barriopedro et al. 2011). Our findings are consistent with those of Shevchenko et al. (2013), who showed that the 2010 HW was record-breaking only in the eastern part of Ukraine while the 1994 HW remained the most severe one over its western part. The exceptionality of the summer of 1994 in Central Europe was also documented by Kyselý (2010), who analysed heat waves using station data from the Czech Republic. This suggests that the ‘regional’ 1994 HW remains the most severe over certain parts of Central and Eastern Europe.

Enhanced severity of HWs in the 1950s and in the past two decades is in accordance with Della-Marta et al. (2007b), who analysed their temporal variability mainly over the western part of Europe. This temporal pattern is related to the Atlantic Multidecadal Oscillation that probably has a substantial impact on European summer temperatures (e.g. Sutton and Hodson 2005; Della Marta et al. 2007a).

The greatest temperature amplitude (8.4°C) observed in the 1983 HW was linked to the extremely warm southern advection with peak on 27 July. Maximum temperatures in the Czech Republic reached 40°C (Krška and Munzar 1984), having established an all time record temperature that held for almost 30 years. The new absolute temperature maximum for the Czech Republic (40.4°C) was measured on 20 August 2012 (Němec 2012), but it was not



a part of a HW due to low persistence of the extreme heat. During the 1983 HW, a record breaking maximum temperature (40.2°C) was measured also in Germany (DWD 2013).

### 6.5.3 Interannual variability of cold spells

Turning to CSs, the winters of 1955/1956 and 1962/1963 were the most extreme over Central Europe in the examined period. These two extreme winters occurred during the period with low values of the North Atlantic Oscillation index (Hurrell and Deser 2010). Cattiaux et al. (2010) regarded the winter of 1962/1963 as the coldest winter since 1949, but the winter of 1955/1956 was pronounced in their analysis as well. Our results are also in good agreement with Walsh and Phillips (2001), who analysed cold outbreaks in the United States and Europe. Because they had focused on the western and northern parts of Europe a direct comparison is not possible, but the identified very cold anomalies in the winters of 1955/1956 and 1962/1963 are listed among the most extreme ones in their study. Moreover, the greatest cold anomaly in January 1987 (according to Walsh and Phillips 2001), was also captured in our analysis as a severe CS.

Although record breaking cold spells and snowfalls were observed across Europe as well as the United States and East Asia during the winter of 2009/2010 (Cohen et al. 2010), no CS was present in our analysis from that season. This relates to the fact that the strongest cold anomaly was observed mainly in western and northern Europe (Cattiaux et al. 2010), while winter weather especially over the eastern part of Central Europe was milder.

## 6.6 Conclusions

The main findings of the study are as follows:

- We proposed a methodology for delimiting major heat waves (HWs) and cold spells (CSs) from gridded data that is based on the persistence of large regional temperature anomalies.
- An extremity index was introduced that reflects joint effects of spatial extent, temperature anomaly and duration of HWs and CSs in order to assess their severity. This index allows analogous characterization of HWs and CSs and, because it involves no 'local' settings, it may be applied also in other regions over the E-OBS domain and for other purposes.

- Using the E OBS gridded data set, we documented major Central European HWs and CSs and analysed their characteristics and interannual variability. These events were visualized in “event based” maps and classified according to their characteristics.
- The most severe HW in Central Europe since 1950 occurred in 1994, followed by the 2006 HW. The severity of HWs was considerably reduced during the 1960–1990 period.
- The cluster analysis revealed 4 types of HWs with different characteristics: those that are 1) spatially widespread and long, 2) weak, 3) moderate, and 4) intense.
- Although the most severe CSs over Central Europe occurred in the beginning of the examined period (during 1955/1956 and 1962/1963), we found the winter of 2011/2012 to be the 6th coldest since 1950/1951 according to the seasonal sum of the extremity index.
- CSs were classified analogously into 4 types with a structure similar to that of HWs: 1) spatially widespread and long, 2) weak, 3) not intense but long, and 4) intense but short. The number of CS types was less obvious and the differences between the types less clear than in the case of HWs.
- The clustering tendency of CDs was considerably greater than was the clustering tendency of HDs. Hence, in spite of the analogous definitions, the number of CSs was larger than the number of HWs. Nevertheless, the number of winter seasons with a CS was smaller than was the number of summer seasons with a HW.
- We established a list of major Central European HWs and CSs and their characteristics. This list can be regularly updated when a new version of the E-OBS data set is released and it might be utilized in further studies focusing on temperature extremes over Europe.

Due to its general definition, the extremity index may be used over different areas to perform comparative studies. The methodology can also be applied to climate model simulations; such analysis evaluating the performance of RCMs for the recent climate will contribute to better understanding RCMs’ strengths and biases in reproducing joint characteristics of the duration, magnitude, and spatial extent of temperature extremes. In addition, the extremity index and additional characteristics might be used to analyze projected changes in major HWs and CSs in a possible future climate.

## Acknowledgments

The authors are grateful to R. Huth for helpful comments on the cluster analysis. We acknowledge the E-OBS data set from the EU-FP6 project ENSEMBLES (<http://ensembles-eu.metoffice.com>). The study was supported by the Czech Science Foundation, project P209/10/2265; the Charles University Grant Agency, project 532313; and the Ministry of Education, project 7AMB12AR005.

## References

- AON (2012) February 2012 Global Catastrophe Recap.  
[http://thoughtleadership.aonbenfield.com/ThoughtLeadership/Documents/201202\\_if\\_monthly\\_cat\\_recap\\_february.pdf](http://thoughtleadership.aonbenfield.com/ThoughtLeadership/Documents/201202_if_monthly_cat_recap_february.pdf)
- Ballester J, Rodó X, Giorgi F (2010) Future changes in Central Europe heat waves expected to mostly follow summer mean warming. *Clim Dyn* 35:1191–1205. doi: 10.1007/s00382-009-0641-5
- Barnett AG, Hajat S, Gasparrini A, Rocklöv J (2012) Cold and heat waves in the United States. *Environ Res* 112:218–224. doi: 10.1016/j.envres.2011.12.010
- Barriopedro D, Fischer EM, Luterbacher J, et al (2011) The hot summer of 2010: redrawing the temperature record map of Europe. *Science* 332:220–224. doi: 10.1126/science.1201224
- Beniston M (2004) The 2003 heat wave in Europe: A shape of things to come? An analysis based on Swiss climatological data and model simulations. *Geophys Res Lett* 31:4. doi: 10.1029/2003GL018857
- Beniston M, Stephenson DB, Christensen OB, et al (2007) Future extreme events in European climate: an exploration of regional climate model projections. *Clim Change* 81:71–95. doi: 10.1007/s10584-006-9226-z
- Black E, Blackburn M, Harrison G, et al (2004) Factors contributing to the summer 2003 European heatwave. *Weather* 59:217–223. doi: 10.1256/wea.74.04
- Cassou C, Terray L, Phillips AS (2005) Tropical Atlantic Influence on European Heat Waves. *J Clim* 18:2805–2811.
- Cattiaux J, Vautard R, Cassou C, et al (2010) Winter 2010 in Europe: A cold extreme in a warming climate. *Geophys Res Lett* 37:L20704. doi: 10.1029/2010GL044613
- Cattiaux J, Yiou P, Vautard R (2012) Dynamics of future seasonal temperature trends and extremes in Europe: a multi-model analysis from CMIP3. *Clim Dyn* 38:1949–1964. doi: 10.1007/s00382-011-1211-1

- Cohen J, Foster J, Barlow M, et al (2010) Winter 2009-2010: A case study of an extreme Arctic Oscillation event. *Geophys Res Lett* 37:L17707. doi: 10.1029/2010GL044256
- Colombo AF, Etkin D, Karney BW (1999) Climate Variability and the Frequency of Extreme Temperature Events for Nine Sites across Canada : Implications for Power Usage. *J Clim* 12:2490–2502.
- De Bono A, Giuliani G, Kluser S, Peduzzi P (2004) Impacts of summer 2003 heat wave in Europe. *UNEP/DEWA/GRID-Europe Environ Alert Bull* 2:1–4.
- Della-Marta PM, Luterbacher J, Weissenfluh H, et al (2007a) Summer heat waves over western Europe 1880–2003, their relationship to large-scale forcings and predictability. *Clim Dyn* 29:251–275. doi: 10.1007/s00382-007-0233-1
- Della-Marta PM, Haylock MR, Luterbacher J, Wanner H (2007b) Doubled length of western European summer heat waves since 1880. *J Geophys Res* 112:D15103. doi: 10.1029/2007JD008510
- DWD (2013) Absolute Maximum Temperature in Germany.  
[http://www.dwd.de/bvbw/generator/DWDWWW/Content/Oeffentlichkeit/KU/KUPK/Wetterrekorde/absolute\\_\\_hoechsttemperaturen\\_\\_brd,templateId=raw,property=publicationFile.pdf/absolute\\_hoechsttemperaturen\\_brd.pdf](http://www.dwd.de/bvbw/generator/DWDWWW/Content/Oeffentlichkeit/KU/KUPK/Wetterrekorde/absolute__hoechsttemperaturen__brd,templateId=raw,property=publicationFile.pdf/absolute_hoechsttemperaturen_brd.pdf)
- Fischer EM, Seneviratne SI, Lüthi D, Schär C (2007) Contribution of land-atmosphere coupling to recent European summer heat waves. *Geophys Res Lett* 34:L06707. doi: 10.1029/2006GL029068
- Fischer EM, Schär C (2010) Consistent geographical patterns of changes in high-impact European heatwaves. *Nat Geosci* 3:398–403. doi: 10.1038/ngeo866
- Gershunov A, Cayan DR, Iacobellis SF (2009) The Great 2006 Heat Wave over California and Nevada: Signal of an Increasing Trend. *J Clim* 22:6181–6203. doi: 10.1175/2009JCLI2465.1
- Giorgi F, Bi X, Pal JS (2004) Mean, interannual variability and trends in a regional climate change experiment over Europe. I. Present-day climate (1961–1990). *Clim Dyn* 22:733–756. doi: 10.1007/s00382-004-0409-x
- Haylock MR, Hofstra N, Klein Tank AMG, et al (2008) A European daily high-resolution gridded data set of surface temperature and precipitation for 1950–2006. *J Geophys Res* 113:D20119. doi: 10.1029/2008JD010201
- Hollander M, Douglas AW (1999) *Nonparametric Statistical Methods*, 2nd edn. John Wiley & Sons, New York
- Hurrell JW, Deser C (2010) North Atlantic climate variability: The role of the North Atlantic Oscillation. *J Mar Syst* 79:231–244. doi: 10.1016/j.jmarsys.2009.11.002

- Huth R, Beck C, Philipp A, et al (2008) Classifications of atmospheric circulation patterns: recent advances and applications. *Ann N Y Acad Sci* 1146:105–152. doi: 10.1196/annals.1446.019
- Huth R, Kyselý J, Dubrovský M (2001) Time Structure of Observed, GCM-Simulated, Downscaled, and Stochastically Generated Daily Temperature Series. *J Clim* 14:4047–4061. doi: [http://dx.doi.org/10.1175/1520-0442\(2001\)014<4047:TSOOGS>2.0.CO;2](http://dx.doi.org/10.1175/1520-0442(2001)014<4047:TSOOGS>2.0.CO;2)
- Jaeger EB, Seneviratne SI (2011) Impact of soil moisture–atmosphere coupling on European climate extremes and trends in a regional climate model. *Clim Dyn* 36:1919–1939. doi: 10.1007/s00382-010-0780-8
- Kalvová J, Nemešová I (1998) Estimating Autocorrelations of Daily Extreme Temperatures in Observed and Simulated Climates. *Theor Appl Climatol* 164:151–164.
- Klein Tank AMG, Wijngaard JB, Können GP, et al (2002) Daily dataset of 20th-century surface air temperature and precipitation series for the European Climate Assessment. *Int J Climatol* 22:1441–1453. doi: 10.1002/joc.773
- Krška K, Munzar J (1984) Temperature peculiarities of the tropic summer 1983 in Czechoslovakia and in Europe. *Meteorol Zprávy* 37:33–40.
- Kyselý J (2002) Temporal fluctuations in heat waves at Prague-Klementinum, the Czech Republic, from 1901-97, and their relationships to atmospheric circulation. *Int J Climatol* 22:33–50. doi: 10.1002/joc.720
- Kyselý J (2010) Recent severe heat waves in central Europe : how to view them in a long-term prospect? *Int J Climatol* 109:89–109. doi: 10.1002/joc1874
- Kyselý J (2008) Influence of the persistence of circulation patterns on warm and cold temperature anomalies in Europe: Analysis over the 20th century. *Glob Planet Change* 62:147–163. doi: 10.1016/j.gloplacha.2008.01.003
- Kyselý J, Plavcová E (2010) A critical remark on the applicability of E-OBS European gridded temperature data set for validating control climate simulations. *J Geophys Res* 115:D23118. doi: 10.1029/2010JD014123
- L'Heureux M, Butler A, Jha B, et al (2010) Unusual extremes in the negative phase of the Arctic Oscillation during 2009. *Geophys Res Lett* 37:1–7. doi: 10.1029/2010GL043338
- Meehl G a, Tebaldi C (2004) More intense, more frequent, and longer lasting heat waves in the 21st century. *Science* 305:994–997. doi: 10.1126/science.1098704
- Meehl G, Arblaster J, Tebaldi C (2007) Contributions of natural and anthropogenic forcing to changes in temperature extremes over the United States. *Geophys Res Lett*. doi: 10.1029/2007GL030948
- Němec L (2012) The Czech temperature record in Dobřichovice on 20 August 2012. *Meteorol Zprávy* 65:145–148.

- Peings Y, Cattiaux J, Douville H (2013) Evaluation and response of winter cold spells over Western Europe in CMIP5 models. *Clim Dyn* 41:3025–3037. doi: 10.1007/s00382-012-1565-z
- Perkins SE, Alexander L V. (2013) On the Measurement of Heat Waves. *J Clim* 26:4500–4517. doi: 10.1175/JCLI-D-12-00383.1
- Plavcová E, Kyselý J (2012) Atmospheric circulation in regional climate models over Central Europe: links to surface air temperature and the influence of driving data. *Clim Dyn* 39:1681–1695. doi: 10.1007/s00382-011-1278-8
- Robine J-M, Cheung SLK, Le Roy S, et al (2008) Death toll exceeded 70,000 in Europe during the summer of 2003. *C R Biol* 331:171–178. doi: 10.1016/j.crv.2007.12.001
- Shevchenko O, Lee H, Snizhko S, Mayer H (2014) Long-term analysis of heat waves in Ukraine. *Int J Climatol* 34:1642–1650. doi: 10.1002/joc.3792
- Schneidereit A, Schubert S, Vargin P, et al (2012) Large-Scale Flow and the Long-Lasting Blocking High over Russia: Summer 2010. *Mon Weather Rev* 140:2967–2981. doi: 10.1175/MWR-D-11-00249.1
- Stefanon M, D’Andrea F, Drobinski P (2012) Heatwave classification over Europe and the Mediterranean region. *Environ Res Lett* 7:014023. doi: 10.1088/1748-9326/7/1/014023
- Stott PA, Stone DA, Allen MR (2004) Human contribution to the European heatwave of 2003. *Nature* 432:610–614. doi: 10.1029/2001JB001029
- Sutton RT, Hodson DLR (2005) Atlantic Ocean Forcing of North American and European Summer Climate. *Science* 309:115–118.
- Thompson DWJ, Wallace JM (1999) Annular Modes in the Extratropical Circulation. Part I: Month-to-Month Variability. *J Clim* 13:1000–1016.
- Toth Z, Szentimrey T (1989) The binormal distribution: A distribution for representing asymmetrical but normal-like weather elements. *J Clim* 3:128–136.
- Van der Linden P, Mitchell JFB (2009) ENSEMBLES: Climate Change and its Impacts: Summary of research and results from the ENSEMBLES project. Met Office Hadley Centre, Exeter
- Vavrus S, Walsh JE, Chapman WL, Portis D (2006) The behavior of extreme cold air outbreaks under greenhouse warming. *Int J Climatol* 26:1133–1147. doi: 10.1002/joc.1301
- Walsh J, Phillips A (2001) Extreme cold outbreaks in the United States and Europe, 1948-99. *J Clim* 14:2642–2658.
- Wilks DS (2011) *Statistical Methods in the Atmospheric Sciences*. Academic Press, Oxford

## 7 Article II: ‘Hot Central-European summer of 2013 in a long-term context’

Ondřej Lhotka<sup>a,b,c</sup> and Jan Kyselý<sup>a,b</sup>

<sup>a</sup> Institute of Atmospheric Physics, Academy of Sciences of the Czech Republic, Prague, Czech Republic

<sup>b</sup> Global Change Research Centre, Academy of Sciences of the Czech Republic, Brno, Czech Republic

<sup>c</sup> Faculty of Science, Charles University, Prague, Czech Republic

**Abstract:** The European summer of 2013 was characterized by very high temperatures that established a new historical maximum in Austria. The extremity of this summer in Europe is assessed based on the E-OBS and ECA&D data sets. At the continental scale, it is ranked as the fifth warmest summer since 1951, with large positive temperature anomalies over Central Europe. According to seasonal heat wave characteristics, the 2013 summer was unprecedented in Kremsmuenster and Graz (both Austria) and ranked as the second or third at other stations with at least 100 years of measurements in the Czech Republic, Slovakia, Croatia and Slovenia. The most intense 2013 heat wave over Central Europe in early August was driven primarily by anticyclonic conditions and was probably amplified by the preceding precipitation deficit. In combination with major flooding in the Danube and Elbe river basins in early June and severe convective storms at the end of July, the hot 2013 summer in Central Europe may represent an analog of a future summer climate that will probably be more prone to both temperature and precipitation extremes.

**Keywords:** summer of 2013; climate variability; temperature records; heat waves; effective precipitation; Central Europe

### 7.1 Introduction

In summer 2013, Europe experienced a series of heat waves that peaked on 8 August, when the highest historically recorded maximum temperature (40.5°C) was measured in Austria (ZAMG 2013). Such extreme events have substantial impacts on society and the natural environment, inasmuch as they cause excess illness and mortality, animal stress, crop failure, forest fires, spread of pests and increased energy demand for cooling (De Bono et al. 2004; Beniston et al. 2007).

The severity of European heat waves has increased over the past two decades (Della-Marta et al. 2007a; Kyselý 2010). Barriopedro et al. (2011) concluded that the European summer of 2010 was record-breaking for the 1500–2010 period, followed by the summers of 2003, 2002 and 2006. The 2010 heat wave had greatest impacts in Eastern Europe, while the

heat wave of 2003 was pronounced mainly in Western Europe (Fink et al. 2004). Beniston (2004) examined the 2003 heat wave and found it to represent an analog for the “shape of things to come” in the late 21<sup>st</sup> century climate. Nevertheless, the major heat wave of 1994 (Kysely 2002) remains the most severe one over large parts of Central and Eastern Europe (Lhotka and Kysely 2014; Shevchenko et al. 2014).

European heat waves are triggered mainly by interruption of the prevailing zonal flow. Pfahl and Wernli (2012) concluded that a substantial part of these extremes was driven by atmospheric blocking and related positive anomalies in the surface radiation budget and in a meridional warm advection. Due to the Arctic Amplification (Francis and Vavrus 2012), these blocking conditions are projected to occur more frequently and be prolonged in future climate, suggesting enhanced occurrence of European heat waves. Beside this, heat waves are expected to become more intense and longer lasting due to the shift of the summer temperature distribution (Ballester et al. 2011). The combination of these factors would probably result in more severe heat waves under global warming conditions (Fischer and Schär 2010), along with the increment of other extremes (IPCC 2012).

Another important factor for the development of heat waves is precipitation deficit. A lack of soil-moisture reduces the latent heat flux and results in an amplification of heat waves (Jaeger and Seneviratne, 2011). An important role of preceding dry soils in enhancing major European heat waves of 1976, 2003 and 2006 was shown by Fischer et al. (2007).

The aim of the present study is to assess the extremity of the 2013 summer in Europe. In the most affected Central European region, the severity of heat waves during this summer is evaluated based on long-term station data series. Finally, an analysis of preceding precipitation, mean sea level pressure, and 500 hPa geopotential height is performed in order to explore possible drivers of the most intense 2013 heat wave over Central Europe.

## **7.2 Data and methods**

The extremity of the 2013 summer is assessed over the European domain (Figure 7.1) using gridded daily mean and maximum temperatures. Southernmost regions and Iceland were excluded due to partially missing data. Temperature data was taken from the E-OBS 10.0 gridded data set (Haylock et al. 2008), which has a spatial resolution of 0.25° and covers the entire land area. European mean summer temperature ( $T_{JJA}$ ) was calculated as an average of all daily mean temperature ( $T_{\text{mean}}$ ) grid point values during the entire season, weighted by their respective areas. Summer was regarded as the period of June to August. High summer



temperatures were assessed through daily maximum temperature ( $T_{\max}$ ) excesses above the 90<sup>th</sup> percentile of summer  $T_{\max}$  distribution (calculated from the 1961–2000 period). These excesses in individual grid points were summed for every summer, and hereafter they are referred to as TS90. In order to assess interannual variability of TS90 on the European scale, this characteristic was averaged over continental grid points, weighted by their respective areas (mean TS90).

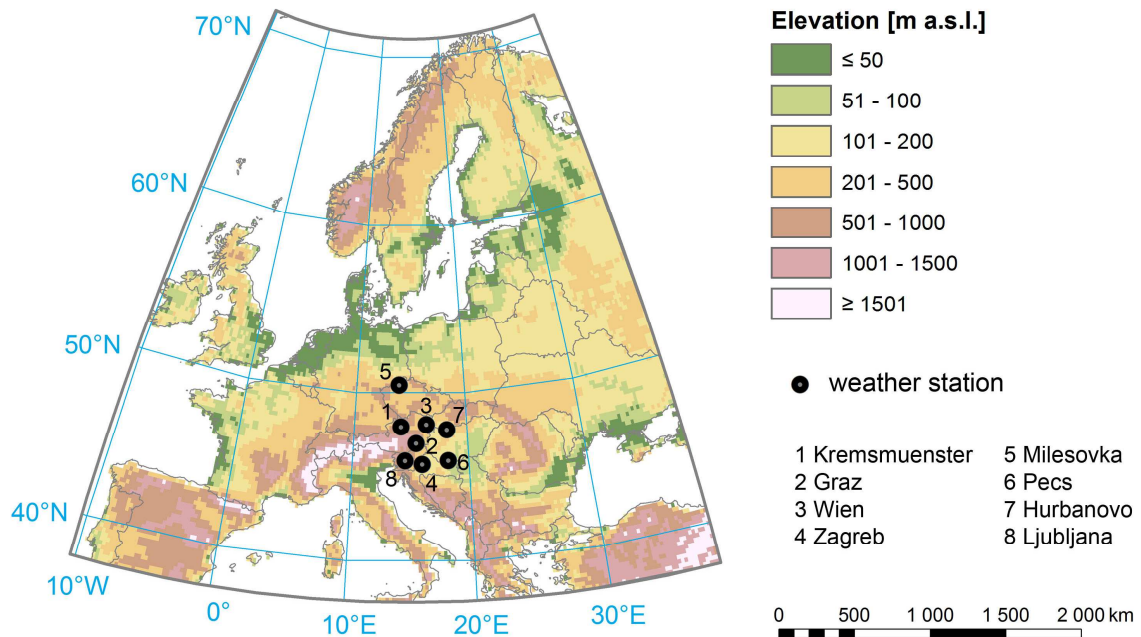


Figure 7.1. European domain, location of the weather stations included in the heat wave analysis and elevation model (GTOPO30) used in the E-OBS gridded data set.

In the Central European region (with largest temperature anomalies in the 2013 summer), the analysis of heat waves was performed using  $T_{\max}$  data from weather stations involved in the European Climate Assessment & Dataset (ECA&D) project (Klein Tank et al. 2002). We selected 8 stations with long-term temperature series (more than 100 years), listed in Table 7.1. No other long-term series involving 2013 is available within ECA&D in this area, including Poland and eastern Slovakia. Although the majority of the stations exhibits some inhomogeneities (Wijngaard et al. 2003), this data set still represents the best source of long-term station data over Central Europe and has been used in a variety of analyses (e.g. Beniston 2013; Simolo et al. 2014).

Table 7.1. Stations included in the heat wave analysis.

Id	Station	Country	Elevation [m a.s.l.]	Start	Missing years
1	Kremsmuenster	Austria	383	1876	
2	Graz	Austria	366	1894	1945
3	Wien	Austria	199	1876	
4	Zagreb	Croatia	157	1881	1886
5	Milesovka	Czech Republic	833	1906	1930–1935
6	Pecs	Hungary	203	1901	
7	Hurbanovo	Slovakia	115	1901	
8	Ljubljana	Slovenia	299	1900	1919–1922, 1925

The definition of a heat wave was based on excesses above the 90<sup>th</sup> percentile of summer  $T_{\max}$ . The minimum duration of a heat wave was set to 3 days, in accordance with the majority of studies (Meehl and Tebaldi 2004; Della-Marta et al. 2007b; Kyselý 2010). The severity of individual heat waves was measured using the sum of  $T_{\max}$  excesses above the 90<sup>th</sup> percentile, hereafter referred as HW90. Table 7.2 summarizes the abbreviations used.

Table 7.2. Description of abbreviations used.

Abbreviation	Data character	Variable	Definition
$T_{JJA}$	gridded	$T_{\text{mean}}$	European mean summer temperature
TS90	gridded	$T_{\max}$	summed daily excesses above the 90 <sup>th</sup> percentile of their distribution within individual grid points in summer
mean TS90	gridded	$T_{\max}$	same as TS90, but averaged over the European domain
HW90	station	$T_{\max}$	summed daily excesses above the 90 <sup>th</sup> percentile of their distribution during individual heat waves in summer

Precipitation data for a detailed analysis of the most intense 2013 heat wave was taken from the E-OBS data set (Haylock et al. 2008). Soil moisture conditions were assessed indirectly through effective precipitation (Byun and Wilhite 1999), calculated as the summed value of daily precipitation with a time-dependent reduction function:

$$\text{Effective precipitation} = \sum_{n=1}^i \left[ \left( \sum_{m=1}^n P_m \right) / n \right]$$

where  $P_m$  is precipitation  $m$  days before and  $i$  is the length of the period considered. We utilized the 3-month period prior to the August 2013 heat wave in order to capture also the Central European floods at the turn of May and June (Blöschl et al. 2013). However, effective precipitation is only little affected by the values at the beginning of the analysed period. Sea level pressure and 500 hPa geopotential height data was taken from the NCEP/NCAR reanalysis (Kalnay et al. 1996).

### **7.3 European mean and extreme summer temperatures**

The average of  $T_{JJA}$  for the 1961–2000 period was 16.9°C. No summer with negative  $T_{JJA}$  anomaly occurred after 1993 and the summers of 2003 and 2010 were markedly above the others, with positive  $T_{JJA}$  anomalies only slightly below +2.0°C. The coldest summer occurred in 1978 and had a negative  $T_{JJA}$  anomaly of –1.1°C. The 5-year running average showed an increase since the mid-1970s, with the greatest values at the end of the series. On the continental scale, the summer of 2013 was ranked as the 5<sup>th</sup> warmest European summer since 1951 (+1.4°C) and its  $T_{JJA}$  was comparable to those of the summers of 2002 and 2006 (Figure 7.2a).

The time series of the annual values of mean TS90 is shown in Figure 7.2b. This characteristic reflects occurrence of major heat waves rather than mean summer temperature. The summer of 2013 was less pronounced in this characteristic and thus it is characterized rather by an absence of cold periods than by occurrence of an extraordinary heat wave on the continental scale.

The relationship between  $T_{JJA}$  and mean TS90 is shown through a scatter plot in Figure 7.2c. Values in individual summers were fitted to a logarithmic trend line, which indicates that a relatively small increase in  $T_{JJA}$  is linked to a substantial increment in heat waves magnitude. A  $T_{JJA}$  increase of 1°C is associated with an approximate doubling of mean TS90.

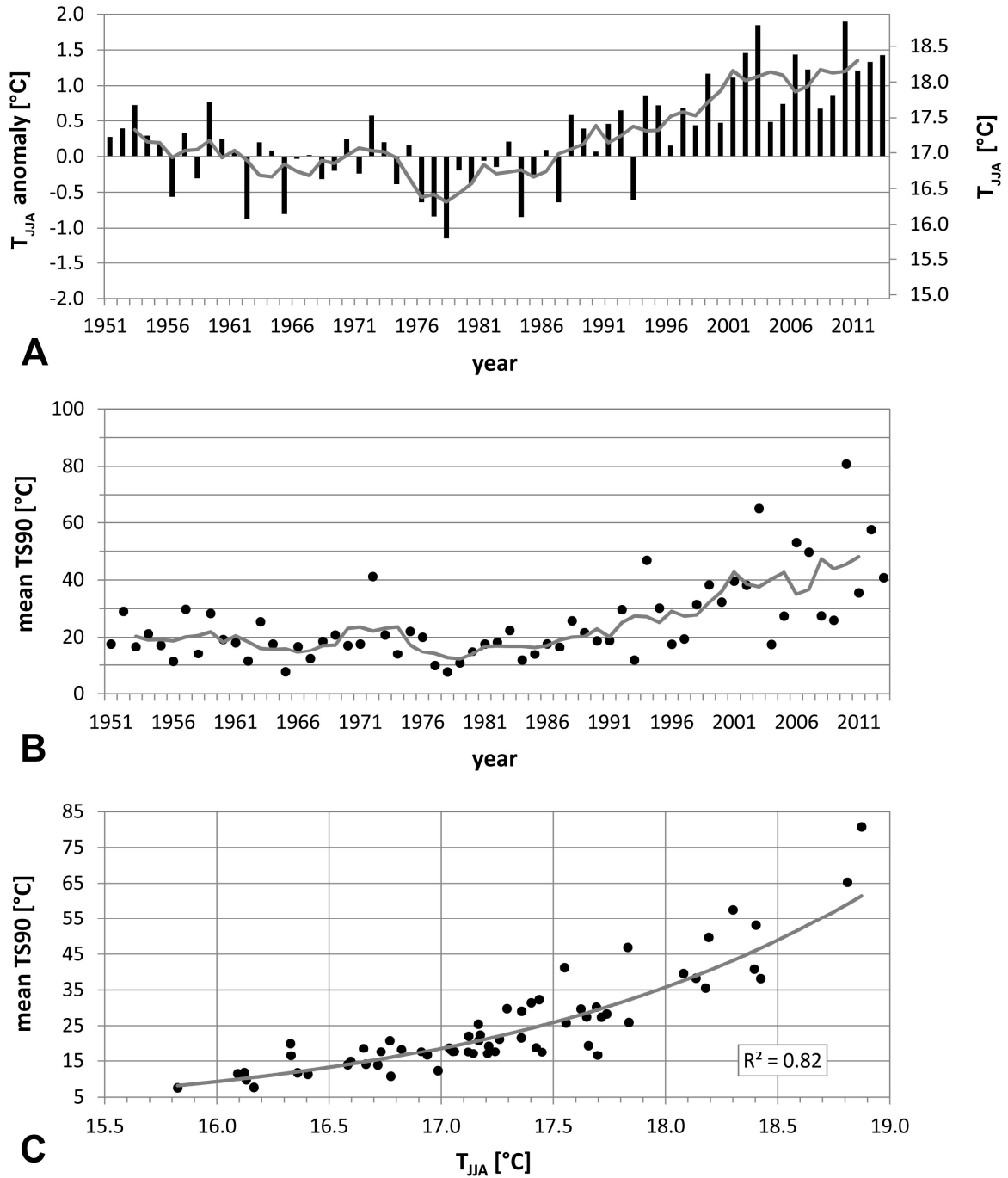


Figure 7.2. (A) European mean summer temperature for the 1951–2013 period and the 5-year running average. The  $T_{JJA}$  anomaly was calculated with respect to the 1961–2000 period. (B) Seasonal sums of positive daily  $T_{max}$  excesses above the 90<sup>th</sup> percentile of the summer  $T_{max}$  distribution averaged over continental Europe (mean TS90) and the 5-year running average. (C) Scatter plot of  $T_{JJA}$  and mean TS90 with a logarithmic trend line and a coefficient of determination ( $R^2$ ), indicating how well data fit a statistical model.

Figure 7.3 shows spatial patterns of seasonal TS90 for the 8 European summers with mean TS90 exceeding 40°C. In the most extreme summer of 2010, the greatest values of TS90 (regionally exceeding 200°C) were observed over a vast area in Eastern Europe. TS90 greater than 200°C also occurred in 2003 over Western Europe and in 2012 over the Balkan Peninsula, but the spatial extents in these cases were smaller than in 2010. In the summer of 2013, the greatest values of TS90 were located over Central Europe. Although these were less pronounced than, for example, the values for the 2010 summer in Eastern Europe, the summer of 2013 was one of the most extreme over the Central-European region. In this area, the severity of heat waves in 2013 was assessed based on long-term station series.

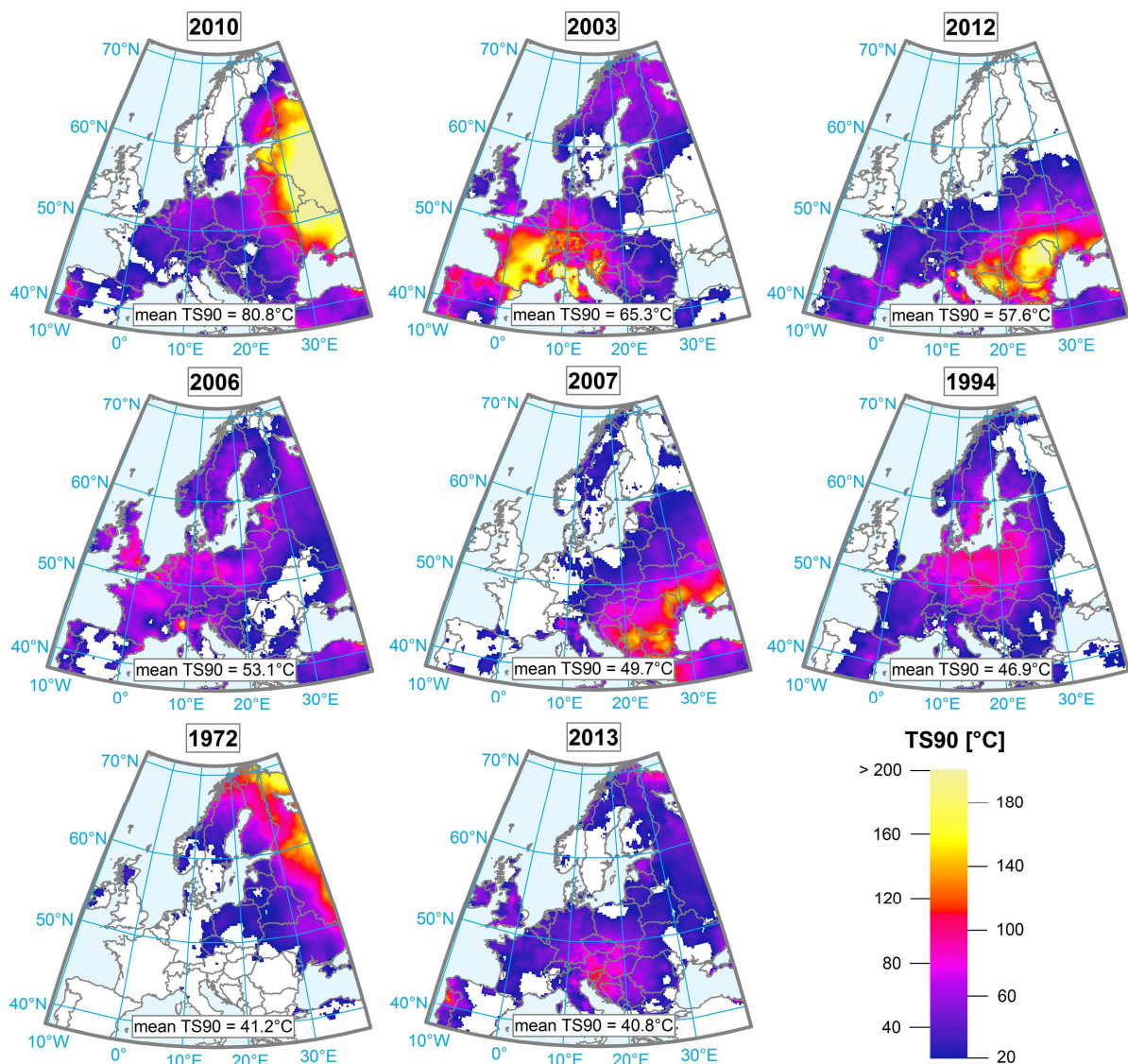


Figure 7.3. Spatial patterns of TS90 for 8 European summers with mean TS90 exceeding 40°C in Europe during 1951–2013. The areas with TS90 below 20°C are in white.

#### **7.4 Long-term variability of Central European heat waves**

We analysed 8 Central-European stations with long-term series of observed data to assess the severity of heat waves during the 2013 summer in a long-term context. Interannual variability of heat waves was calculated based on HW90 (Section 7.2).

The majority of stations showed the largest magnitude of heat waves in the past two decades (Figure 7.4). This maximum was preceded by considerable decrease of heat wave severity in the 1960s and 1970s. The stations located to the south had secondary maxima during the 1940s and 1950s, which were especially pronounced in Pecs where heat waves in the summers of 1946, 1950, and 1952 were the most severe for the entire period of observation. In Kremsmuenster, the secondary maximum was located at the end of the 19<sup>th</sup> century, but this phenomenon was not observed at the other stations with available data. This is discussed in more detail in Section 7.6.

In Kremsmuenster and Graz (Austria), the seasonal sum of HW90 in 2013 was largest for the entire period of observation. Heat waves were especially severe in Kremsmuenster, where the seasonal sum of HW90 in this summer was 125°C, while the second largest value since 1876 was only 74°C. At Miletovka (Czech Republic), Wien (Austria), Hurbanovo (Slovakia), Ljubljana (Slovenia), and Zagreb (Croatia), the seasonal sum of HW90 in 2013 was ranked as the second or the third largest one. The recent tendency to hot summers may also be illustrated by the fact that the seasonal sums of HW90 in the last two years of data (2012, 2013) were among the three highest values since the beginning of available data in Ljubljana, Zagreb and Hurbanovo. The extreme 2013 heat waves in Kremsmuenster are examined in detail in the next section.

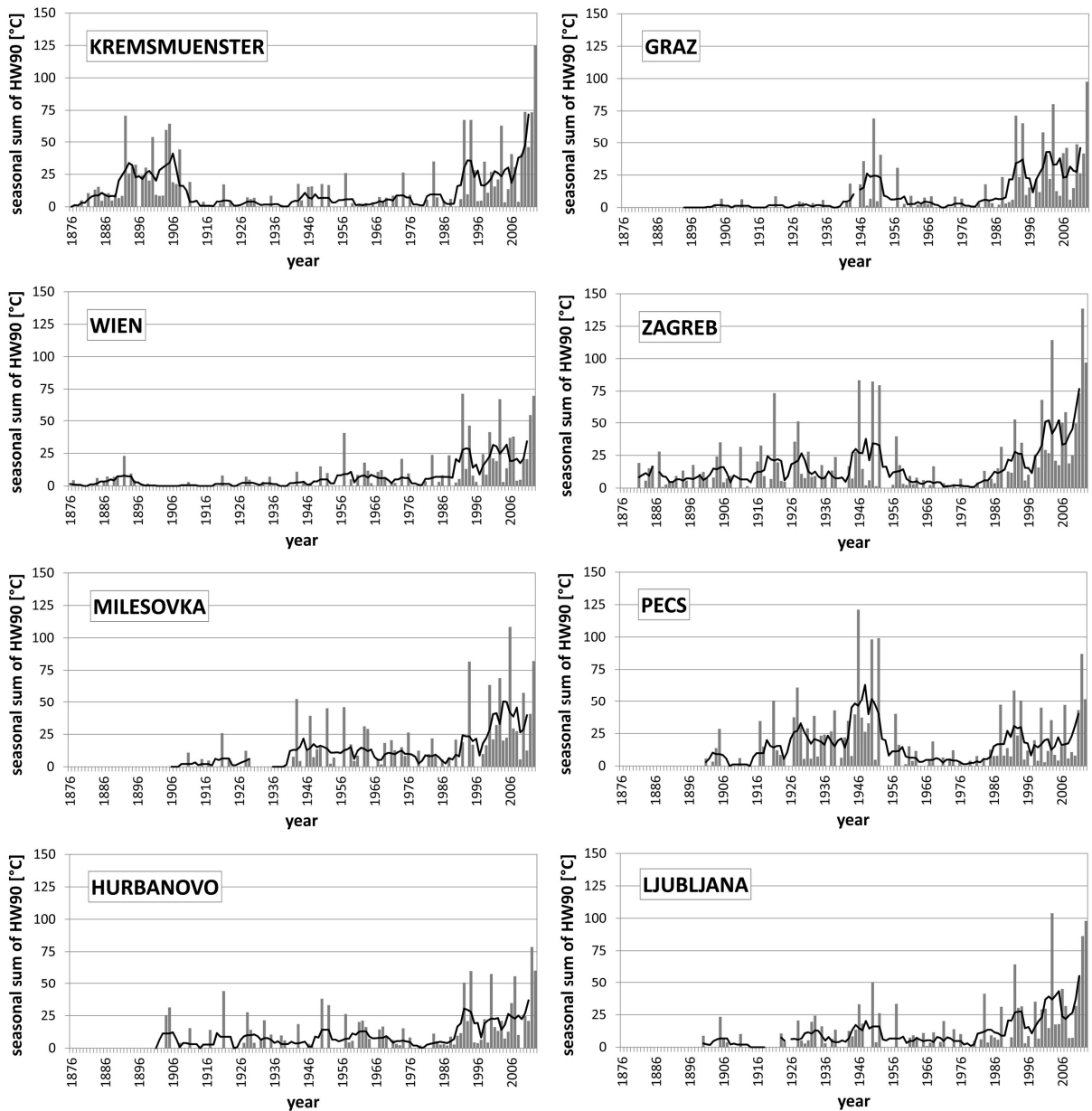


Figure 7.4. Long-term variability of heat waves at 8 Central-European stations. The grey bars indicate seasonal sums of HW90. Black line represents the 5-year running average, and its interruption denotes missing data.

### 7.5 Description of the 2013 heat waves and driving mechanisms

During the summer of 2013, 3 heat waves with total duration of 27 days occurred in Kremsmuenster. The most intense was the heat wave between 1 and 8 August that had the mean daily excess above the 90<sup>th</sup> percentile of summer  $T_{\max}$  distribution of 6.0°C (Figure 7.5). The record-breaking maximum temperature for Austria (40.5°C) occurred during this event and was measured in Bad Deutsch-Altenburg on 8 August. The 90<sup>th</sup> percentile of summer

$T_{\max}$  distribution was exceeded in 6 more days during 2013, but these days did not meet the minimum length criterion for heat waves.

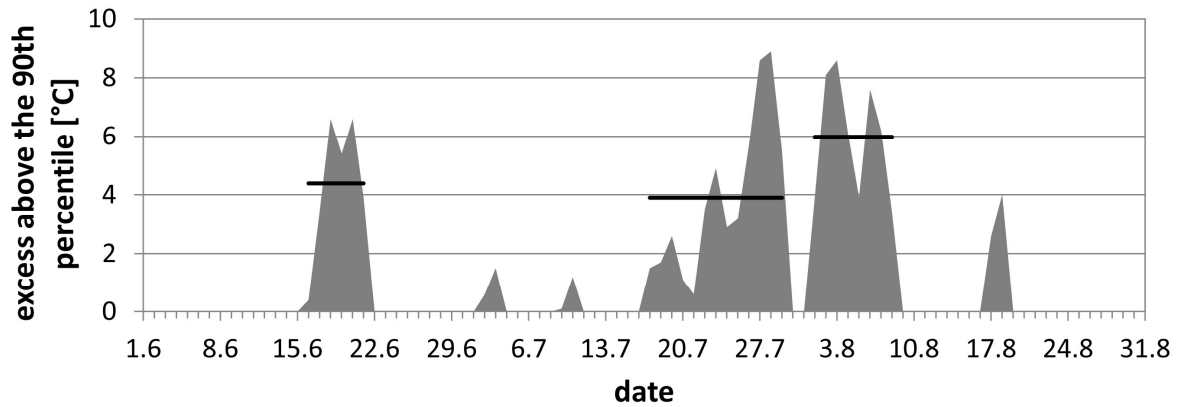


Figure 7.5.  $T_{\max}$  excesses above the 90<sup>th</sup> percentile of the summer  $T_{\max}$  distribution in Kremsmuenster during the summer of 2013. Horizontal black lines indicate the mean daily values of the  $T_{\max}$  excesses during the heat waves that have been detected in this summer.

A more detailed analysis of the most intense August 2013 heat wave was made in order to reveal the driving factors of this event. The greatest average of  $T_{\max}$  anomalies from their mean value during the heat wave was located in southern regions of Central Europe. These anomalies reached nearly 10°C in Austria and Slovenia and anomalies exceeding 5°C were observed over large parts of Central Europe. Temperatures were close to the long-term mean for this period of year in the rest of Europe (Figure 7.6a).

The spatial pattern of the effective precipitation anomaly at onset of the heat wave (Figure 7.6b) showed drier conditions in the area of large temperature anomalies. In this region, the lowest values of the effective precipitation were only about 25% of their mean values for this period of the year, thus indicating a soil-moisture deficit that might have led to an amplification of the heat wave. However, this deficit was not so pronounced on the continental scale, since some areas (e.g. the Iberian Peninsula or south-eastern Ukraine) had even greater precipitation deficits. By contrast, a precipitation surplus was observed over north-western Europe.

A large high-pressure area over Central Europe extending from the Mediterranean is found in the composite map of sea level pressure for the August 2013 heat wave period (Figure 7.6c). This circulation pattern together with a low-pressure system located over the British Isles controlled an advection of warm air masses into Central Europe. The area of high



pressure was centred over Austria, and this supported clear-sky conditions and related positive anomalies in the surface radiation budget. The high-pressure ridge is also evident from the composite map of the 500 hPa geopotential height (Figure 7.6d).

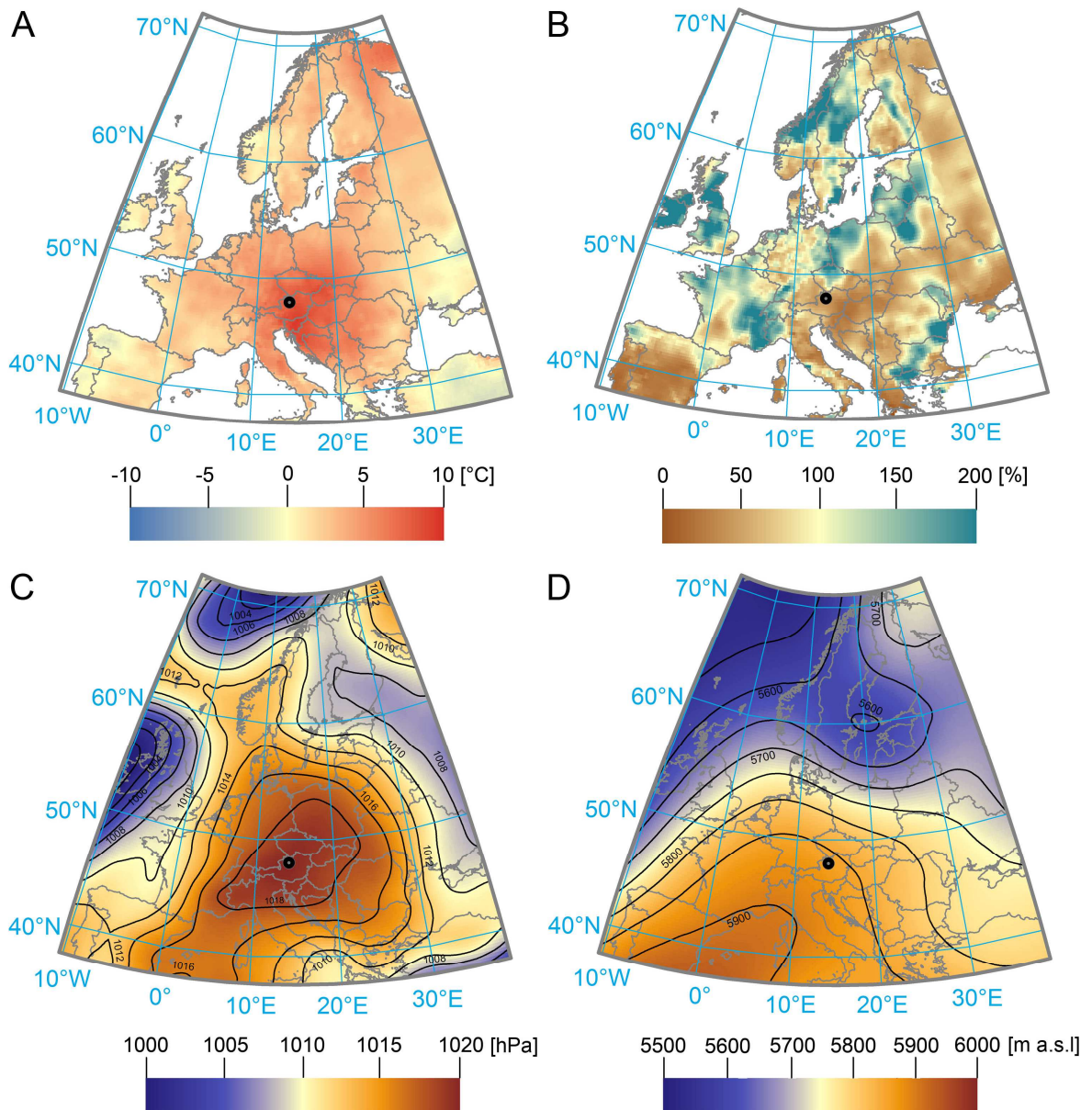


Figure 7.6. A) Average  $T_{\max}$  anomalies for 1–8 August 2013 relative to its mean value for this period of year. B) Effective precipitation for 1 May – 31 July 2013 relative to its mean value for this period of year. C) Mean sea level pressure for 1–8 August 2013. D) Mean 500 hPa geopotential height for 1–8 August 2013. The mean values were calculated over the 1961–2000 period. The black dot represents the Kremsmuenster station.

## 7.6 Discussion and conclusions

As concluded by Hartmann et al. (2013), it is certain that global mean surface temperature has increased since the late 19th century. Moreover, according to paleoclimatic reconstructions, the past two decades were warmest since 1500 (Popa and Kern 2009; Luterbacher et al. 2004). The record-breaking European summer of 2010 (Barriopedro et al. 2011) remained the warmest on the continental scale, but the summer of 2013 was more severe in certain regions over Central Europe.

In relation to the shift of the European summer mean temperature distribution and to the increase of its variability (Schär et al. 2004), heat waves have become more frequent and severe in the past two decades. According to seasonal heat wave characteristics, the 2013 summer was the most severe on record at 2 out of the 8 stations in Central Europe, and ranked second or third at 5 other stations with long-term data. By contrast, the greatest severity of heat waves in Pecs was observed in the mid-20<sup>th</sup> century. A similar pattern was reported by Kysely (2002) for Basel (Switzerland), thus indicating that this feature may be typical for more southerly stations.

The enhanced severity of heat waves in Kremsmuenster at the end of the 19<sup>th</sup> century does not correspond to other long-term analyses of heat waves (Della-Marta et al. 2007a; Kysely 2010). The so-called early instrumental warm-bias was identified at this station, which affected temperature measurements at least until 1870 (Böhm et al. 2010). Inhomogeneities in long-term European data sets were identified also at other locations (Wijngaard et al. 2003; Winkler 2009; Brunet et al. 2011) and some stations are influenced by an urban heat island. However, its effect is relatively small on summer  $T_{\max}$  (Wilby 2003). The greatest severity of the recent heat waves is evident at the majority of examined locations, including stations on a mountain summit (Milesovka) and in small towns (Hurbanovo, Kremsmuenster), and thus is quite robust.

The mean sea level pressure field during the August 2013 heat wave over Central Europe corresponds to the second canonical correlation analysis mode between sea level pressure and the heat wave index (Della-Marta et al. 2007b). A similar anticyclonic circulation pattern over Central Europe was also found conducive to heat waves by Kysely (2008). The effective precipitation anomaly at the onset of the heat wave reveals a soil-moisture deficit in the area of pronounced temperature anomalies. This is in accordance with previous studies showing that the majority of European heat waves were preceded by a precipitation deficit (Fink et al. 2004; Fischer et al. 2007). By contrast, the substantial precipitation deficit over the Iberian

Peninsula was not associated with a heat wave, probably due to a westerly advection and more cyclonic conditions. The precipitation surplus over north-western Europe (including north-western parts of Central Europe) was probably linked to intense mesoscale convective systems that hit France, the United Kingdom and Germany at the end of July. These thunderstorms and associated hailstorms were related to the so-called “Spanish Plume” (Holley et al. 2014) and caused record-breaking economic losses (in billions of euro) across Germany (Kreibich et al. 2014).

In general, the early-August 2013 heat wave exhibited both favourable synoptic conditions and a lack of preceding rainfall over most of Central Europe that probably had an amplifying effect on the heat wave’s magnitude. In combination with major flooding in the Danube and Elbe river basins during early June (Blöschl et al. 2013) and severe convective storms at the end of July, the 2013 summer may indeed represent “a shape of things to come” for future summer climate – a climate probably more prone to both temperature and precipitation extremes.

### **Acknowledgments**

We acknowledge the E-OBS dataset from the EU-FP6 project ENSEMBLES (<http://ensembles-eu.metoffice.com>), the data providers in the ECA&D project (<http://www.ecad.eu>), and NCEP Reanalysis data provided by the NOAA/OAR/ESRL PSD. The study was supported by the Czech Science Foundation, project P209/10/2265.

### **References**

- Ballester J, Rodó X, Giorgi F (2010) Future changes in Central Europe heat waves expected to mostly follow summer mean warming. *Clim Dyn* 35:1191–1205. doi: 10.1007/s00382-009-0641-5
- Barriopedro D, Fischer EM, Luterbacher J, et al (2011) The hot summer of 2010: redrawing the temperature record map of Europe. *Science* 332:220–224. doi: 10.1126/science.1201224
- Beniston M (2004) The 2003 heat wave in Europe: A shape of things to come? An analysis based on Swiss climatological data and model simulations. *Geophys Res Lett* 31:4. doi: 10.1029/2003GL018857
- Beniston M (2013) Exploring the behaviour of atmospheric temperatures under dry conditions in Europe: evolution since the mid-20th century and projections for the end of the 21st century. *Int J Climatol* 33:457–462. doi: 10.1002/joc.3436

- Beniston M, Goyette S (2007) Changes in variability and persistence of climate in Switzerland: Exploring 20th century observations and 21st century simulations. *Glob Planet Change* 57:1–15. doi: 10.1016/j.gloplacha.2006.11.004
- Blöschl G, Nester T, Komma J, et al (2013) The June 2013 flood in the Upper Danube Basin, and comparisons with the 2002, 1954 and 1899 floods. *Hydrol Earth Syst Sci* 17:5197–5212. doi: 10.5194/hess-17-5197-2013
- Böhm R, Jones PD, Hiebl J, et al (2010) The early instrumental warm-bias: a solution for long central European temperature series 1760–2007. *Clim Change* 101:41–67. doi: 10.1007/s10584-009-9649-4
- Brunet M, Asin J, Sigró J, et al (2011) The minimization of the screen bias from ancient Western Mediterranean air temperature records: an exploratory statistical analysis. *Int J Climatol* 31:1879–1895.
- Byun H-R, Wilhite DA (1999) Objective Quantification of Drought Severity and Duration. *J Clim* 12:2747–2757.
- De Bono A, Giuliani G, Kluser S, Peduzzi P (2004) Impacts of summer 2003 heat wave in Europe. *UNEP/DEWA/GRID-Europe Environ Alert Bull* 2:1–4.
- Della-Marta PM, Haylock MR, Luterbacher J, Wanner H (2007a) Doubled length of western European summer heat waves since 1880. *J Geophys Res* 112:D15103. doi: 10.1029/2007JD008510
- Della-Marta PM, Luterbacher J, Weissenfluh H, et al (2007b) Summer heat waves over western Europe 1880–2003, their relationship to large-scale forcings and predictability. *Clim Dyn* 29:251–275. doi: 10.1007/s00382-007-0233-1
- Fink AH, Brücher T, Krüger A, et al (2004) The 2003 European summer heatwaves and drought - synoptic diagnosis and impacts. *Weather* 59:209–216. doi: 10.1256/wea.73.04
- Fischer EM, Seneviratne SI, Lüthi D, Schär C (2007) Contribution of land-atmosphere coupling to recent European summer heat waves. *Geophys Res Lett* 34:L06707. doi: 10.1029/2006GL029068
- Fischer EM, Schär C (2010) Consistent geographical patterns of changes in high-impact European heatwaves. *Nat Geosci* 3:398–403. doi: 10.1038/ngeo866
- Francis JA, Vavrus SJ (2012) Evidence linking Arctic amplification to extreme weather in mid-latitudes. *Geophys Res Lett* 39:L06801. doi: 10.1029/2012GL051000
- Hartmann DL, Klein Tank AMG, Rusticucci M (2013) Observations: Atmosphere and Surface. In: *Climate Change 2013: The Physical Science Basis. Contribution of Working Group I to the Fifth Assessment Report of the Intergovernmental Panel on Climate Change*. Cambridge University Press, Cambridge, United Kingdom and New York, NY, USA, pp 161–218

- Haylock MR, Hofstra N, Klein Tank AMG, et al (2008) A European daily high-resolution gridded data set of surface temperature and precipitation for 1950–2006. *J Geophys Res* 113:D20119. doi: 10.1029/2008JD010201
- Holley DM, Dorling SR, Steele CJ, Earl N (2014) A climatology of convective available potential energy in Great Britain. *Int J Climatol*. doi: 10.1002/joc.3976
- IPPC (2012) *Managing the Risks of Extreme Events and Disasters to Advance Climate Change Adaptation. A Special Report of Working Groups I and II of the Intergovernmental Panel on Climate Change*. Cambridge University Press, Cambridge, United Kingdom and New York, NY, USA
- Jaeger EB, Seneviratne SI (2011) Impact of soil moisture–atmosphere coupling on European climate extremes and trends in a regional climate model. *Clim Dyn* 36:1919–1939. doi: 10.1007/s00382-010-0780-8
- Kalnay E, Kanamitsu M, Kistler R, et al (1996) The NCEP/NCAR 40-year reanalysis project. *Bull Am Meteorol Soc* 77:437–471.
- Klein Tank AMG, Wijngaard JB, Können GP, et al (2002) Daily dataset of 20th-century surface air temperature and precipitation series for the European Climate Assessment. *Int J Climatol* 22:1441–1453. doi: 10.1002/joc.773
- Kreibich H, Bubeck P, Kunz M, et al (2014) A review of multiple natural hazards and risks in Germany. *Nat Hazards*. doi: 10.1007/s11069-014-1265-6
- Kyselý J (2002) Temporal fluctuations in heat waves at Prague-Klementinum, the Czech Republic, from 1901–97, and their relationships to atmospheric circulation. *Int J Climatol* 22:33–50. doi: 10.1002/joc.720
- Kyselý J (2010) Recent severe heat waves in central Europe : how to view them in a long-term prospect? *Int J Climatol* 109:89–109. doi: 10.1002/joc.1874
- Kyselý J (2008) Influence of the persistence of circulation patterns on warm and cold temperature anomalies in Europe: Analysis over the 20th century. *Glob Planet Change* 62:147–163. doi: 10.1016/j.gloplacha.2008.01.003
- Lhotka O, Kyselý J (2014) Characterizing joint effects of spatial extent, temperature magnitude and duration of heat waves and cold spells over Central Europe. *Int J Climatol*. doi: 10.1002/joc.4050
- Luterbacher J, Dietrich D, Xoplaki E, et al (2004) European Seasonal and Annual Temperature Variability, Trends and Extremes Since 1500. *Science* 303:1499–1503.
- Meehl GA, Tebaldi C (2004) More intense, more frequent, and longer lasting heat waves in the 21st century. *Science* 305:994–997. doi: 10.1126/science.1098704
- Pfahl S, Wernli H (2012) Quantifying the relevance of atmospheric blocking for co-located temperature extremes in the Northern Hemisphere on (sub-)daily time scales. *Geophys Res Lett* 39:L12807. doi: 10.1029/2012GL052261

- Popa I, Kern Z (2008) Long-term summer temperature reconstruction inferred from tree-ring records from the Eastern Carpathians. *Clim Dyn* 32:1107–1117. doi: 10.1007/s00382-008-0439-x
- Shevchenko O, Lee H, Snizhko S, Mayer H (2014) Long-term analysis of heat waves in Ukraine. *Int J Climatol* 34:1642–1650. doi: 10.1002/joc.3792
- Schär C, Vidale PL, Lüthi D, et al (2004) The role of increasing temperature variability in European summer heatwaves. *Nature* 427:332–336. doi: 10.1038/nature02230.1.
- Simolo C, Brunetti M, Maugeri M, Nanni T (2014) Increasingly warm summers in the Euro–Mediterranean zone: mean temperatures and extremes. *Reg Environ Chang* 14:1825–1832. doi: 10.1007/s10113-012-0373-7
- Wijngaard JB, Klein Tank a. MG, Konnen GP (2003) Homogeneity of 20th century European daily temperature and precipitation series. *Int J Climatol* 23:679–692. doi: 10.1002/joc.906
- Wilby RL (2003) Past and projected trends in London’s urban heat island. *Weather* 58:251–260.
- Winkler P (2009) Revision and necessary correction of the long-term temperature series of Hohenpeissenberg, 1781–2006. *Theor Appl Climatol* 98:259–268. doi: 10.1007/s00704-009-0108-y
- ZAMG (2013) New temperature record: 40.5° C in Bad Deutsch-Altenburg. <http://www.zamg.ac.at/cms/de/klima/news/neuer-hitze-rekord-40-5deg-c-in-bad-deutsch-altenburg>. Accessed 16 Jan 2014

# 8 Article III: ‘Spatial and temporal characteristics of heat waves over Central Europe in an ensemble of regional climate model simulations’

Ondřej Lhotka<sup>a,b</sup> and Jan Kyselý<sup>a</sup>

<sup>a</sup> Institute of Atmospheric Physics, Academy of Sciences of the Czech Republic, Prague, Czech Republic

<sup>b</sup> Faculty of Science, Charles University, Prague, Czech Republic

**Abstract:** The study examines the capability of regional climate models (RCMs) to reproduce spatial and temporal characteristics of severe Central European heat waves. We analysed an ensemble of 7 RCM simulations driven by the ERA-40 reanalysis over the 1961–2000 period, in comparison to observed data from the E-OBS gridded dataset. Heat waves were defined based on regionally significant excesses above the model-specific 95% quantile of summer daily maximum air temperature distribution and their severity was described using the extremity index. The multi-model mean reflected the observed characteristics of heat waves quite well, but considerable differences were found among the individual RCMs. The RCMs had a tendency to simulate too many heat waves that were shorter but their temperature peak was more pronounced on average compared to E-OBS. Deficiencies were found also in reproducing interannual and interdecadal variability of heat waves. Using as an example the most severe Central European heat wave that occurred in 1994, we demonstrate that its magnitude was underestimated in all RCMs and that this bias was linked to overestimation of precipitation during and before the heat wave. By contrast, a simulated precipitation deficit during summer 1967 in the majority of RCMs contributed to an ‘erroneous’ heat wave. This shows that land–atmosphere coupling is crucial for developing severe heat waves and its proper reproduction in climate models is essential for obtaining credible scenarios of future heat waves.

**Keywords:** heat waves; regional climate models; land–atmosphere coupling; spatial characteristics; interannual variability; ENSEMBLES project

## 8.1 Introduction

Heat waves (periods of extremely high air temperature in summer) are important phenomena of the European climate. Extraordinary heat waves that were observed in the past two decades, mainly the extreme 2003 heat wave in France (Black et al. 2004) and the extraordinarily hot summer of 2010 in Russia (Schneider et al. 2012), have attracted much interest in the climatological community. Heat waves have major impacts on terrestrial ecosystems, water resources, forestry, agriculture, the power industry and human health (e.g. De Bono et al. 2004; Beniston et al. 2007; Barriopedro et al. 2011). Due to the expected rise in global mean air temperature (IPCC 2013) and projected strengthening of atmospheric

blocking over the Euro-Atlantic region due to Arctic Amplification (Francis and Vavrus 2012), there are concerns that the losses caused by heat waves will be increasing. Meehl and Tebaldi (2004) and Seneviratne et al. (2012) analysed outputs of global climate models (GCMs) to demonstrate that heat waves will become more frequent and intense in a future climate. In addition, Fischer and Schär (2010) emphasized that the most pronounced changes would occur in low-altitude river basins affecting many densely populated urban centres. To verify the credibility of these projections, model outputs for recent climate must be evaluated against observed data.

The evaluation of modelled daily maximum temperature in summer ( $T_{\max}$ ) over Europe was performed by many authors. Kjellström et al. (2007) examined  $T_{\max}$  from several regional climate models (RCMs) from the PRUDENCE project (Christensen and Christensen 2007). The RCMs (driven by the HadGEM GCM) generally tend to underestimate  $T_{\max}$  in Scandinavia and the British Isles while they overestimate  $T_{\max}$  in Southern and Eastern Europe. This bias was larger in the tails of the  $T_{\max}$  distribution. A similar  $T_{\max}$  pattern over Europe was reported by Nikulin et al. (2011), who examined the RCA3 regional climate model (Samuelsson et al. 2011) driven by the ERA-40 reanalysis (Uppala et al. 2005). Christensen et al. (2008) found larger warm biases in extremely warm conditions with the implication that climate models may not properly represent future warmer conditions correctly.

Over Central Europe, RCMs tend to slightly underestimate  $T_{\max}$  (Kjellström et al. 2007, Nikulin et al. 2011). Plavcová and Kyselý (2011) evaluated  $T_{\max}$  in RCM simulations from the ENSEMBLES project (van der Linden and Mitchell 2009). Their results were consistent with majority of previous works, indicating negative biases of modelled  $T_{\max}$  over Central Europe. It should be noted, however, that Kjellström et al. (2010) reported that the biases in this region are the smallest of all those across the entire ENSEMBLES-RCMs domain.

Central Europe recently experienced exceptionally high temperatures in August 2012, when the new all-time temperature record (40.4°C) was set in the Czech Republic (Němec 2012). In summer 2013, moreover, Central Europe was affected by a series of heat waves that peaked on 8 August, when the new absolute maximum temperature (40.5°C) was measured in Austria. The previous all-time temperature record for Austria (39.9°C) had been set only a few days earlier, on 3 August, 2013 (ZAMG 2013).

Compared to  $T_{\max}$  simulation, a proper reproduction of heat waves is even more challenging. This requires not only a good simulation of the right tail of the  $T_{\max}$  distribution



but also of the persistence of extremely high  $T_{\max}$ . The capability of RCMs to simulate heat waves over Europe was evaluated by Vautard et al. (2013). They used a high resolution ( $0.11^\circ$ ) ensemble of RCM simulations from the CORDEX project (Giorgi et al. 2009). Due to the absence of observed gridded data in very high resolution, they interpolated model outputs to the ECA&D stations (Klein Tank et al. 2002) using the nearest-neighbour method with elevation adjustment. Modelled  $T_{\max}$  in Central Europe still suffered from biases, which influenced the characteristics of modelled heat waves that were too persistent and severe.

Many papers have focused on potential sources of these biases, and especially on atmospheric circulation and land–atmosphere coupling. Although the relationship between atmospheric circulation and surface air temperature in Europe is most significant in winter (e.g. Cattiaux et al. 2012), extreme high summer temperatures are also related to specific circulation patterns (Della-Marta et al. 2007; Kyselý 2008). The capability of RCMs to reproduce circulation indices (flow direction, strength and vorticity) in Central Europe was investigated by Plavcová and Kyselý (2012). Driven by the ERA-40 reanalysis, the utilized RCMs reproduced the circulation indices relatively well. These results are in concordance with Blenkinsop et al. (2009), who evaluated simulated circulation indices over England. Plavcová and Kyselý (2012) also demonstrated that differences between frequency distributions of circulation indices were higher when the model ensemble contained one RCM driven by various GCMs. On the contrary, these differences were smaller when the model ensemble involved various RCMs driven by one GCM. This reflects the fact that atmospheric circulation is primarily given by lateral boundary conditions and is little modified by individual RCMs.

The significant influence of land–atmosphere coupling on high summer air temperatures was shown by Fischer et al. (2007) who performed RCM simulations of  $T_{\max}$  during the most severe European heat waves with coupled and uncoupled soil-moisture scheme. They found major differences between these two types of simulations, thus indicating that improper simulation of soil-moisture content can dramatically alter a reproduction of  $T_{\max}$  and heat waves. These results were confirmed by Jaeger and Seneviratne (2010) who studied RCM simulations of  $T_{\max}$  over Europe under several soil-moisture scenarios. A reduction of soil-moisture content led to increase of  $T_{\max}$  and prolonged mean heat wave length.

Although a lot of work has been done to evaluate summer  $T_{\max}$  in RCM simulations (including an attribution of biases) and a number of studies examined heat wave characteristics for individual grid points as well, little attention has been given to evaluating

heat waves as *spatial* temperature patterns. In this study, we analysed spatial and temporal characteristics of heat waves in an ensemble of RCM simulations from the ENSEMBLES project. These simulated heat waves were evaluated against observed ones delimited from the E-OBS gridded dataset (Haylock et al. 2008). We investigated the capability of RCMs to reproduce their spatial extent, interannual variability, temperature amplitude and length. Furthermore, the capability of RCMs to reproduce the most severe Central European heat wave observed in 1994 (Lhotka and Kysely, 2014) was analysed, and simulation of an ‘erroneous’ heat wave at the turn of July and August, 1967 was examined in detail. Because soil-moisture feedback can significantly alter the heat wave pattern (e.g. Fischer et al. 2007), we focused on this aspect when studying variations among individual RCMs during these events.

## **8.2 Data and methods**

### 8.2.1 Regional climate model simulations

We examined 7 RCM runs driven by the ERA-40 reanalysis from the ENSEMBLES project (Table 8.1). The simulations cover the 1961–2000 period. The model runs were selected on the basis of their cartographic projection (rotated latitude/longitude grid with South Pole coordinates  $-39.25$  N,  $18.00$  E and  $25$  km resolution). This specification corresponds to the E-OBS gridded dataset ( $0.22^\circ$  rotated grid version). In addition, all RCMs have metadata available. The number of vertical levels in the RCMs varies from 24 (SMHIRCA) to 40 (KNMI-RACMO2), orography was adopted from the GTOPO30 dataset (except for METO-HC\_Had, which uses the US Navy 10' dataset). Each RCM utilizes its own land–surface scheme with different types of land cover with specific behaviours and have several soil layers for modelling heat and moisture storage and fluxes. An example of how these processes are described in one of the RCMs is given in Samuelsson et al. (2011). The depth of model bottom varies across individual RCMs, and that creates some difficulties when analysing soil moisture conditions. Further descriptions of individual models are available in metadata files at the ENSEMBLES RT3 data portal (<http://ensemblesrt3.dmi.dk/>).

Table 8.1. Examined RCMs driven by ERA-40 reanalysis.

Acronym	Institution	Model
C4IRCA3	Community Climate Change Consortium for Ireland	RCA ver. 3
ETHZ-CLM	Federal Institute of Technology in Zurich	CLM ver. 2.4.6
KNMI-RACMO2	Royal Netherlands Meteorological Institute	RACMO ver. 2.1
METNOHIRHAM	Norwegian Meteorological Institute	HIRHAM ver. 2
METO-HC_Had	Hadley Centre	HadRM ver. 3Q0
MPI-M-REMO	Max-Planck Institute	REMO ver. 5.7
SMHIRCA	Swedish Meteorological and Hydrological Institute	RCA ver. 3

### 8.2.2 Area of interest

The analysis was performed over Central Europe as defined by 1,000 grid points (40×25) and covering an area of 625,000 km<sup>2</sup> (Figure 8.1). This region is located in the area within approximately 47–53° N and 8–22° E. It includes Germany (excluding northern areas and the Rhineland), northern Austria, the Czech Republic, the south-western part of Poland, Slovakia (excluding its eastern part) and northern Hungary.

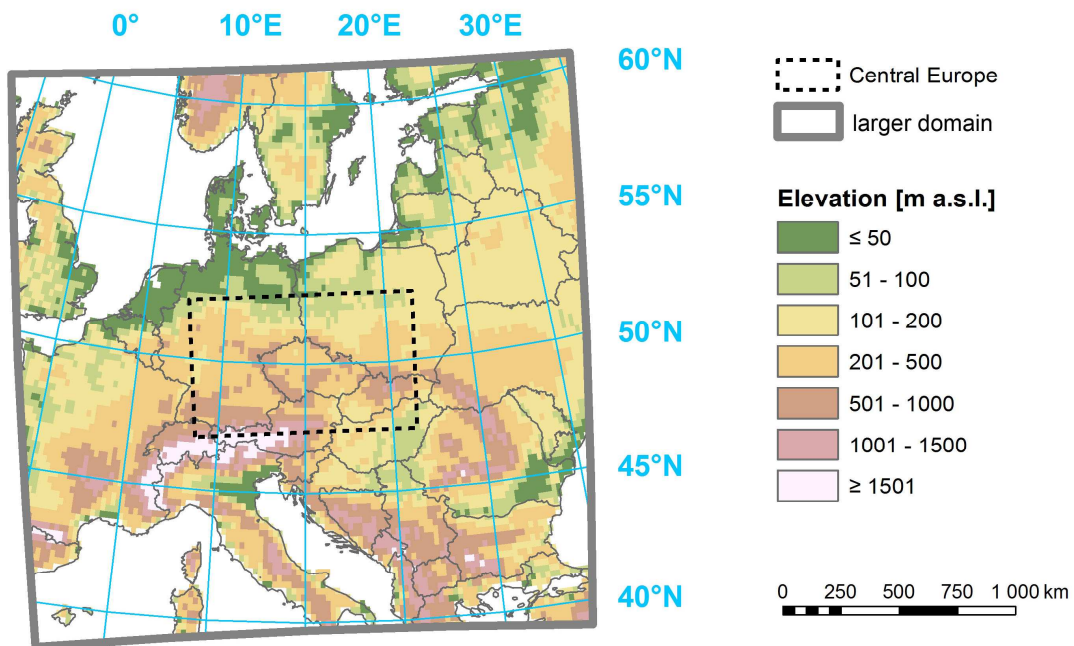


Figure 8.1. Definition of Central Europe (black dashed polygon), the larger domain (grey solid polygon) and the elevation model (GTOPO30) used in the E-OBS 9.0 gridded dataset.

### 8.2.3 Datasets utilized

To evaluate spatial and temporal characteristics of Central European heat waves, we examined modelled time series of  $T_{\max}$  that had a length of 3,680 days for each RCM (92 days in each summer over the 1961–2000 period; summer was regarded as the period between 1 June and 31 August). Observed data (E-OBS) for the same period were taken from the E-OBS 9.0 gridded dataset (Haylock et al. 2008) with the same projection and resolution as the modelled data.

For evaluating precipitation rates during and before heat waves, we used modelled daily precipitation data. This data was compared with observed precipitation from the E-OBS gridded dataset (Haylock et al. 2008). Due to different thickness of soil layers among individual RCMs and various depths of RCM bottoms, it is impossible to compare simulated soil moisture content directly between individual RCMs. Inasmuch as wet soils yield a high evaporative fraction (e.g. Small and Kurc 2003), soil moisture conditions were estimated on its basis. The evaporative fraction (EF) is defined as the ratio between latent heat flux ( $Q_e$ ) and available energy (sum of latent heat flux and sensible heat flux ( $Q_e+Q_h$ )) and it is related to the Bowen ratio ( $\beta$ ):

$$EF = \frac{Q_e}{Q_e + Q_h} = \frac{1}{1 + \beta}$$

### 8.2.4 Definition of heat wave

The definition of a heat wave (HW) was based on the persistence of hot days (HDs) and is the same as that in Lhotka and Kyselý (2014), who dealt with HWs in the E-OBS gridded dataset. For each day in summer, daily maximum air temperature ( $T_{\max}$ ) in each grid point over Central Europe was transformed into  $T_{\max}$  deviation by subtracting the grid point specific 95% quantile of summer  $T_{\max}$  distribution (calculated from the 1961–2000 period). Any day was considered a HD when the average of these  $T_{\max}$  deviations over all grid points in Central Europe (Figure 8.1) was greater than zero. Thus, a HD can occur only if a substantial part of Central Europe is affected by  $T_{\max}$  above the 95% quantile.

A HW over Central Europe was defined as a period of at least three consecutive HDs. For this period, the grid maps of positive  $T_{\max}$  deviations (excesses) were summed into a cumulative map. The relatively strict criteria allow identifying only major HWs that are presumed to have considerable impacts on the natural environment and society. This

definition was applied for both simulated and observed data. Due to biases in the modelled 95% quantile of the  $T_{\max}$  distribution and because our intention was to focus on spatial and temporal characteristics of HWs rather than the  $T_{\max}$  bias itself, we utilized respective 95% quantiles (calculated for each RCM) when delimiting HWs from modelled data. The respective quantiles were applied also by Vautard et al. (2013) who evaluated HWs in CORDEX-RCM simulations over Europe.

To describe the severity of individual HWs, we used a heat wave extremity index ( $I_{hw}$ ; Lhotka and Kysely 2014) that is calculated from a cumulative map of positive  $T_{\max}$  deviations. Values of individual grid points ( $TSmax'$ ) are summed up and scaled by the total number of grid points in Central Europe (1,000):

$$I_{hw} = \frac{1}{1000} \sum_{i=1}^n (TSmax')_i [^{\circ}C]$$

where  $n$  is the number of grid points with a positive  $T_{\max}$  deviation in a cumulative map. This index uses summed deviations over the whole period during which a HW persists, and hence it captures joint effects of temperature magnitude, spatial extent and also length of a HW. Detailed evaluation and discussion of the extremity index is given in Lhotka and Kysely (2014).

### 8.2.5 Heat wave characteristics

In addition to using  $I_{hw}$ , we evaluated several other characteristics of HWs. The temperature amplitude ( $T_{amp}$ ) is the highest daily value of  $T_{\max}$  deviations from the 95% quantile of summer  $T_{\max}$  distribution during the HW (in any grid point in Central Europe) and represents an anomaly of its peak temperature. The length of a HW ( $L$ ) is the number of days during which a HW persists (the number of consecutive HDs). The spatial extent ( $A$ ) is given by an area where the  $T_{\max}$  deviations from the 95% quantile of summer  $T_{\max}$  distribution were positive for at least 3 days. This is the only characteristic that was calculated over the larger domain (Figure 8.1) in order to capture the larger-scale pattern associated with each HW. The larger domain is defined by 10,000 grid points (100×100), but we excluded grid points over the sea and used only 7,016 continental grid points in order to allow a comparison with E-OBS. Although HWs were visualised over this larger region, grid points outside

Central Europe were not taken into account when calculating  $I_{hw}$ ,  $T_{amp}$  and  $L$ . The characteristics of HWs are summarized in Table 8.2.

Table 8.2. Characteristics of heat waves.

Abbreviation	Description	Units	Domain
$I_{hw}$	heat wave extremity index	°C	Central Europe
$T_{amp}$	temperature amplitude	°C	Central Europe
$L$	length	days	Central Europe
$A$	spatial extent	km <sup>2</sup>	larger domain

The ratio between the total duration of HWs and the total number of HDs indicates whether HDs have a high clustering tendency (a ratio close to 1), or whether HDs tend to occur separately throughout summer (a ratio close to 0). This ratio is hereafter referred as the clustering index ( $I_{cl}$ ).

#### 8.2.6 Temporal autocorrelation

Persistence of  $T_{max}$  over Central Europe was assessed by temporal autocorrelation computed as Pearson product-moment coefficients for lagged data pairs, which is the most commonly used method (Wilks 2011). For each day in summer,  $T_{max}$  values across 1,000 grid points over Central Europe were averaged into a regionally averaged  $T_{max}$ , which was used to compute correlation coefficients. Since the  $T_{max}$  series is not continuous, we computed correlation coefficients individually for each summer and averaged them thereafter.

### 8.3 Evaluation of heat wave characteristics and temporal variability in RCMs

During the 1961–2000 period, the RCMs simulated 104.6 hot days on average (Table 8.3), which is comparable to E-OBS (105). By contrast, the multi-model mean of the total duration of HWs was larger than in E-OBS, which is due to a higher clustering tendency of hot days in the RCM simulations (manifested in greater values of  $I_{cl}$ ). The temperature amplitude was overestimated in the majority of the RCMs, and especially in METO-HC\_Had. This RCM suffered from unrealistically hot isolated grid points that caused the highest average temperature amplitude (14.3°C), far exceeding the observed value (6.0°C). The average length of HWs was too short in modelled data, and the only RCM that simulated too long HWs on average was KNMI-RACMO2. Although the multi-model mean of simulated spatial extent was similar to E-OBS, large variations were present among individual RCMs. SMHIRCA simulated low average values (796,100 km<sup>2</sup>), while the spatial extent of HWs was

considerably enhanced in KNMI-RACMO2 and METNOHIRHAM (Table 8.3). Pronounced differences among the RCMs exist also in average and total extremity index. For example, both average and total  $I_{hw}$  were more than twice as great in KNMI-RACMO2 as in SMHIRCA (Table 8.3). In the multi-model mean, the average value of  $I_{hw}$  (characteristic of a single HW) was underestimated while the total  $I_{hw}$  was overestimated, which is related to the greater number of HWs in modelled data.

Table 8.3. Comparison of HW characteristics in RCM simulations and observed data (1961–2000).

	HD	HW	HW duration	$I_{cl}$	$T_{amp}$	L	A	Average $I_{hw}$	Total $I_{hw}$
C4IRCA3	102	13	48	0.47	6.1	3.7	924.3	5.5	71.6
ETHZ-CLM	102	13	49	0.48	7.2	3.8	945.4	7.8	100.9
KNMI-RACMO2	111	13	69	0.62	6.4	5.3	1259.2	10.6	137.6
METNOHIRHAM	112	14	62	0.55	8.3	4.4	1279.2	9.8	136.6
METO-HC_Had	101	12	47	0.47	14.3	3.9	1016.6	10.6	126.7
MPI-M-REMO	99	14	49	0.49	7.9	3.5	937.1	6.1	84.7
SMHIRCA	105	14	53	0.50	5.1	3.8	796.1	4.9	68.5
Multi-model mean	104.6	13.3	53.9	0.51	7.9	4.1	1022.5	7.9	103.8
E-OBS	105	9	42	0.40	6.0	4.7	924.5	9.1	81.7

HD – number of HDs, HW – number of HWs, HW duration – total duration of HWs [days],  $I_{cl}$  – clustering index of HDs,  $T_{amp}$  – average temperature amplitude of HWs [°C], L – average length of HWs [days], A – average spatial extent of HWs [thousands km<sup>2</sup>], Average  $I_{hw}$  – average heat wave extremity index [°C], Total  $I_{hw}$  – total heat wave extremity index [°C].

Because  $I_{cl}$  was overestimated in all RCMs, we evaluated a temporal autocorrelation of regionally averaged  $T_{max}$  among individual RCMs in comparison to E-OBS (Figure 8.2). In general, most RCMs (except for METO-HC\_Had) exhibited slightly greater values of autocorrelation coefficients than E-OBS. The lowest values of  $I_{cl}$  in C4IRCA3 and METO-HC\_Had are linked to relatively low correlation coefficients (but still higher than the observed one in the case of C4IRCA3). The second highest value of  $I_{cl}$  in METNOHIRHAM is accompanied by the highest correlation coefficients, particularly for lags of 2 days and more. Although the relationship between  $I_{cl}$  and the correlation coefficients is not perfectly expressed, the results suggest that the generally enhanced clustering tendency of hot days in the RCMs is related to an overestimated autocorrelation of  $T_{max}$ .

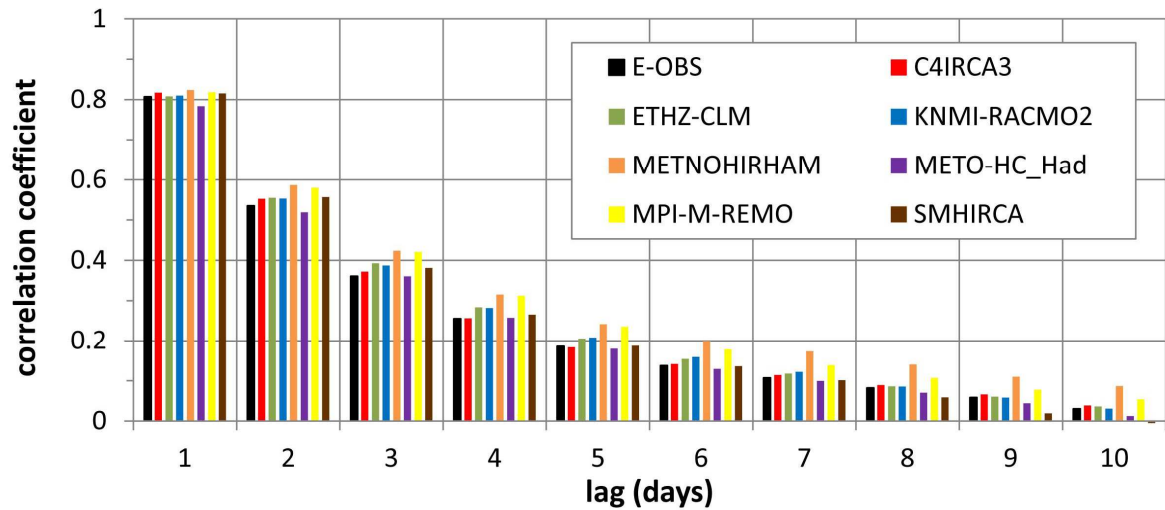


Figure 8.2. Temporal autocorrelation of regionally averaged  $T_{max}$  in RCM simulations and E-OBS during the 1961–2000 period.

The substantial overestimation of the total  $I_{hw}$  by the RCMs was analysed with respect to precipitation rates during the HWs (Table 8.4). The observed summer precipitation climatology (238.8 mm) and the average summer daily precipitation (2.6 mm) over Central Europe were simulated reasonably well in all RCMs and they are captured almost perfectly by the multi-model mean. In E-OBS, the average daily precipitation during HWs was 0.9 mm, which is approximately one third of average summer daily precipitation (35%). This ratio was considerably underestimated in KNMI-RACMO2 (9%) that simulated virtually no precipitation during HWs, which is probably related to the generally overestimated severity of heat waves in this RCM (expressed by the greatest value of average  $I_{hw}$  as well as total  $I_{hw}$ ). Overestimated values of total  $I_{hw}$  in ETHZ-CLM, METNOHIRHAM and METO-HC\_Had are also linked to low average daily precipitation during the HWs, while lower values of total  $I_{hw}$  in the rest of the RCMs are associated with higher average daily precipitation during HWs.



Table 8.4. Precipitation rates during the HWs in RCM simulations and observed data (1961–2000).

	R_JJA [mm]	R_day [mm/day]	R_HW-day [mm/day]	%
C4IRCA3	247.7	2.7	0.9	31.7
ETHZ-CLM	233.3	2.5	0.3	10.8
KNMI-RACMO2	192.4	2.1	0.2	9.1
METNOHIRHAM	199.7	2.2	0.4	20.2
METO-HC_Had	281.3	3.1	0.7	23.5
MPI-M-REMO	239.8	2.6	1.4	52.7
SMHIRCA	291.0	3.2	1.3	42.2
Multi-model mean	240.7	2.6	0.7	28.3
E-OBS	238.8	2.6	0.9	35.3

R\_JJA – summer precipitation climatology (1961–2000), R\_day – average summer daily precipitation, R\_HW-day – average daily precipitation during the HWs, % – the ratio (given as percentage) between R\_HW-day and R\_day.

Interannual variability of modelled hot days and HWs in each RCM and E-OBS is shown in Figure 8.3. Generally, the RCMs had a tendency to overestimate the number of hot days and severity of HWs in the first decade (1961–1970), especially METNOHIRHAM. In 1967, all RCMs simulated more hot days compared to E-OBS. Moreover, all RCMs simulated at least one HW in 1967 while no HW occurred in E-OBS that year.

The 1971–1990 period was typical for a small number of hot days and low  $I_{hw}$  values in E-OBS. This feature was well depicted by the majority of RCMs, however, KNMI-RACMO2 and METO-HC\_Had clearly simulated too many hot days and HWs. On the contrary, METNOHIRHAM simulated no HW and very few hot days in this period. It should be noted that the observed 1974, 1976 and 1983 HWs were not captured by most RCMs. In addition, MPI-M-REMO simulated a very high annual sum of  $I_{hw}$  in 1986 while the sum of  $I_{hw}$  in 1986 was equal to 0 in E-OBS.

The last analysed decade (1991–2000) was punctuated by the extreme summers of 1992 and 1994. These severe HWs were only reasonably well reproduced in ETHZ-CLM, KNMI-RACMO2 and METNOHIRHAM while the rest of the RCMs failed to simulate major HWs in these years. In addition, METNOHIRHAM and MPI-M-REMO simulated very high annual sums of  $I_{hw}$  and severe HWs in 1996, which contradicts observations.

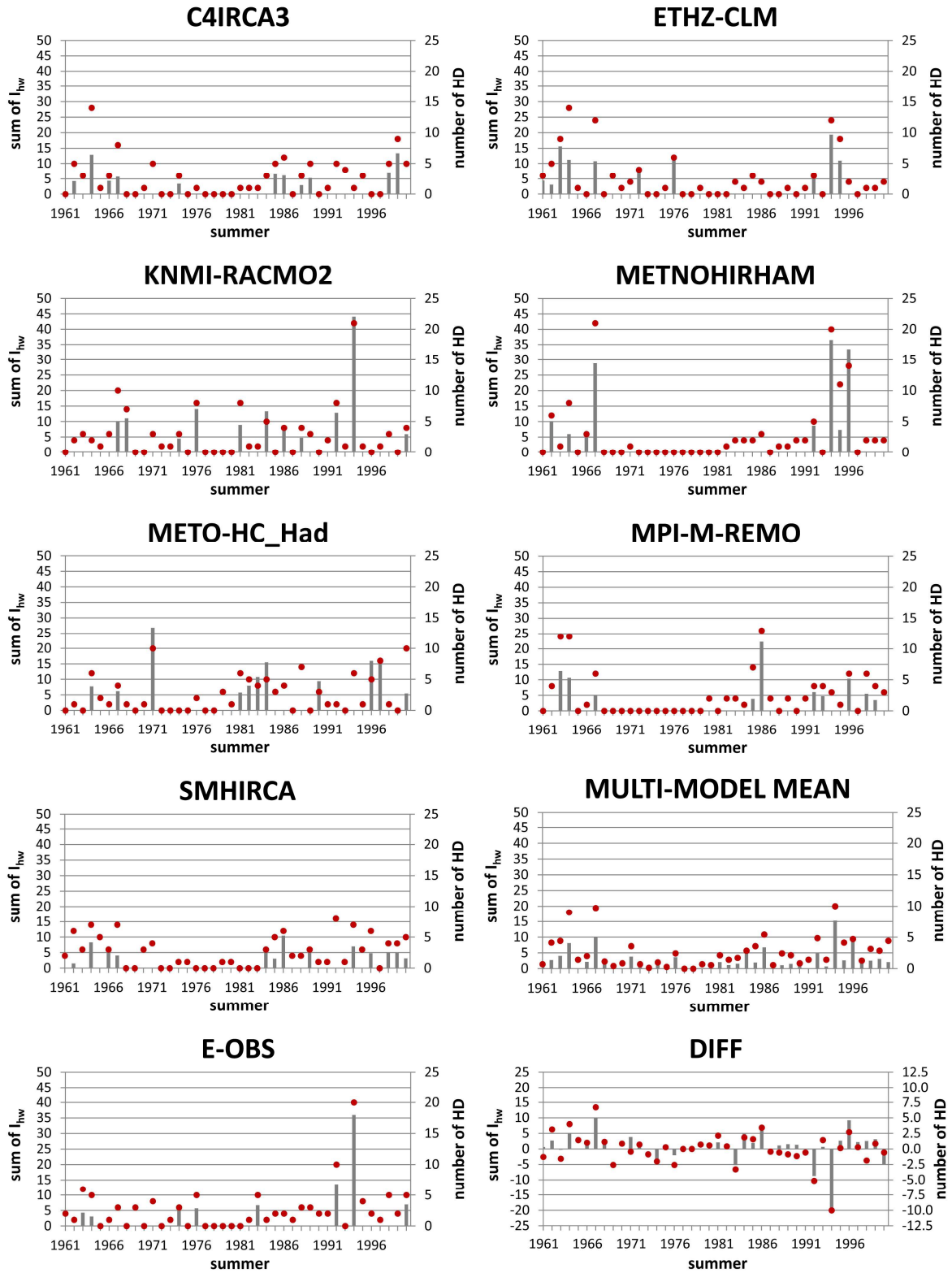


Figure 8.3. Temporal variability of the number of hot days (HD, red dots) and the annual sum of the heat wave extremity index ( $I_{hw}$ , grey bars) in RCM simulations and observed data during the 1961–2000 period. DIFF represents the difference between the multi-model mean and E-OBS.

The difference between the multi-model mean and E-OBS showed that the RCMs overestimated the severity of HWs mainly in 1967 and 1996 while the severity of HWs was underestimated in 1992 and especially in 1994. Possible causes of these discrepancies for the summers of 1994 and 1967 are investigated in detail in Sections 8.4 and 8.5, respectively.

#### **8.4 Reproduction of the 1994 heat wave in RCMs**

In this section, we investigated the capability of RCMs to reproduce the most severe Central European HW (according to  $I_{hw}$ ) that occurred in 1994 and persisted for 15 days (July 23 – August 6). This was a record breaking HW across Central Europe over the 1950–2012 period for which E-OBS data were available (Lhotka and Kyselý 2014). For the 15-day heat wave period, we summed the grid maps of positive daily  $T_{max}$  deviations for each RCM into the cumulative maps in order to obtain simulated temperature patterns. While all RCMs agreed with E-OBS that  $T_{max}$  deviations were largest in the area north of Central Europe, we found major differences between the observed 1994 HW pattern and individual RCM simulations (Figure 8.4).

Relatively good reproduction of the major 1994 HW was found in ETHZ-CLM, KNMI-RACMO2 and METNOHIRHAM. In particular, ETHZ-CLM and METNOHIRHAM simulated the spatial distribution of cumulative temperature deviations quite well, however, the  $I_{hw}$  was slightly reduced (Figure 8.4). In KNMI-RACMO2, a distinct area of extreme hot anomalies (sum of temperature deviations above the 95% quantile of summer  $T_{max}$  distribution  $> 50^{\circ}\text{C}$ ) was simulated over north-eastern Germany, north-western Poland and southern Sweden. On the contrary, the south-eastern part of Central Europe was only little affected, thus resulting in a lower  $I_{hw}$  also in this RCM. In the rest of the RCMs, the severity of the 1994 HW was substantially underestimated. Especially C4IRCA3, MPI-M-REMO and SMHIRCA simulated only small temperature anomalies, thus resulting in low values of  $I_{hw}$  (Figure 8.4). In 3 RCMs (C4IRCA3, METO-HC\_Had, MPI-M-REMO), no HW according to the definition applied was simulated during the period corresponding to the observed HW.

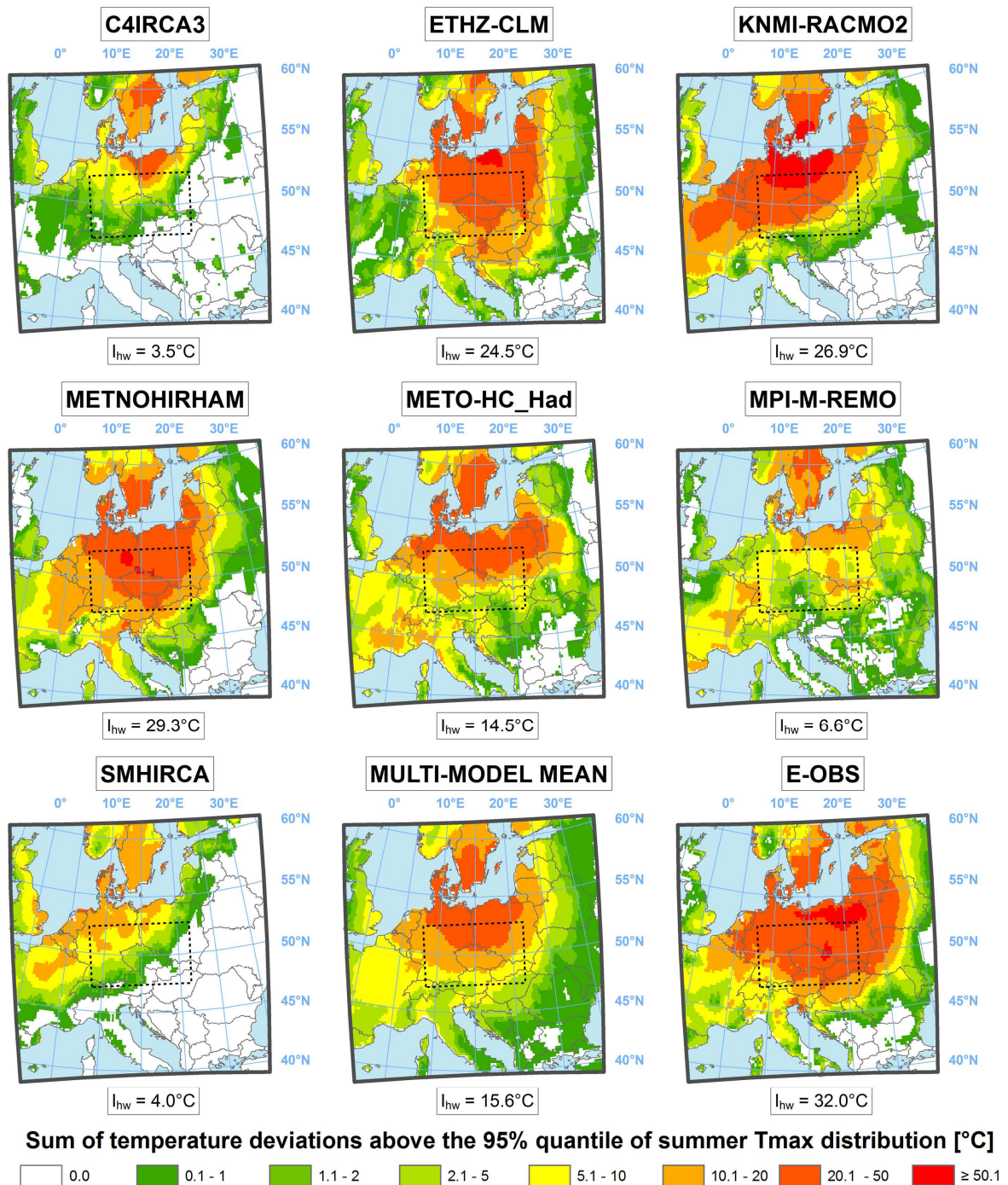


Figure 8.4. Cumulative maps of positive  $T_{max}$  deviations between 23 July and 6 August 1994 for each RCM, the multi-model mean and E-OBS.

In order to determine the causes of these large differences among the RCMs, we analysed the simulated precipitation and soil-moisture conditions. First, we evaluated the accumulated amount of precipitation in the RCMs averaged over Central Europe during the 1994 HW (Figure 8.5).

In E-OBS, the accumulated average precipitation over Central Europe during the 1994 HW was 7.3 mm, which is considerably below the normal precipitation amount for this period (36.3 mm). We found large differences in this characteristic among the RCM simulations and a clear relationship to the simulated temperature patterns. The reproduction of precipitation during the 1994 HW was most realistic in ETHZ-CLM and METNOHIRHAM (Figure 8.5), i.e. in the two RCMs with the most realistic temperature patterns (Figure 8.4). In these RCMs, the accumulated average precipitation was close to E-OBS. Almost no precipitation was simulated by KNMI-RACMO2 (the third RCM with a pronounced HW) during the whole period of the 1994 HW. By contrast, the rest of the RCMs substantially overestimated precipitation over Central Europe during the period corresponding to the observed HW, especially MPI-M-REMO and METO\_HC-Had. This suggests that quite realistic reproduction of temperature patterns for the 1994 HW in ETHZ-CLM and METNOHIRHAM was linked to credible simulation of precipitation rates during this period. Almost no precipitation in KNMI-RACMO2 was probably related to unrealistically hot anomalies in the northern part of Central Europe, while considerably overestimated precipitation rates (by a factor of 3–6) in C4IRCA, METO-HC\_Had, MPI-M-REMO and SMHIRCA were associated with reduced temperature patterns during the HW period.

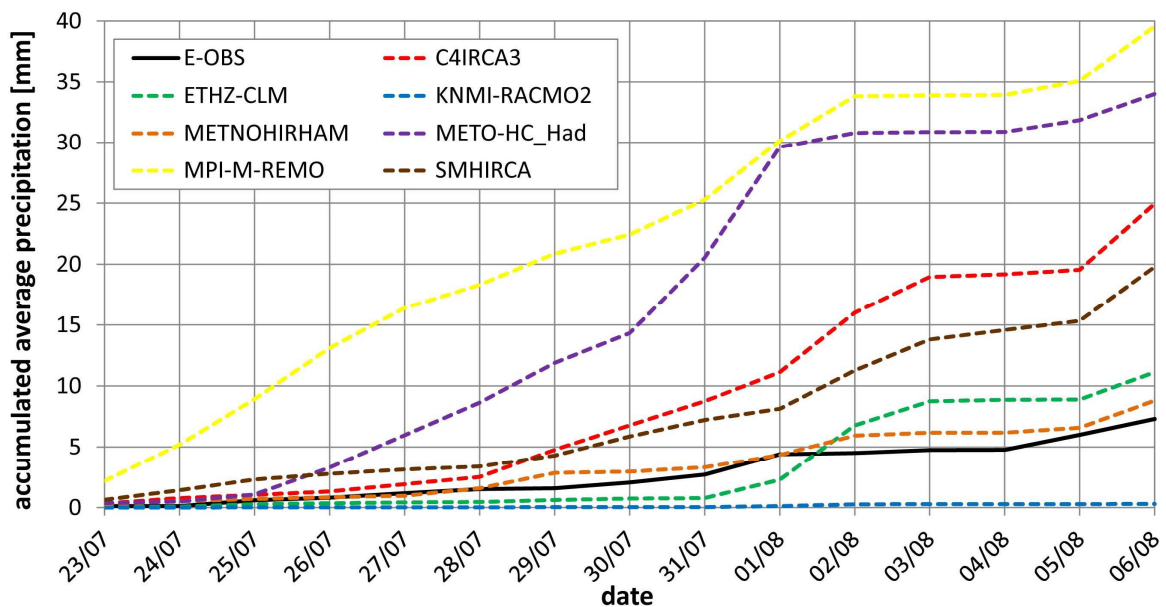


Figure 8.5. Accumulated average precipitation over Central Europe during the 1994 heat wave (23 July – 6 August).

We also investigated the precipitation amount over Central Europe in the early-summer period preceding the HW (from 1 June to 22 July). The precipitation deficit was simulated by all RCMs but it was less pronounced than in E-OBS (Table 8.5). While this might have contributed to the fact that the 1994 HW was simulated as less severe over Central Europe (according to  $I_{hw}$ ) in all RCMs, we found no relationship between the precipitation rates in the previous period and the simulated temperature patterns for the 1994 HW in individual RCMs. In fact, the deficits were larger in those RCMs that did not reproduce the HW.

Table 8.5. Precipitation rates for the period 1 June – 22 July.

	R_1961–2000 [mm]	R_1994 [mm]	%
C4IRCA3	148.5	104.5	70.4
ETHZ-CLM	137.4	114.7	83.5
KNMI-RACMO2	117.5	95.5	81.3
METNOHIRHAM	123.6	111.6	90.3
METO-HC_Had	178.1	143.9	80.8
MPI-M-REMO	150.0	120.3	80.2
SMHIRCA	171.1	125.4	73.3
Multi-model mean	146.6	116.6	79.5
E-OBS	142.6	94.4	66.2

R\_1961–2000 – the 1961–2000 climatology of precipitation amount during June 1 – July 22, R\_1994 – precipitation in year 1994 during June 1 – July 22, % – the ratio (expressed as percentage) between the 1994 precipitation and the 1961–2000 climatology.

The development of evaporative fraction (EF) during the 1994 HW is shown in Figure 8.6. EF is the ratio between the latent heat flux and the available energy (Section 8.2.3). These variables are not available in E-OBS, so our analysis was limited to inter-comparison of the RCMs. Above-average EF values (moister conditions) during the 1994 HW period were simulated by MPI-M-REMO (0.82), SMHIRCA (0.81) and C4IRCA (0.77) in which weak temperature patterns were found for the 1994 HW (Figure 8.4). Below-average values of EF (drier conditions), simulated in the rest of the RCMs (METO-HC\_Had (0.59), ETHZ-CLM (0.60), METNOHIRHAM (0.62), KNMI-RACMO2 (0.67)), were related to the more pronounced temperature anomalies (Figure 8.4), although this link was not well expressed compared to the precipitation amount during the HW. It is noteworthy that although METO-HC\_Had simulated high precipitation rates (Figure 8.5) its mean EF was lowest (Figure 8.6).



Moreover, KNMI-RACMO2 had moderate EF values (Figure 8.6) despite almost no precipitation simulated (Figure 8.5). This issue is discussed in more detail in Section 8.6.4.

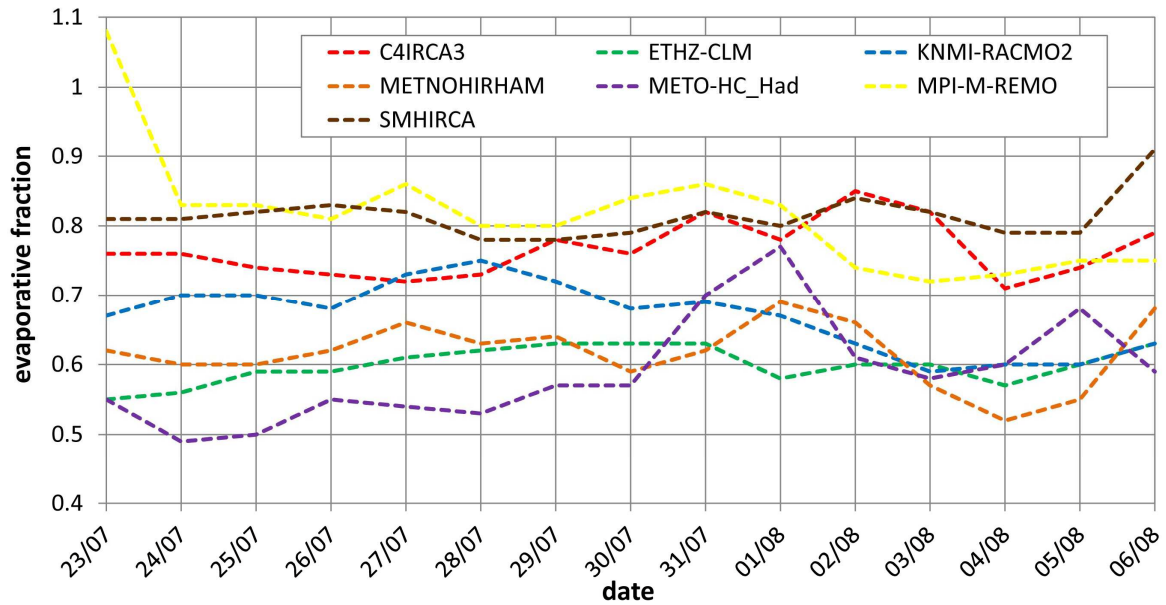


Figure 8.6. Development of evaporative fraction over Central Europe during the 1994 heat wave (23 July – 6 August).

### 8.5 ‘Erroneous’ 1967 heat wave in RCM simulations

All examined RCMs except ETHZ-CLM simulated a HW between 31 July and 4 August 1967 while only a single hot day was observed during this period in E-OBS. Analogously to Section 8.4, we summed the grid maps of positive  $T_{\max}$  deviations for each RCM into cumulative maps in order to obtain simulated temperature patterns for this period that were compared against observations (Figure 8.7). In E-OBS, only small positive  $T_{\max}$  anomalies were found over Central Europe that resulted in a low value for  $I_{hw}$  (Figure 8.7). By contrast, all RCMs considerably enhanced temperature patterns, especially METNOHIRHAM that simulated a severe HW over Central Europe.

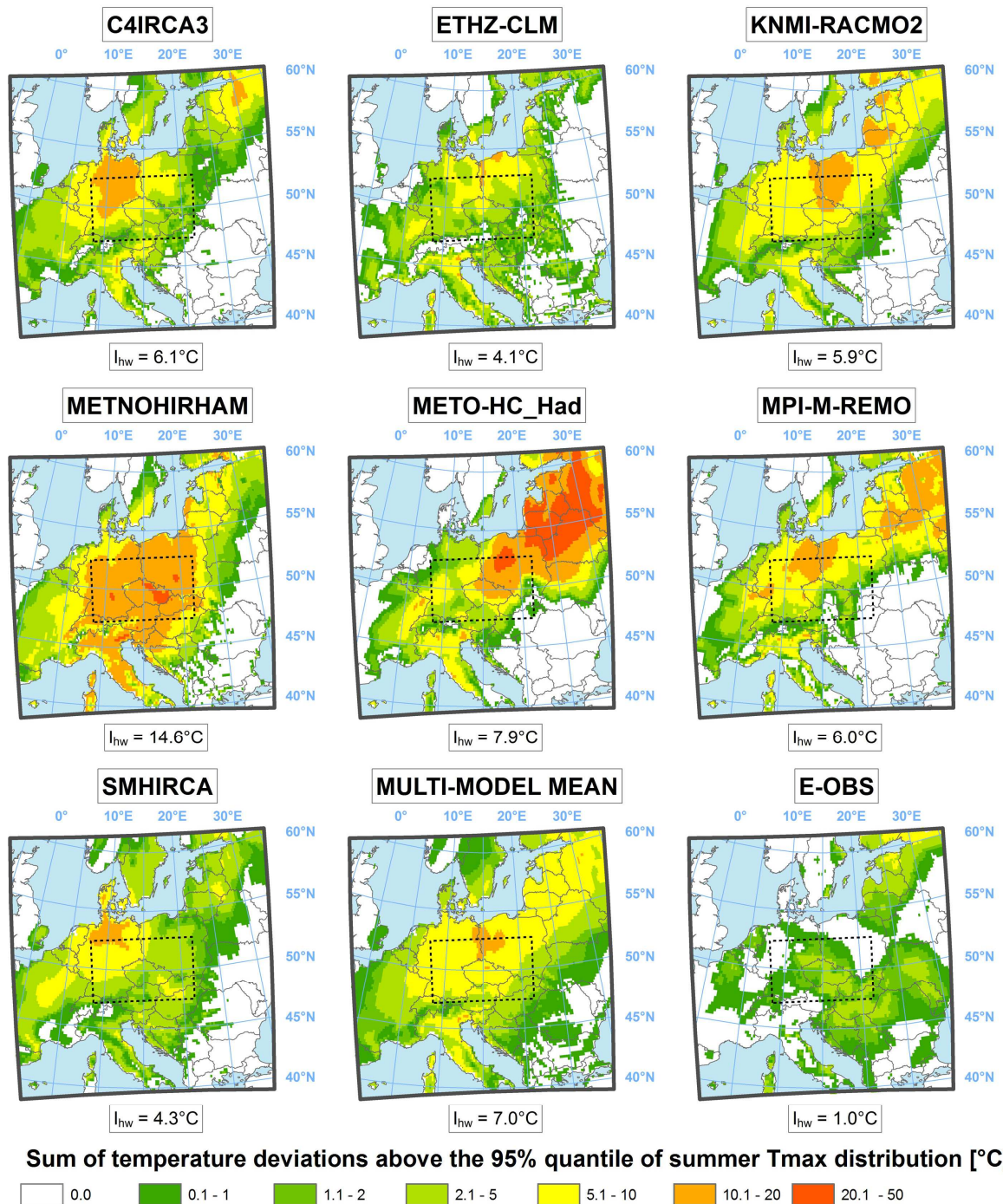


Figure 8.7. Cumulative maps of positive  $T_{max}$  deviations between 31 July and 4 August 1967 for each RCM, the multi-model mean and E-OBS.

As in Section 8.4, we evaluated the accumulated amount of precipitation averaged over Central Europe between 31 July and 4 August 1967. The accumulated precipitation in E-OBS for the examined period was 17.3 mm (Figure 8.8), which was slightly more than the average precipitation for this period of year (13.2 mm). Precipitation was considerably underestimated



in all RCMs, which supported development of the ‘erroneous’ HW. The lowest amount of precipitation (1.3 mm) was simulated by METNOHIRHAM, in which temperature anomalies over Central Europe were most pronounced. A similar amount of precipitation (1.6 mm) in KNMI-RACMO2 was associated with much less pronounced temperature anomalies (Figure 8.7), but this RCM has generally very low precipitation amounts during heat waves (Section 8.3). Between one-third and one-half of the observed precipitation was simulated for the HW period in the remaining RCMs.

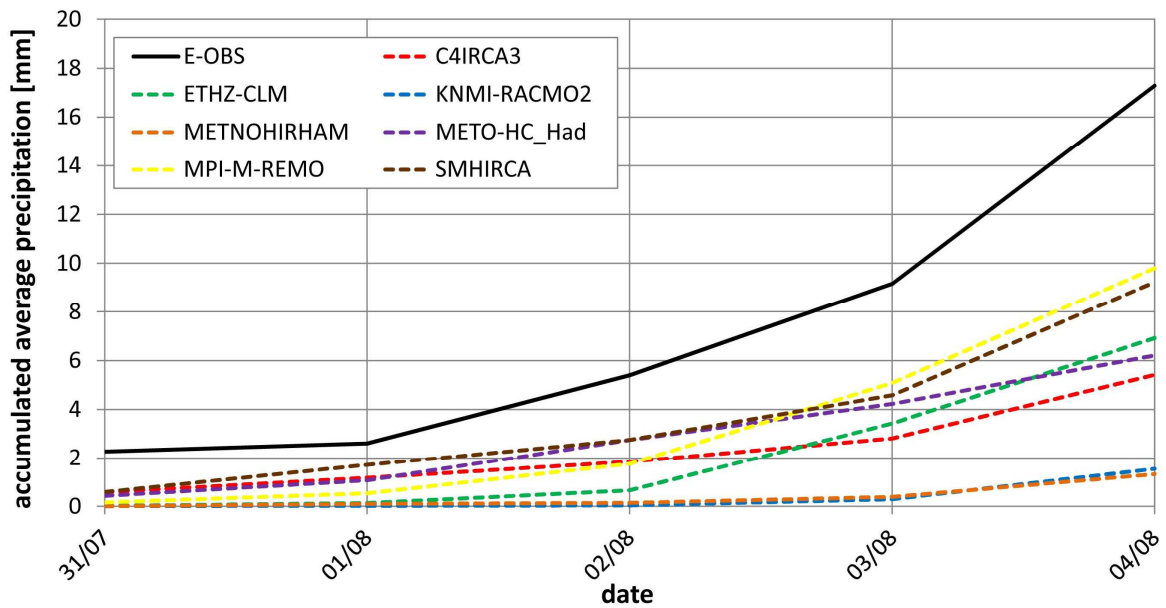


Figure 8.8. Accumulated average precipitation over Central Europe between 31 July and 4 August 1967.

The precipitation in the RCMs and E-OBS during the preceding period from 1 June to 30 July is given in Table 8.6. In observed data, the precipitation amount was only slightly below the 1961–2000 climatology (91%). In the majority of the RCMs, by contrast, considerable precipitation deficits were simulated, especially in METNOHIRHAM (41%). The combination of this major precipitation deficit and almost no precipitation during the simulated HW most probably contributed to the greatest temperature anomalies among all the RCMs. The precipitation deficit in June and July and reduced soil moisture in the other RCMs (except for METO-HC\_Had) have also supported the development of a HW at the turn of July and August in their simulations.

Table 8.6. Precipitation rates for the period June 1 – July 30.

	R_1961–2000 [mm]	R_1967 [mm]	%
C4IRCA3	168.9	134.4	79.6
ETHZ-CLM	156.5	104.5	66.8
KNMI-RACMO2	133.8	91.1	68.1
METNOHIRHAM	138.6	56.8	41.0
METO-HC_Had	202.1	231.8	114.7
MPI-M-REMO	170.7	122.2	71.6
SMHIRCA	195.2	149.7	76.7
Multi-model mean	166.5	123.4	74.1
E-OBS	162.2	147.9	91.2

R\_1961–2000 – the 1961–2000 climatology of precipitation amount during 1 June – 30 July, R\_1967 – precipitation in year 1967 during 1 June – 30 July, % – the ratio (expressed as percentage) between the 1967 precipitation and the 1961–2000 climatology.

## 8.6 Discussion

### 8.6.1 Evaluation of spatial and temporal characteristics of simulated heat waves

In evaluating spatial and temporal characteristics of heat waves, substantial differences became apparent among individual RCMs and between the RCMs and observations. Inasmuch as we calculated 95% quantiles of  $T_{\max}$  distribution for each RCM separately to delimit heat waves, these errors were not caused by simple  $T_{\max}$  biases.

The clustering index of hot days (the ratio between the total duration of heat waves and the total number of hot days) revealed a generally greater clustering tendency for hot days in the RCMs than in the observed data. Higher temporal autocorrelation of summer  $T_{\max}$  found in most RCMs, and particularly for lags of 2 days and more, is likely associated with the enhanced clustering tendency of hot days.

Vautard et al. (2013) showed that RCMs from the CORDEX project (Giorgi et al. 2009) tend to overestimate amplitude and persistence of heat waves, even when respective percentiles (calculated for each RCM) are used. The greater mean amplitude of heat waves accords with our study, but a comparison of persistence is more complex. Vautard et al. (2013) demonstrated that all RCMs overestimated the number of heat waves that persisted more than a few days at the expense of shorter events, and the overestimation generally increased with duration. Such attribute was not present in our study, since only KNMI-RACMO2 simulated a longer heat wave than was observed (18 days long heat wave between

25 July and 11 August, 1994), and the average length of heat waves was shorter in most RCMs compared to observation.

These seemingly contrasting results are probably associated with different definitions of events. While our definition of a heat wave was based on at least 3 consecutive hot days and a larger area's being affected, Vautard et al. (2013) evaluated also single-day events and no requirement on their spatial extent was imposed. This definition, then, resulted in substantially greater number of events. Moreover, a higher respective temperature quantile (95%) was applied in our study. If single-day events would be included in our study as well, then the average length of HWs would decrease more in observed than simulated data (as the clustering index of hot days is smaller in the observed data) and the results would be more consistent. Increasing overestimation for heat waves of longer duration (Vautard et al. 2013) is also consistent with greater overestimation of autocorrelation of daily  $T_{\max}$  for longer lags, as found for most RCMs in our study.

Substantial biases in precipitation rates during heat waves among the RCMs were detected; these differences were linked to the total extremity index of heat waves and may be related to different convection schemes. The influence of convection schemes on the heat wave development in RCM simulations was recently studied by Stegehuis et al. (2014), who demonstrated their crucial role for a simulation of heat waves.

The general overestimation of heat waves severity in the 1960s and its contrasting underestimation in the 1990s is related to underestimated temperature trends in the RCM simulations. Lorenz and Jacob (2010) showed that most RCMs from the ENSEMBLES project driven by the ERA-40 reanalysis failed to simulate the observed temperature trend properly. This feature was consistent in all domains over Europe.

### 8.6.2 Reproduction of the 1994 heat wave

Using as an example the most severe Central European heat wave observed between 23 July and 6 August 1994, we demonstrated that the temperature patterns were model-dependent and differed considerably from observations in most RCMs. Since RCMs driven by the ERA-40 reanalysis reproduce persistence of weather regimes (Sanchez-Gomez et al. 2009) and flow indices (Plavcová and Kyselý 2012) over Central Europe relatively well, we focused on land–atmosphere coupling as a possible driver for the errors in simulations of this event.

The importance of realistically simulating soil-moisture conditions in RCMs for the development of heat waves was emphasized by Fischer et al. (2007) and Vautard et al. (2013). We identified a pronounced overestimation of precipitation amount during the period of the 1994 heat wave in all RCM simulations that considerably underestimated the magnitude of the temperature pattern (4 out of 7), while the simulated precipitation was much closer to reality in the 3 RCMs that captured the 1994 heat wave reasonably well. This is also in accordance with model simulations performed by Jaeger and Seneviratne (2010), who concluded that heat waves are strongly affected by the total amount of soil-moisture.

Since Fischer et al. (2007) found no precipitation deficit in Central Europe in spring 1994, we analysed the preceding precipitation amount only from 1 June to the onset of the July–August 1994 heat wave. The precipitation deficit was present in all examined RCMs, but it was smaller in each case than that actually observed and was not linked to the magnitude of the temperature pattern of the 1994 heat wave. This suggests that the precipitation deficit during this heat wave was more important for its development than was the preceding precipitation amount. However, the slightly overestimated early-summer precipitation in all RCM simulations might also have contributed to the general underestimation of the July–August 1994 heat wave.

### 8.6.3 ‘Erroneous’ 1967 heat wave in RCM simulations

Analogously to the most severe Central European heat wave in 1994, we investigated also the substantial overestimation of  $T_{\max}$  and the ‘erroneous’ heat wave that appeared in 6 out of 7 RCMs between 31 July and 4 August 1967. During this period, all RCMs simulated considerably lower precipitation amounts compared to observed data. Although the precipitation was underestimated by a factor of 2–10, the relationship between the magnitude of temperature pattern and precipitation during this event was weaker than in case of the 1994 heat wave and it was probably not the only major source of errors.

The analysis of preceding precipitation rates revealed a major deficit in METNOHIRHAM that simulated the most pronounced temperature pattern over Central Europe in 1967. This suggests that these errors were caused by a joint effect of precipitation underestimation during this event amplified by the preceding precipitation deficit and associated drying. The importance of dry soils in driving and/or enhancing heat waves was reported by several previous studies (e.g. Fischer et al. 2007). Errors in the 1994 heat wave simulations, by contrast, were caused primarily by incorrect simulation of precipitation during

this event, while the role of the preceding precipitation deficit was relatively small. This is probably related also to the different lengths of the events.

#### 8.6.4 Evaporative fraction during the 1967 and 1994 heat waves

Since the examined RCMs have different thickness of soil layers and a various soil depths, we analysed soil-moisture conditions in the RCMs indirectly through evaporative fraction (Section 8.2.3). Although this micrometeorological characteristic is today measured worldwide within the FLUXNET project (Baldocchi et al. 2001), measurements of evaporative fraction before the beginning of the 21<sup>st</sup> century were rather sparse. The typical annual values for evaporative fraction range from 0.01 in very dry areas to 0.8 in quite humid regions (Jung et al. 2011). According to Hartmann (1994), the estimated average value of evaporative fraction over Europe is 0.6, and Fischer et al. (2007) pointed out that the evaporative fraction was about 0.1 during the severe 1976 heat wave over the British Isles.

Hence, the simulated evaporative fraction during the 1994 heat wave seems to be overestimated (average values among the RCMs range from 0.6 to 0.8). A systematic overestimation of evapotranspiration, which is closely related to evaporative fraction, was found by Mueller and Seneviratne (2014) in GCMs, and it is possible that a similar bias is also present in the examined RCMs.

We found some signs of suspicious relationships between precipitation and evaporative fraction in our study. Although KNMI-RACMO2 simulated virtually no precipitation over Central Europe during the whole 1994 heat wave, the evaporative fraction in this RCM was relatively high. In addition, KNMI-RACMO2 underestimated precipitation amount in the period preceding the heat wave, which is inconsistent with the high evaporative fraction. Meijgaard et al. (2008) noted that the RACMO 2.1 land surface scheme was modified since the previous model simulated insufficient soil drying. The suspiciously high evaporative fraction might be related to the persistence of this issue also in the examined KNMI-RACMO2 simulation. A similar feature was found in METNOHIRHAM that simulated high values of evaporative fraction during the ‘erroneous’ 1967 heat wave (around 0.9, not shown), despite the fact that this RCM simulated considerable precipitation deficit in the early summer and during the heat wave. By contrast, METO-HC\_Had had low evaporative fraction, despite relatively high precipitation rates during the 1994 heat wave. The low evaporative fraction might enable a development of relatively hot conditions despite substantially overestimated precipitation during this event. These results suggest that realistic reproduction of soil

moisture is a critical issue in the RCMs, and this is particularly relevant for heat waves and the credibility of their scenarios in a possible future climate.

#### 8.6.5 Performance of individual RCMs

The main features of the individual RCMs with respect to the simulation of spatial and temporal heat wave characteristics over Central Europe can be summarized as follows:

C4IRCA3 simulated the average temperature amplitude and spatial extent of heat waves well. By contrast, the 1994 heat wave was poorly reproduced, interannual variability of heat waves was distorted and the total heat wave extremity index was slightly underestimated.

ETHZ-CLM simulated temperature amplitude and spatial extent of the heat waves reasonably well. The 1994 heat wave was also captured. Some insufficiencies were found in the simulated interannual variability of heat waves, and the total heat wave extremity index was overestimated.

KNMI-RACMO2 best reproduced the interannual variability and its simulation of the 1994 heat wave was relatively good too. By contrast, this RCM substantially overestimated the spatial extent and total extremity index of heat waves, which is probably related to large underestimation of precipitation during heat waves.

METNOHIRHAM best reproduced the 1994 heat wave and it simulated relatively well the average length of heat waves. However, this RCM suffered most from ‘erroneous’ severe heat waves in 1967 and 1996 when no heat waves were observed. Similarly to KNMI-RACMO2, the spatial extent and total extremity index of heat waves were substantially overestimated.

METO-HC\_Had had difficulties in reproducing the characteristics and the interannual variability of heat waves. The largest drawbacks were found in temperature amplitude, which was simulated unrealistically due to isolated hot grid points.

MPI-M-REMO simulated the spatial extent and total extremity index of heat waves relatively well. By contrast, the average length of heat waves was considerably underestimated, the 1994 heat wave was not properly reproduced and the interannual variability of heat waves was distorted.

SMHIRCA substantially underestimated temperature amplitude, spatial extent and total extremity index of heat waves. The reproduction of the 1994 heat wave was poor and the interannual variability of heat waves was simulated insufficiently.

Although there is no single RCM that outperforms others as to the simulation of all heat wave characteristics over Central Europe, ETHZ-CLM performed relatively well in most characteristics. Previous studies (Christensen et al. 2010; Holtanová et al. 2012) indicated that KNMI-RACMO2 performed best among RCMs from the ENSEMBLES project. The drawbacks of KNMI-RACMO2 found in our study suggest important limitations in reproducing temporal and spatial structure of daily temperatures also in this RCM. The RCMs with the worst simulation of heat waves over Central Europe in the examined ensemble were probably METO-HC\_Had and SMHIRCA.

## 8.7 Conclusions

We investigated the ability of RCMs to reproduce spatial and temporal characteristics of heat waves over Central Europe, using the ensemble of 7 RCM simulations driven by the ERA-40 reanalysis over the 1961–2000 period. We utilized the E-OBS 9.0 gridded dataset as a source of observed data. Since soil-moisture feedback enhances temperature amplitude and prolongs duration of heat waves, we also focused on land–atmosphere coupling in the RCM simulations during the most severe Central European heat wave in 1994 as well as during an ‘erroneous’ heat wave found in the RCM simulations in 1967. The main conclusions are as follows:

- The RCMs simulated more heat waves despite the fact that the number of hot days is almost the same as in the observed data. The overestimation of the clustering tendency of hot days is probably related to enhanced temporal autocorrelation of summer  $T_{\max}$ , particularly for lags of 2 days and more.
- On average, heat waves tended to be shorter but with a too-pronounced temperature peak in most RCMs. The spatial extent and heat wave extremity index were reproduced reasonably well in the ensemble mean, although considerable differences were found among individual RCMs.
- Substantial variations in precipitation rates during heat waves in the RCMs were found, and they were related to the total extremity index of heat waves.
- We found major differences among the RCMs when reproducing interannual and interdecadal variability of heat waves and hot days. In general, the RCMs overestimated the severity of heat waves and the number of hot days in the 1960s and underestimated both during the extreme 1992 and 1994 summers.

- Focusing on the ability of the RCMs to reproduce the most severe 1994 heat wave, we found considerable differences between observations and the RCMs that were linked to the simulated precipitation during this event. Only those RCMs that reproduced the precipitation deficit captured the 1994 heat wave reasonably well, while the heat wave was weak or entirely missing in all RCMs that substantially overestimated precipitation during this period.
- Analogously, unrealistically overestimated temperature anomalies in 1967 in all RCMs were related to unrealistic precipitation deficits simulated during the heat wave as well as in the preceding early-summer period.
- The evaporative fraction was suspiciously high in the RCMs during the 1994 heat wave. This suggests a possible contribution of other factors such as cloud cover and associated downward radiation that might strongly affect heat wave development in the RCMs. Moreover, the link between simulated evaporative fraction and precipitation was poorly expressed, indicating deficiencies in land surface schemes among the RCMs.
- Although there is no single RCM that outperforms others as to the simulation of all heat wave characteristics over Central Europe, ETHZ-CLM performed relatively well in most characteristics. By contrast, METO-HC\_Had and SMHIRCA were probably the least performing RCMs in the examined ensemble as to the simulation of heat waves over Central Europe.

Regional climate models have become a powerful tool for exploring impacts of global climate change on a regional scale. Further work is needed to determine the relationships between extreme high temperature, atmospheric circulation, soil-moisture conditions, cloud cover and associated incoming shortwave radiation in RCM simulations. Evaluating these driving processes before and during simulated heat waves can provide a better attribution of errors in reproducing such extreme events. It is important to better understand the strengths and weaknesses of RCMs also for assessing the credibility of projected regional changes of heat waves in future climate and, ultimately, for improving the RCMs.

### **Acknowledgments**

The RCM data were obtained from the ENSEMBLES project database funded within the EU-FP6 (<http://ensemblesrt3.dmi.dk/>). We also acknowledge the E-OBS dataset from the same



project (<http://ensembles-eu.metoffice.com>) and the data providers in the ECA&D project (<http://www.ecad.eu>). The study was supported by the Czech Science Foundation, project P209/10/2265. We thank anonymous reviewers for useful comments that helped improve the original manuscript.

## References

- Baldocchi D, Falge E, Gu L, et al. (2001) FLUXNET : A New Tool to Study the Temporal and Spatial Variability of Ecosystem-Scale Carbon Dioxide, Water Vapor, and Energy Flux Densities. *Bull Am Meteorol Soc* 82:2415–2434. doi: 10.1175/1520-0477(2001)082<2415:FANTTS>2.3.CO;2
- Barriopedro D, Fischer EM, Luterbacher J, et al. (2011) The hot summer of 2010: redrawing the temperature record map of Europe. *Science* 332:220–224. doi: 10.1126/science.1201224
- Beniston M, Stephenson DB, Christensen OB, et al. (2007) Future extreme events in European climate: an exploration of regional climate model projections. *Clim Change* 81:71–95. doi: 10.1007/s10584-006-9226-z
- Black E, Blackburn M, Harrison G, et al. (2004) Factors contributing to the summer 2003 European heatwave. *Weather* 59:217–223. doi: 10.1256/wea.74.04
- Blenkinsop S, Jones PD, Dorling SR, Osborn TJ (2009) Observed and modelled influence of atmospheric circulation on central England temperature extremes. *Int J Climatol* 29:1642–1660. doi: 10.1002/joc.1807
- Cattiaux J, Yiou P, Vautard R (2012) Dynamics of future seasonal temperature trends and extremes in Europe: a multi-model analysis from CMIP3. *Clim Dyn* 38:1949–1964. doi: 10.1007/s00382-011-1211-1
- Christensen JH, Christensen OB (2007) A summary of the PRUDENCE model projections of changes in European climate by the end of this century. *Clim Change* 81:7–30. doi: 10.1007/s10584-006-9210-7
- Christensen JH, Boberg F, Christensen OB, Lucas-Picher P (2008) On the need for bias correction of regional climate change projections of temperature and precipitation. *Geophys Res Lett* 35:L20709. doi: 10.1029/2008GL035694
- Christensen J, Kjellström E, Giorgi F, et al. (2010) Weight assignment in regional climate models. *Clim Res* 44:179–194. doi: 10.3354/cr00916
- De Bono A, Giuliani G, Kluser S, Peduzzi P (2004) Impacts of summer 2003 heat wave in Europe. *UNEP/DEWA/GRID-Europe Environ Alert Bull* 2:1–4.

- Della-Marta PM, Luterbacher J, Weissenfluh H, et al. (2007) Summer heat waves over western Europe 1880–2003, their relationship to large-scale forcings and predictability. *Clim Dyn* 29:251–275. doi: 10.1007/s00382-007-0233-1
- Fischer EM, Seneviratne SI, Lüthi D, Schär C (2007) Contribution of land-atmosphere coupling to recent European summer heat waves. *Geophys Res Lett* 34:L06707. doi: 10.1029/2006GL029068
- Fischer EM, Schär C (2010) Consistent geographical patterns of changes in high-impact European heatwaves. *Nat Geosci* 3:398–403. doi: 10.1038/ngeo866
- Francis JA, Vavrus SJ (2012) Evidence linking Arctic amplification to extreme weather in mid-latitudes. *Geophys Res Lett* 39:L06801. doi: 10.1029/2012GL051000
- Giorgi F, Jones C, Asrar G (2009) Addressing climate information needs at the regional level: the CORDEX framework. *WMO Bull* 58:175–183.
- Hartmann DL (1994) *Global Physical Climatology*. Academic Press, San Diego
- Haylock MR, Hofstra N, Klein Tank AMG, et al. (2008) A European daily high-resolution gridded data set of surface temperature and precipitation for 1950–2006. *J Geophys Res* 113:D20119. doi: 10.1029/2008JD010201
- Holtanová E, Mikšovský J, Kalvová J, et al. (2012) Performance of ENSEMBLES regional climate models over Central Europe using various metrics. *Theor Appl Climatol* 108:463–470. doi: 10.1007/s00704-011-0542-5
- International Panel on Climate Change (IPCC) (2013) *Climate Change 2013: The Physical Science Basis. Contribution of Working Group I to the Fifth Assessment Report of the Intergovernmental Panel on Climate Change*. Cambridge University Press, Cambridge, United Kingdom and New York, NY, USA, p 1535.
- Jaeger EB, Seneviratne SI (2010) Impact of soil moisture–atmosphere coupling on European climate extremes and trends in a regional climate model. *Clim Dyn* 36:1919–1939. doi: 10.1007/s00382-010-0780-8
- Jung M, Reichstein M, Margolis HA., et al. (2011) Global patterns of land-atmosphere fluxes of carbon dioxide, latent heat, and sensible heat derived from eddy covariance, satellite, and meteorological observations. *J Geophys Res* 116:G00J07. doi: 10.1029/2010JG001566
- Kjellström E, Bärring L, Jacob D, et al. (2007) Modelling daily temperature extremes: recent climate and future changes over Europe. *Clim Change* 81:249–265. doi: 10.1007/s10584-006-9220-5
- Kjellström E, Boberg F, Castro M, et al. (2010) Daily and monthly temperature and precipitation statistics as performance indicators for regional climate models. *Clim Res* 44:135–150. doi: 10.3354/cr00932

- Klein Tank AMG, Wijngaard JB, Konnen GP, et al. (2002) Daily dataset of 20th-century surface air temperature and precipitation series for the European Climate Assessment. *Int J Climatol* 22:1441–1453. doi: 10.1002/joc.773
- Kyselý J (2008) Influence of the persistence of circulation patterns on warm and cold temperature anomalies in Europe: Analysis over the 20th century. *Glob Planet Change* 62:147–163. doi: 10.1016/j.gloplacha.2008.01.003
- Lhotka O, Kyselý J (2014) Characterizing joint effects of spatial extent, temperature magnitude and duration of heat waves and cold spells over Central Europe. *Int. J. Climatol.* doi: 10.1002/joc.4050
- Lorenz P, Jacob D (2010) Validation of temperature trends in the ENSEMBLES regional climate model runs driven by ERA40. *Clim Res* 44:167–177. doi: 10.3354/cr00973
- Meehl GA, Tebaldi C (2004) More intense, more frequent, and longer lasting heat waves in the 21st century. *Science* 305:994–997. doi: 10.1126/science.1098704
- Meijgaard E van, Ulft LH van, Bosveld FC, et al. (2008) The KNMI regional atmospheric climate model RACMO version 2.1. Tech report; TR – 302 43.
- Mueller B, Seneviratne SI (2014) Systematic land climate and evapotranspiration biases in CMIP5 simulations. *Geophys Res Lett* 41:128–134. doi: 10.1002/2013GL058055
- Němec L (2012) The Czech temperature record in Dobřichovice on 20 August 2012. *Meteorol Zprávy* 65:145–148.
- Nikulin G, Kjellström E, Hansson U, et al. (2011) Evaluation and future projections of temperature, precipitation and wind extremes over Europe in an ensemble of regional climate simulations. *Tellus A* 63A:41–55. doi: 10.1111/j.1600-0870.2010.00466.x
- Plavcová E, Kyselý J (2011) Evaluation of daily temperatures in Central Europe and their links to large-scale circulation in an ensemble of regional climate models. *Tellus A* 63A:763–781. doi: 10.1111/j.1600-0870.2011.00514.x
- Plavcová E, Kyselý J (2012) Atmospheric circulation in regional climate models over Central Europe: links to surface air temperature and the influence of driving data. *Clim Dyn* 39:1681–1695. doi: 10.1007/s00382-011-1278-8
- Samuelsson P, Jones CG, Willén U, et al. (2011) The Rossby Centre Regional Climate model RCA3: model description and performance. *Tellus A* 63A:4–23. doi: 10.1111/j.1600-0870.2010.00478.x
- Sanchez-Gomez E, Somot S, Déqué M (2009) Ability of an ensemble of regional climate models to reproduce weather regimes over Europe-Atlantic during the period 1961–2000. *Clim Dyn* 33:723–736. doi: 10.1007/s00382-008-0502-7
- Schneidereit A, Schubert S, Vargin P, et al. (2012) Large-Scale Flow and the Long-Lasting Blocking High over Russia: Summer 2010. *Mon Weather Rev* 140:2967–2981. doi: 10.1175/MWR-D-11-00249.1

- Seneviratne SI, Nicholls N, Easterling D, et al. (2012) Changes in climate extremes and their impacts on the natural physical environment. *Manag. Risks Extrem. Events Disasters to Adv. Clim. Chang. Adapt.* Cambridge University Press, Cambridge, UK, and New York, NY, USA, pp 109–230
- Small EE, Kurc SA. (2003) Tight coupling between soil moisture and the surface radiation budget in semiarid environments: Implications for land-atmosphere interactions. *Water Resour Res* 39:1–14. doi: 10.1029/2002WR001297
- Stegehuis A, Vautard R, Ciais P, Teuling R (2014) Simulating European heatwaves with WRF – a multi-physics ensemble approach. *Geophys. Res. Abstr.* Vol. 16. pp EGU2014–12613
- Uppala SM, Kallberg PW, Simmons AJ, et al. (2005) The ERA-40 re-analysis. *Q J R Meteorol Soc* 131:2961–3012. doi: 10.1256/qj.04.176
- van der Linden P, Mitchell JFB (2009) ENSEMBLES: Climate Change and its Impacts: Summary of research and results from the ENSEMBLES project. Met Office Hadley Centre, Exeter
- Vautard R, Gobiet A, Jacob D, et al. (2013) The simulation of European heat waves from an ensemble of regional climate models within the EURO-CORDEX project. *Clim Dyn* 41:2555–2575. doi: 10.1007/s00382-013-1714-z
- Wilks DS (2011) *Statistical Methods in the Atmospheric Sciences.* 676.
- Zentralanstalt für Meteorologie und Geodynamik (ZAMG) (2013) New temperature record: 40.5° C in Bad Deutsch-Altenburg. <http://www.zamg.ac.at/cms/de/klima/news/neuer-hitze-rekord-40-5deg-c-in-bad-deutsch-altenburg>. Accessed 16 Jan 2014

## 9 Article IV: ‘Climate change scenarios of heat waves in Central Europe and their uncertainties’

Ondřej Lhotka<sup>1,2,3</sup>, Jan Kyselý<sup>1,2</sup> and Aleš Farda<sup>2,4</sup>

<sup>1</sup> Institute of Atmospheric Physics CAS, Prague, Czech Republic

<sup>2</sup> Global Change Research Centre CAS, Brno, Czech Republic

<sup>3</sup> Faculty of Science, Charles University, Prague, Czech Republic

<sup>4</sup> Czech Hydrometeorological Institute, Prague, Czech Republic

**Abstract:** The study examines climate change scenarios of Central European heat waves with a focus on related uncertainties in a large ensemble of regional climate model (RCM) simulations from the EURO-CORDEX and ENSEMBLES projects. Historical runs (1970–1999) driven by global climate models (GCMs) are evaluated against the E-OBS gridded data set in the first step. Although the RCMs are found to reproduce the frequency of heat waves quite well, those RCMs with the coarser grid (25 and 50 km) considerably overestimate the frequency of severe heat waves. This deficiency is improved in higher-resolution (12.5 km) EURO-CORDEX RCMs. In the near future (2020–2049), heat waves are projected to be nearly twice as frequent in comparison to the modelled historical period, and the increase is even larger for severe heat waves. Uncertainty originates mainly from the selection of RCMs and GCMs because the increase is similar for all concentration scenarios. For the late 21<sup>st</sup> century (2070–2099), a substantial increase in heat wave frequencies is projected, the magnitude of which depends mainly upon concentration scenario. Three to four heat waves per summer are projected in this period (compared to less than one in the recent climate) and severe heat waves are likely to become a regular phenomenon. This increment is primarily driven by a positive shift of temperature distribution, but changes in its scale and enhanced temporal autocorrelation of temperature also contribute to the projected increase in heat wave frequencies.

**Keywords:** heat waves; climate change; regional climate models; CORDEX; Central Europe

### 9.1 Introduction

Heat waves are one of the main concerns in relation to the ongoing climate change. The severity of heat waves has increased across European regions in the recent decades (Della-Marta et al. 2007; Kyselý 2010; Valeriánová et al. 2015). The most notable events occurred in 2003 over Western Europe (Fink et al. 2004) and in 2010 over Eastern Europe and Russia (Schneidereit et al. 2012). Recently, Central Europe was affected by several extraordinary heat waves in summer 2015, during which the highest historically recorded daily maximum temperature ( $T_{\max}$ , 40.3°C) was measured in Germany (DWD 2015). Central Europe experienced extremely hot weather conditions also in summer 2013, which ranked as the fifth

warmest since 1951 at the continental scale, and the heat wave severity broke historical records at several stations with long-term measurement (Lhotka and Kyselý 2015b). In 2013, the highest historically recorded  $T_{\max}$  (40.5°C) was reached in Austria (ZAMG 2013) and the highest temperature for the Czech Republic (40.4°C) was observed one year earlier, in August 2012 (Holtanová et al. 2015). It is estimated that the probability of severe heat waves has increased by a factor of 2–4 due to climate change (Coumou and Rahmstorf 2012), and Fischer and Knutti (2015) concluded that about 75% of hot extremes over land in the past six decades are attributable to the observed warming.

Heat waves cause excess illness and mortality, losses in agricultural production, forest fires, increased energy demand for cooling, and other related hazards (Beniston et al. 2007), and there is growing evidence that the European agricultural sector will need to adopt suitable adaptation strategies in relation to more frequent heat stress (Iglesias et al. 2012). The 2003 heat waves caused 70,000 excess deaths in Europe, mainly in the elderly population (Robine et al. 2008), and the 2010 heat wave in Russia was associated with a death toll of 55,000 (Barriopedro et al. 2011). Bastos et al. (2014) showed that both events led to a marked decrease of plant productivity. In addition, numerous wildfires that occurred in 2010 caused continuous episodes of extreme air pollution in several Russian cities (Konovalov et al. 2011).

In general, heat waves are expected to become more frequent, more intense, and longer lasting in a future climate (Meehl and Tebaldi 2004; Lau and Nath 2014; Lemonsu et al. 2014). More specifically, based on ENSEMBLES regional climate models (RCMs) driven by global climate models (GCMs) forced by the SRES A1B scenario, Fischer and Schär (2010) showed that the occurrence of heat waves is projected to increase substantially by the end of the 21<sup>st</sup> century in most European regions and their peak temperature may be enhanced by approximately 5°C. These changes are usually reported to be driven rather by higher mean temperature than by larger temperature variability (Ballester et al. 2010). There is nevertheless a considerable spread among individual climate models, causing substantial uncertainties in future projections.

The evaluation of uncertainties is fundamental for any application (Déqué et al. 2012) and presents a key challenge for adaptation planning. Uncertainties in climate projections originate from three main sources: the choice of emission/concentration scenario, internal variability of climate, and model uncertainties (Hawkins and Sutton 2009). Concentration scenarios represent possible ways of human society's development that alter a radiative forcing on climate (Moss et al. 2010), mainly through a modification of atmospheric

chemistry and land-cover changes. In the extratropics, the uncertainty based on internal climate variability is mainly associated with atmospheric dynamics, dominated at the hemispheric scale by annular modes (Deser et al. 2012), such as the North Atlantic Oscillation (Hurrell and Deser 2010). The model uncertainty arises from the nature of model design, as different RCMs exhibit various internal behaviour and their simulations are driven by different GCMs.

Identifying typical features of individual models related to heat waves in the historical climate is crucial for credible interpretation of their projections. Kjellström et al. (2007) demonstrated that RCMs tend to underestimate high summer temperatures over Scandinavia and the British Isles, while an overestimation was found over Eastern Europe, the Mediterranean, and the Iberian Peninsula. In Central Europe, a negative bias of daily maximum temperature is often reported (Nikulin et al. 2011; Plavcová and Kyselý 2011), but Kjellström et al. (2010) showed that this bias is one of the smallest across the European domain. Reproduction of heat waves nevertheless requires not only a good simulation of the right tail of a temperature distribution but also of the persistence of high temperatures. The capability of RCMs to simulate heat waves over Europe was evaluated by Vautard et al. (2013), who found that biases in modelled temperature influenced characteristics of heat waves that were too persistent and severe. A different approach to defining heat waves was adopted by Lhotka and Kyselý (2015c), who took into account their temperature magnitude, length, and spatial extent. Simulated heat waves were then shorter but more frequent, and their peak temperatures were substantially overestimated.

Previous studies on climate change scenarios have not evaluated in detail the aforementioned uncertainties when analyzing heat waves in a future climate. The focus of the present study is on uncertainties connected with the choice of emission/concentration scenario (RCP 4.5, RCP 8.5, and SRES A1B), model resolution (12.5, 25, and 50 km), and the climate model (31 RCM × GCM combinations). The changes and uncertainties are assessed for the near future (2020–2049) and the late 21<sup>st</sup> century (2070–2099). An evaluation of the RCMs is performed against the E-OBS gridded data set over the 1970–1999 historical period. Since the study involves a large ensemble of RCMs with various characteristics, this approach allows analysing magnitude of projected changes with respect to the related uncertainties.

## 9.2 Data and methods

### 9.2.1 Area of interest and observed data

Heat waves are analysed over Central Europe that is situated approximately between 47–53°N and 8–22°E (Figure 9.1). The area contains 4,160 (80 × 52), 1,040 (40 × 26), or 260 (20 × 13) grid points, depending on horizontal grid spacing of a particular data (12.5, 25 or 50 km, respectively). This region's location is designed for the most common rotated pole grid and is identical for observed data and all 3 horizontal grid spacings of the RCMs. The E-OBS 11.0 gridded data set (0.22 rotated grid, Haylock et al. 2008) is used as a source of observations. This data set covers whole continental Europe over the 1950–2014 period, but the evaluation of model simulations is performed during the shorter 1970–1999 period due to the limited time span of modelled data.

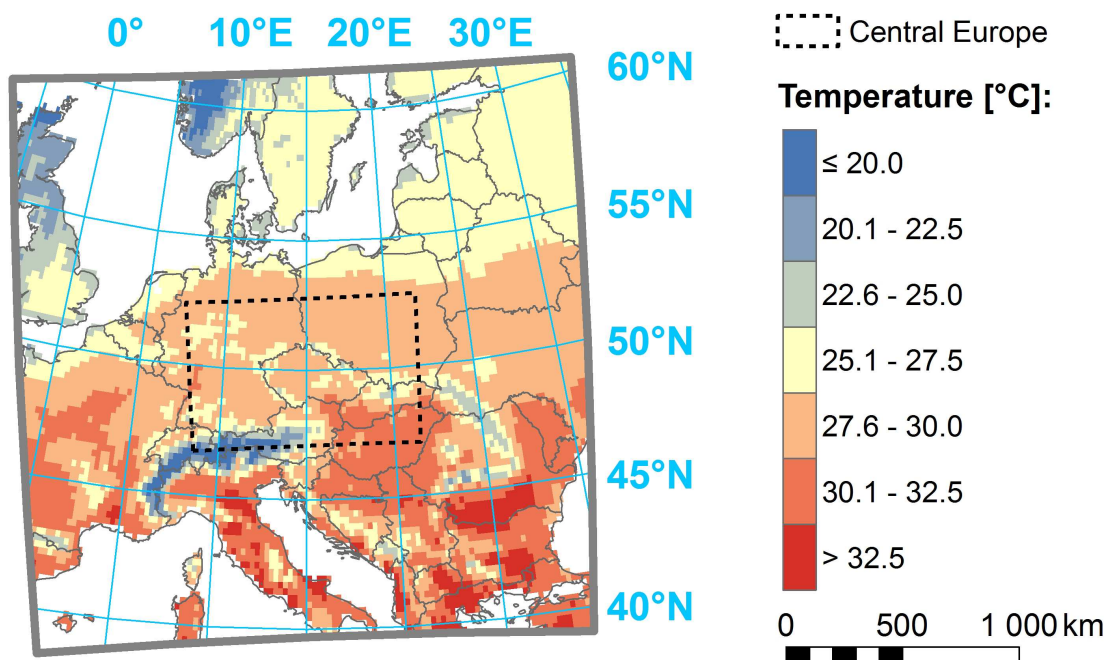


Figure 9.1. Definition of Central Europe (black dashed polygon) and the 90<sup>th</sup> percentile of summer daily maximum temperature calculated for the 1970–1999 period (colour shading) in the E-OBS 11.0 gridded data set.



### 9.2.2 Climate model simulations

Modelled data are taken from the EURO-CORDEX (Jacob et al. 2014) and ENSEMBLES (van der Linden and Mitchell 2009) projects. While EURO-CORDEX provides RCM simulations in 50 km and 12.5 km resolutions driven by RCP scenarios (van Vuuren et al. 2011), the ENSEMBLES project is valuable in that it provides RCMs in the 25 km resolution forced by the SRES A1B scenario (Arnell et al. 2004). Individual RCMs had been subjected to various upgrades during the time period between the ENSEMBLES project phase and the EURO-CORDEX simulations. The EURO-CORDEX models investigated in this study had improved their respective sets of physical parameterizations while keeping their basic principles from the ENSEMBLES stage. Another notable change is the use of more recent surface properties data sets and improved restart techniques, for example in RCA4 (Strandberg et al. 2014) and CLM (Davin et al. 2011). The majority of the model simulations are available up to the end of the 21<sup>st</sup> century (Table 9.1), and all simulations have available their historical runs (1970–1999) driven by the same GCM.

Table 9.1. Number of model simulations from the EURO-CORDEX and ENSEMBLES projects for the near future and the late 21<sup>st</sup> century. Decimal numbers represent the horizontal grid spacing, “RCP” or “SRES” denote the concentration scenario.

	2020–2049	2070–2099
CORDEX - 0.11 - RCP 4.5	10	10
CORDEX - 0.11 - RCP 8.5	10	10
CORDEX - 0.44 - RCP 4.5	13	13
CORDEX - 0.44 - RCP 8.5	13	13
ENSEMBLES - 0.22 - SRES A1B	16	13
Total	62	59

Individual model simulations from the EURO-CORDEX project are listed in Table 9.2. These models have 0.11° (12.5 km) or 0.44° (50 km) horizontal grid spacing and are forced by the RCP 4.5 or RCP 8.5 scenarios. The RCP 4.5 scenario represents stabilization of concentrations without overshooting effective radiative forcing (ERF) of 4.5 W/m<sup>2</sup> relative to pre-industrial values (~650 ppm CO<sub>2</sub> equivalent). This is achieved by implementing mitigation policies (Thomson et al. 2011). The total ERF is 2.3 W/m<sup>2</sup> in year 2020, 3.4 W/m<sup>2</sup> in 2050, 3.8 W/m<sup>2</sup> in 2070, and 3.9 W/m<sup>2</sup> in 2100 (Prather et al. 2013). By contrast, the RCP 8.5 scenario represents a long-term large energy demand without implementation of mitigation policies, thus leading to high greenhouse gas emissions (Riahi et al. 2011). This

scenario is presumed to reach ERF of  $8.5 \text{ W/m}^2$  ( $\sim 1370$  ppm CO<sub>2</sub> equivalent) and the total anthropogenic ERF is  $2.3 \text{ W/m}^2$  in year 2020,  $4.4 \text{ W/m}^2$  in 2050,  $5.9 \text{ W/m}^2$  in 2070, and  $8.0 \text{ W/m}^2$  in 2100 (Prather et al. 2013). It should be mentioned that the CORDEX ensemble may be unbalanced due to the majority of RCA4 RCM simulations (especially in the  $0.44^\circ$  grid), which has to be taken into account when interpreting the model outputs.

Table 9.2. RCM  $\times$  GCM matrix for the EURO-CORDEX project. “g12” (“g50”) denotes simulations available only in the 12.5 (50) km grid and “G” denotes simulations available in both grids. All simulations are forced by both RCP 4.5 and RCP 8.5 scenarios.

	CCCma	CNRM	CSIRO	HadGEM	ICHEC	IPSL	MIROC	MPI	NCC	NOAA
CLM-CCLM		g12			g12			G		
DMI-HIRHAM					G					
KNMI-RACMO					G					
SMHI-RCA4	g50	G	g50	G	G	G	g50	G	g50	g50

The ENSEMBLES project contains 16 simulations that use rotated grid and the  $0.22^\circ$  (25 km) horizontal grid spacing (Table 9.3). These simulations are forced by the SRES A1B concentration scenario that represents rapid economic growth with increasing globalisation, fast technological change, and low population increase (Arnell et al. 2004). The total anthropogenic ERF is  $2.2 \text{ W/m}^2$  in year 2020,  $4.2 \text{ W/m}^2$  in 2050,  $5.3 \text{ W/m}^2$  in 2070, and  $6.0 \text{ W/m}^2$  in 2100 (Prather et al. 2013).

Table 9.3. RCM  $\times$  GCM matrix for the ENSEMBLES project. “X” denotes simulations covering the whole 1970–2099 period while “I” represents the limited 1970–2050 period. Hadley Centre (HC) models are considered as three individual simulations, due to their different climatic responses to radiative forcing.

	ARPEGE	BCM	CGCM3	ECHAM5	HadCM3Q0	HadCM3Q3	HadCM3Q16	IPSL
C4I-RCA3							X	
DMI-HIRHAM	X	X		X				
ETHZ-CLM					X			
GKSS-CLM								I
HC-HadRM3Q0					X			
HC-HadRM3Q3						X		
HC-HadRM3Q16							X	
KNMI-RACMO				X				
MPI-REMO				X				
NO-HIRHAM		I			I			
SMHI-RCA3		X		X		X		

In some studies, a relatively large numbers of gaps in RCM  $\times$  GCM matrices were completed using statistical methods for data reconstruction. Nevertheless, Heinrich et al. (2014) showed that seasonal mean climate change of the ENSEMBLES RCM projections is not significantly biased due to the lack of driving GCMs. This technique is therefore not employed in the present study, and we analyse only the available simulations.

### 9.2.3 Definition of heat wave

Heat waves are defined with respect to their temperature magnitude, length, and spatial extent. First, all data are recalculated to the  $0.44^\circ$  (50 km) grid through averaging 4 (16) respective grid cells when transforming the original 25 km (12.5 km) grid. Inasmuch as a sensitivity study had shown the occurrence of heat waves to be identical in selected  $0.22^\circ$  (25 km) data sets and in their recalculated  $0.44^\circ$  versions, we found this approach useful for direct comparison of heat wave characteristics among all data sets involved. An analogous procedure was applied by Kotlarski et al. (2014) when comparing the performance of CORDEX and ENSEMBLES models driven by reanalyses. We note that some heat wave characteristics (e.g. temperature amplitude) cannot be directly compared between different resolutions, and this approach also overcomes the issue with the missing observed  $0.11^\circ$  (12.5 km) grid data for the evaluation of historical runs.

The definition of heat waves is based on the occurrence of hot days over Central Europe and is similar to that proposed in Lhotka and Kyselý (2015a). A hot day occurs when the average of  $T_{\max}$  deviations from the 90<sup>th</sup> percentile of their summer distribution is positive over Central Europe (calculated in the 1970–1999 period). The percentiles are calculated individually for observed data and each model simulation in order to remove a  $T_{\max}$  bias. This approach is suitable when focusing rather on behaviour of the right tail of the  $T_{\max}$  distribution and the spatial and temporal structure of daily temperatures (which are essential for heat waves) than on the  $T_{\max}$  bias itself. The use of the respective percentiles has already been employed in previous studies (Ballester et al. 2010; Fischer and Schär 2010; Vautard et al. 2013). In future time slices, the calculated percentiles from the historical period are kept. A heat wave is defined by at least three consecutive hot days. Therefore, a heat wave is regarded as a several days long period with high temperatures over large Central European areas.

### 9.2.4 Heat wave characteristics

Four characteristics of a heat wave are calculated so that each event is described by (i) temperature amplitude, (ii) length, (iii) spatial extent, and (iv) extremity index. Temperature amplitude is the highest daily  $T_{\max}$  excess above the 90<sup>th</sup> percentile of the summer  $T_{\max}$  distribution during a heat wave (at any grid point in Central Europe) and represents the temperature anomaly of its peak. Length is the number of consecutive hot days that form a heat wave (minimum of 3 hot days). Spatial extent is represented by an area where  $T_{\max}$  deviations above the 90<sup>th</sup> percentile of summer  $T_{\max}$  distribution are positive for at least 3 successive days, and it is given as a ratio (1.0 means that whole Central Europe is affected by a heat wave). The extremity index is adopted from Lhotka and Kyselý (2015a) and is defined as a sum of positive  $T_{\max}$  deviations in all Central European grid points during a heat wave, scaled by the total number of (recalculated) grid points over Central Europe (260). This index captures joint effects of temperature, length, and spatial extent of heat waves. An example of the heat wave definition and calculation of its characteristics is given in Figure 9.2.

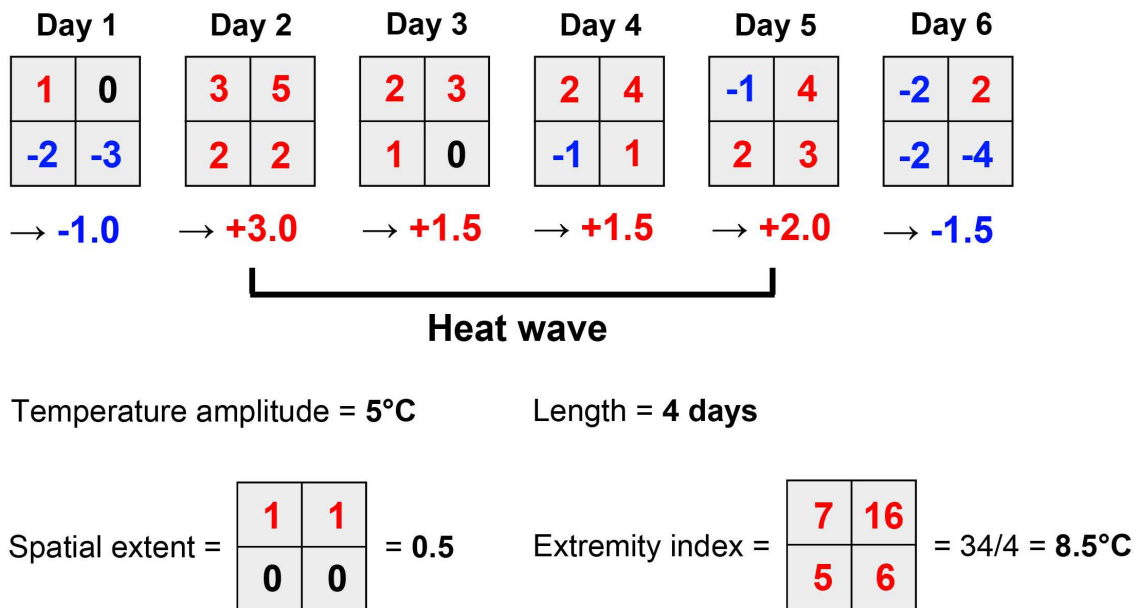


Figure 9.2. Theoretical example of the heat wave definition and calculation of heat wave characteristics over a hypothetical area represented by 4 grid points. Positive (red), negative (blue), and zero (black) deviations from the 90<sup>th</sup> percentile of summer  $T_{\max}$  distribution are shown.

### 9.2.5 Temporal autocorrelation and statistical testing

Analogously to Lhotka and Kysely (2015c), persistence of  $T_{\max}$  over Central Europe is analysed by temporal autocorrelation computed as Pearson product moment coefficients for lagged data pairs. For each day in summer,  $T_{\max}$  values across 260 grid points over Central Europe are averaged into a regionally averaged  $T_{\max}$ , which is used to compute correlation coefficients. Since the summer  $T_{\max}$  series is not continuous, we calculated correlation coefficients individually for each summer and averaged them thereafter. Statistical significance of changes in temporal autocorrelation is assessed using the two-sided Wilcoxon rank sum test. This non-parametric test is chosen because the criterion of data normality is not always met.

### 9.3 Observed heat waves and evaluation of historical RCM simulations

Because the study includes evaluating performance of the RCMs' historical simulations, observed heat wave characteristics are analysed first. In the E-OBS data, 22 heat waves are found in the 1970–1999 period (7.3 heat waves per decade). Their temperature amplitude ranges from 4.1 to 9.8°C, the length varies from 3 days (by definition) to 16 days, the spatial extent ranges from 0.24 to 1, and the extremity index varies from 2.5 to 51.4°C. Median values of heat wave characteristics are 5.7°C (temperature amplitude), 4 days (length), 0.64 (spatial extent), and 7.4°C (extremity index, Figure 9.3). Hereafter, a heat wave is considered “severe” when all its characteristics are equal to or exceed these median values.

Only 5 of the 22 heat waves (in 1971, 1974, 1976, 1992, and 1994) meet this severe heat wave criterion (1.7 severe heat waves per decade). The heat wave of 1994 is exceptional due to its length (16 days) and a very high extremity index. This long-lasting event affected whole Central Europe, but its temperature amplitude is not extremely pronounced (Figure 9.3). Larger-scale temperature patterns associated with each severe heat wave are shown in Figure 9.4.

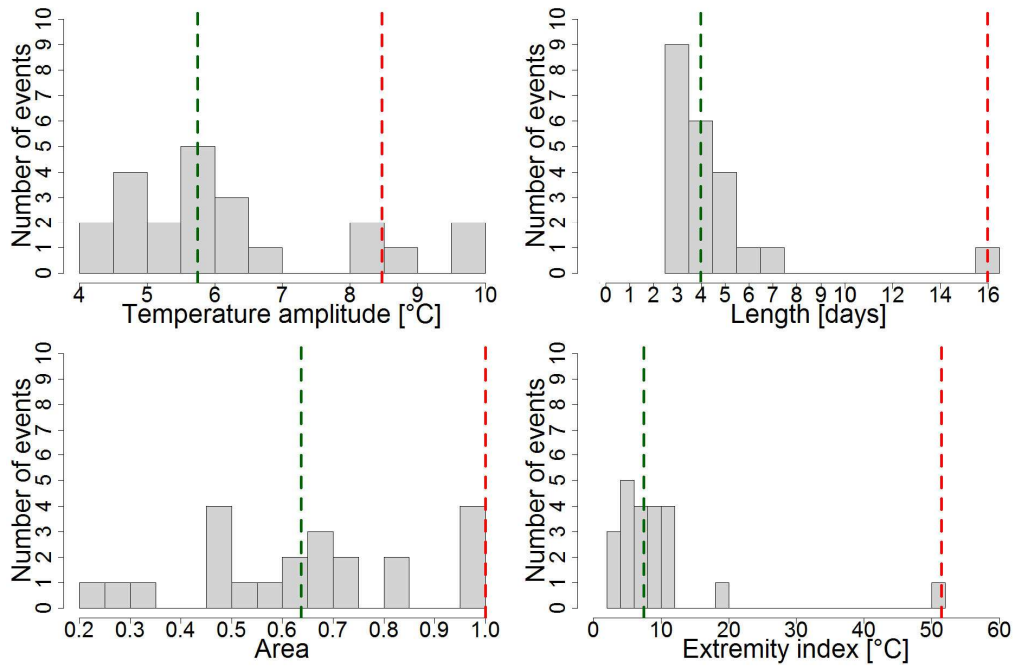


Figure 9.3. Histograms of heat wave characteristics (temperature amplitude, length, spatial extent, extremity index) for observed heat waves in the 1970–1999 period. Green vertical lines represent median values and red vertical lines indicate values for the extraordinary 1994 heat wave.

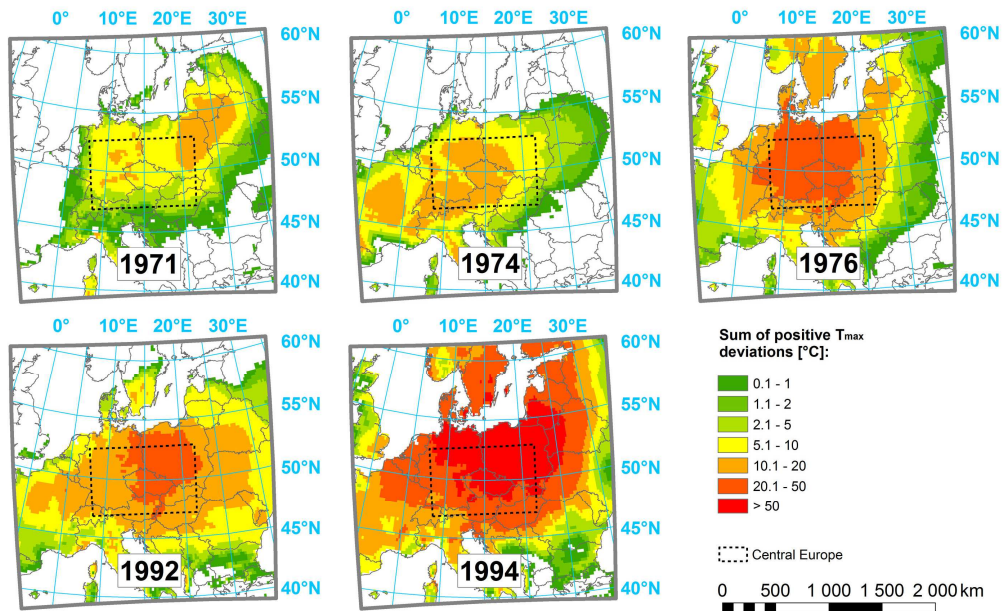


Figure 9.4. Severe heat waves over Central Europe during the 1970–1999 period. Colour shading represents the sum of positive  $T_{\max}$  deviations from the 90<sup>th</sup> percentile of its summer distribution. Note that only grid points located within the Central European domain are used to compute heat wave characteristics.

Evaluation of simulated frequencies of heat waves and severe heat waves is performed individually for (i) EURO-CORDEX RCMs with the  $0.11^\circ$  grid, (ii) EURO-CORDEX RCMs with the  $0.44^\circ$  grid, and (iii) ENSEMBLES RCMs with the  $0.22^\circ$  km grid. These groups are hereafter referred to as COR11, COR44, and ENS22, respectively. In all three groups, frequencies of ‘all’ heat waves are reproduced considerably better compared to severe heat waves. Although a large variance is present in ENS22, the observed frequency of heat waves (7.3/decade) fits into the simulated interquartile range (IQR). The IQR in COR11 and COR44 is beyond the observed frequency, but the variance is smaller and no substantial outliers are present in COR11. For severe heat waves, a large overestimation of their frequencies is found, which is mainly linked to substantial overestimation of median temperature amplitude in the RCMs. Although the observed frequency of severe heat waves (1.7/decade) is located in the lower quartile in all three RCM groups (Figure 9.5a,b,c), the higher-resolution COR11 performed best, because the RCMs in this group are able to capture median spatial extent of heat waves reasonably well. On the other hand, an event with equal or higher characteristics compared to the exceptional heat wave that occurred in 1994 (temperature amplitude =  $8.5^\circ\text{C}$ , length = 16 days, spatial extent = 1.0, extremity index =  $51.4^\circ\text{C}$ ) was found only in 3 of the 39 model simulations for the historical period.

Changes in temporal autocorrelation of regionally averaged  $T_{\max}$  (hereafter simply referred as autocorrelation) are assessed for lags from 1 to 10 days. In E-OBS, the autocorrelation for lag 1 is 0.85 and then it decreases exponentially to 0.06 for lag 10. COR11 and COR44 (historical simulations) significantly underestimate the autocorrelation for the first two lags (Table 9.4). This underestimation is particularly pronounced and highly significant for the lag of 1 day (at the 1% significance level). By contrast, the autocorrelation was overestimated from lag 5 compared to E-OBS, but these changes are found to be insignificant. In ENS22, the autocorrelation is significantly enhanced for lags 4–9, while the underestimation for lag 1 is small and insignificant (Table 9.4).

In order to investigate an effect of model resolution on the simulation of heat wave and severe heat wave frequencies, eight models from the CORDEX project which are available in both grids (Table 9.2) were selected (Figure 9.5d,e). The overall patterns of probability density functions (PDFs) are similar to those in Figure 9.5a,b, which means that the differences between COR11 and COR44 are related to different model resolutions rather than different composition of ensembles in these groups.

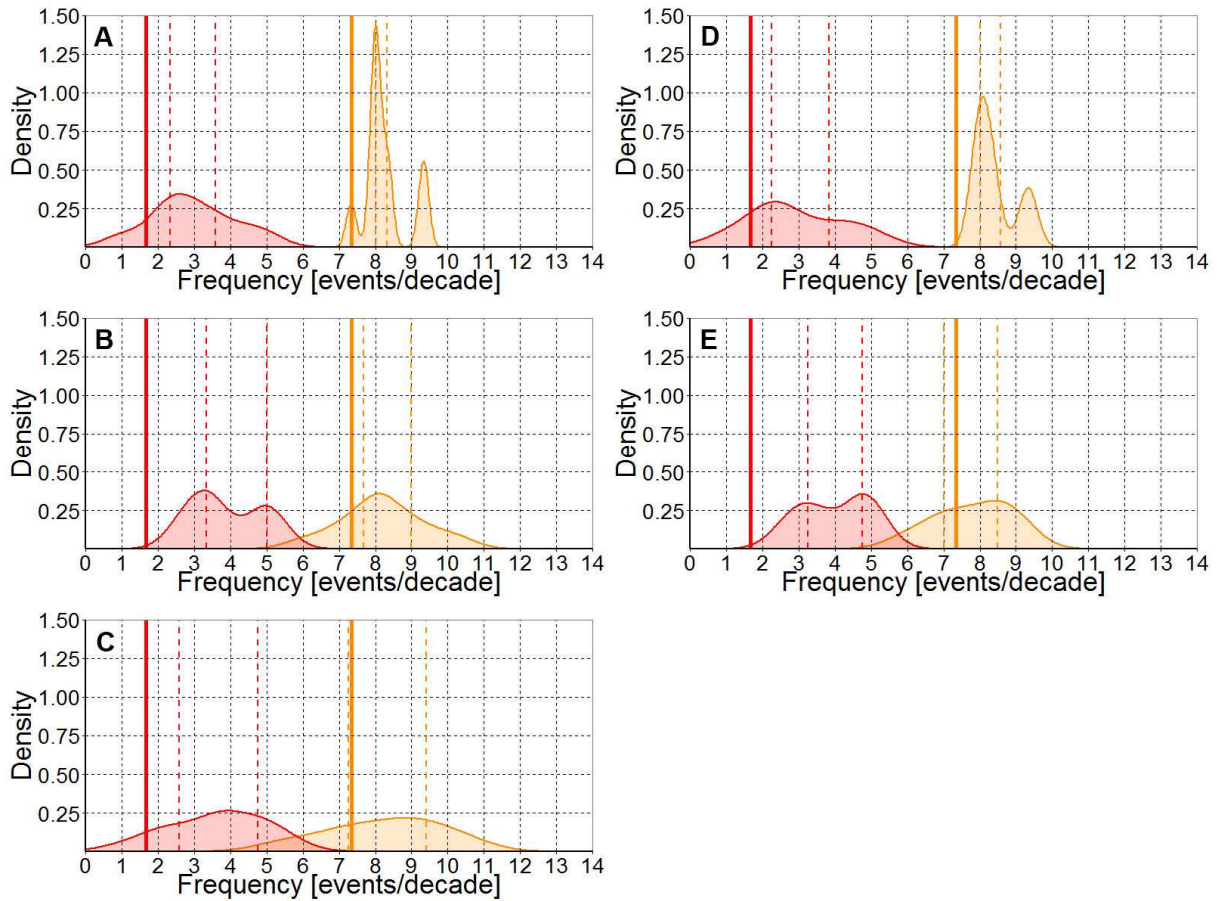


Figure 9.5. Probability density functions (PDFs) of heat waves (orange) and severe heat waves (red) frequencies for (A) COR11, (B) COR44, and (C) ENS22. CORDEX models that are available in both grids (which allows for a fair comparison) are shown in (D) – 0.11° grid and (E) – 0.44° grid. Solid vertical lines represent the frequency in E-OBS while dashed vertical lines delimit the interquartile ranges of model historical simulations.

Table 9.4. Temporal autocorrelation of summer daily maximum temperature for the historical period (1970–1999). L1–L10 represents lags from 1 to 10 days, bold (bold underlined) values are significantly different from E-OBS at the 5% (1%) significance level.

	L1	L2	L3	L4	L5	L6	L7	L8	L9	L10
E-OBS	0.85	0.61	0.42	0.30	0.22	0.17	0.14	0.11	0.08	0.06
COR11	<b><u>0.79</u></b>	<b><u>0.53</u></b>	0.38	0.30	0.24	0.19	0.16	0.13	0.11	0.09
COR44	<b><u>0.80</u></b>	<b><u>0.53</u></b>	0.38	0.29	0.23	0.18	0.15	0.13	0.10	0.08
ENS22	0.83	0.61	0.46	<b><u>0.37</u></b>	<b><u>0.31</u></b>	<b><u>0.26</u></b>	<b><u>0.21</u></b>	<b><u>0.18</u></b>	<b><u>0.15</u></b>	0.11



#### 9.4 Heat wave scenarios and uncertainties for near future and late 21<sup>st</sup> century

In the near future time slice (2020–2049), both heat waves and severe heat waves are projected to become more frequent in comparison to the modelled historical climate (1970–1999). Relatively large uncertainty was found, inasmuch as the IQRs for frequencies of these events are considerably widened compared to the historical simulations. The largest increment of the heat wave frequency is present in CORDEX groups forced by the ‘low concentration’ RCP 4.5 scenario, however, it should be noted that differences among scenarios are small in this period. There is no clear dependence on model resolution, because in both COR11 and COR44 groups heat waves and severe heat waves are projected to be more enhanced under RCP 4.5 (Figure 9.6).

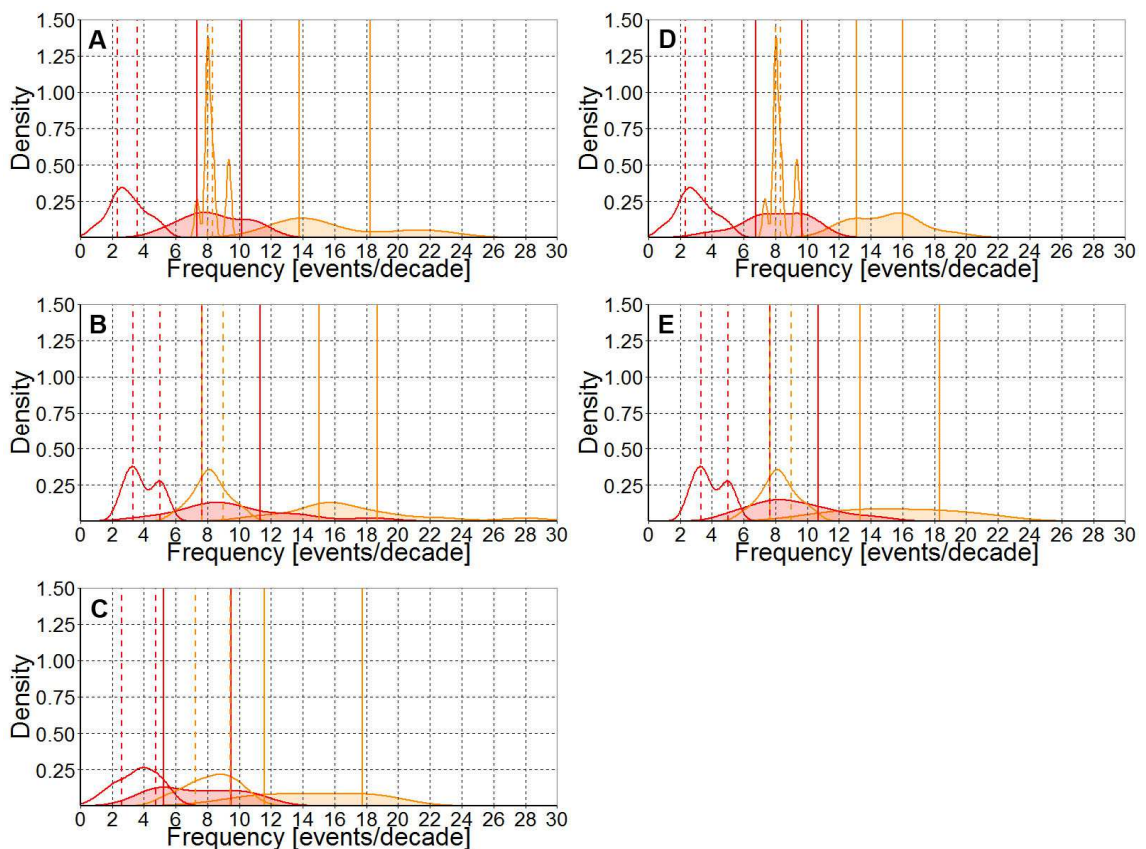


Figure 9.6. Probability density functions (PDFs) of heat waves (orange) and severe heat waves (red) frequencies for (A, B) COR11 and COR44 forced by the RCP 4.5 scenario, (C) ENS22 forced by the SRES A1B scenario and (D, E) COR11 and COR44 forced by the RCP 8.5 scenario. Solid vertical lines delimit the interquartile ranges of model simulations for the near future while dashed vertical lines represent the interquartile ranges of model simulations for the historical runs.

The frequency of heat waves is projected to be nearly twice higher compared to the modelled historical period. The largest increase is found for COR44 forced by RCP 4.5, which relates to the largest change in the scale of the  $T_{\max}$  distribution and also enhanced temporal autocorrelation (Table 9.5). Although the increase in median  $T_{\max}$  is comparable across all model groups, the location of the 90<sup>th</sup> percentile is particularly shifted in COR44 forced by RCP 4.5. The lowest increment of the heat wave frequency was present in ENSEMBLES simulations, which corresponds with generally negative changes in temporal autocorrelation of  $T_{\max}$  and only a small positive change of the scale parameter. A link between the increment of heat waves and changes in temporal autocorrelation is poorly expressed in this period, compared to the shift of the 90<sup>th</sup> percentile (Figure 9.7).

Table 9.5. Projected changes in shift and scale of summer daily maximum temperature distributions and temporal autocorrelation for the near future (2020–2049) compared to their respective historical runs. MED (P90) represents changes in median and the 90<sup>th</sup> percentile of summer daily maximum temperature (°C) over Central Europe. L1–L10 represents lags from 1 to 10 days, bold values are significant at the 5% significance level. ‘%’ represents percentage of the 90<sup>th</sup> percentile increase that is explained by the shift of median.

	MED	P90	%	L1	L2	L3	L4	L5	L6	L7	L8	L9	L10
COR11 – RCP 4.5	+1.1	+1.5	73	+0.01	+0.02	+0.02	+0.02	+0.02	+0.03	+0.03	+0.03	+0.02	+0.02
COR44 – RCP 4.5	+1.3	+1.9	68	+0.06	+0.04	+0.04	+0.04	<b>+0.04</b>	<b>+0.04</b>	<b>+0.04</b>	<b>+0.04</b>	<b>+0.04</b>	<b>+0.03</b>
COR11 – RCP 8.5	+1.2	+1.5	80	+0.01	+0.01	+0.01	+0.01	+0.01	+0.02	+0.02	+0.02	+0.02	+0.02
COR44 – RCP 8.5	+1.3	+1.7	76	+0.05	+0.03	+0.02	+0.02	+0.03	+0.02	+0.02	+0.02	+0.03	<b>+0.03</b>
ENS22 – SRES A1B	+1.3	+1.4	93	0.00	-0.01	-0.01	-0.02	-0.02	-0.02	-0.02	-0.02	-0.01	0.00

In general, severe heat waves are expected to be more enhanced than heat waves (by a factor of 2–3 compared to historical simulations) and their frequency is projected to become comparable to the frequency of all heat waves in the 1970–1999 period. It should be emphasized, however, that the model simulations considerably overestimated the severe heat wave frequencies in the recent climate, and thus this projection might be biased. Analogously to the historical period, the frequency of exceptional events with magnitude equal to or higher than the 1994 heat wave is analysed. In the 30-year period 2020–2049, 29 of the 62 model simulations project at least one such event, and 6 RCM simulations project this type of event to occur at least once per decade. These exceptional heat waves are found in all model groups and they are not linked to specific concentration scenarios. Despite the substantial increment

of these events compared to the historical simulations, they are still rather rare in the near future projections.

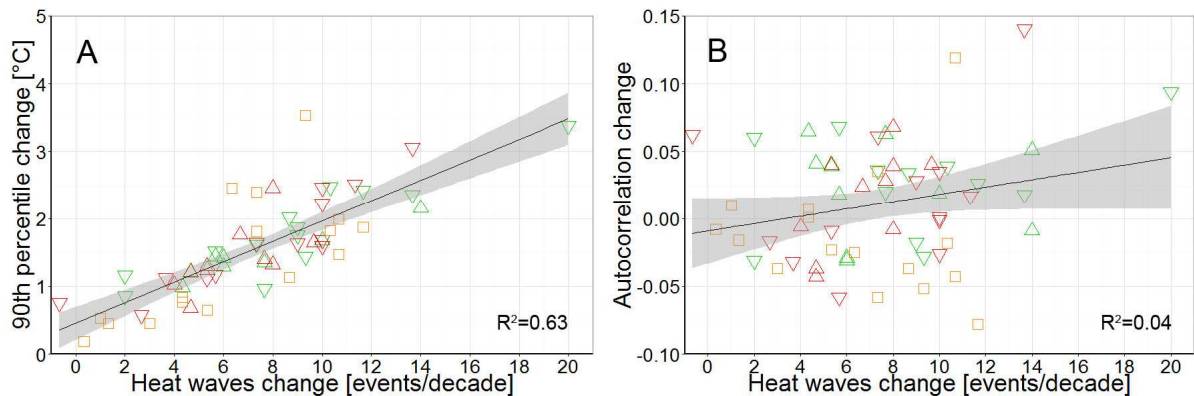


Figure 9.7. Relationships between (A) changes in 90<sup>th</sup> percentile and heat waves frequency and (B) changes in temporal autocorrelation and heat waves frequency in near future (2020–2049). Green colour represent simulations using the low-concentration RCP 4.5 scenario, orange colour depicts mid-concentration SRES A1B and red colour represents high-concentration RCP 8.5. Standard triangles illustrate simulations with 12.5 km grid, squares represents 25 km grid and inverse triangles depicts 50 km grid. Linear regression lines with 95% confidence interval are fitted.

Changes of heat wave and severe heat wave frequencies are clearly linked to the concentration scenarios in the late 21<sup>st</sup> century time slice (2070–2099). The largest increases of these events are found in COR11 and COR44 driven by RCP 8.5. In these groups, the frequency of heat waves is projected to be enhanced by a factor of 4–5 compared to the historical simulations, indicating 3–4 heat waves per year on average at the end of the 21<sup>st</sup> century. By contrast, the increase in the heat wave occurrence is roughly halved under the RCP 4.5 scenario (about two heat waves per year on average). ENS22, with the SRES A1B scenario, projects an increase between the two RCP scenarios, which is in line with the average effective radiative forcing for 2070–2099 (Figure 9.8). The largest increment under RCP 8.5 is related to a large shift of the  $T_{\max}$  distribution and positive significant changes in temporal autocorrelation of  $T_{\max}$  (Table 9.6). A relationship between the increment of heat waves and changes in temporal autocorrelation is tighter in this period compared to near future, but changes in frequency of heat waves are mainly driven by temperature increase and increase in temporal autocorrelation has only a secondary effect (Figure 9.9).

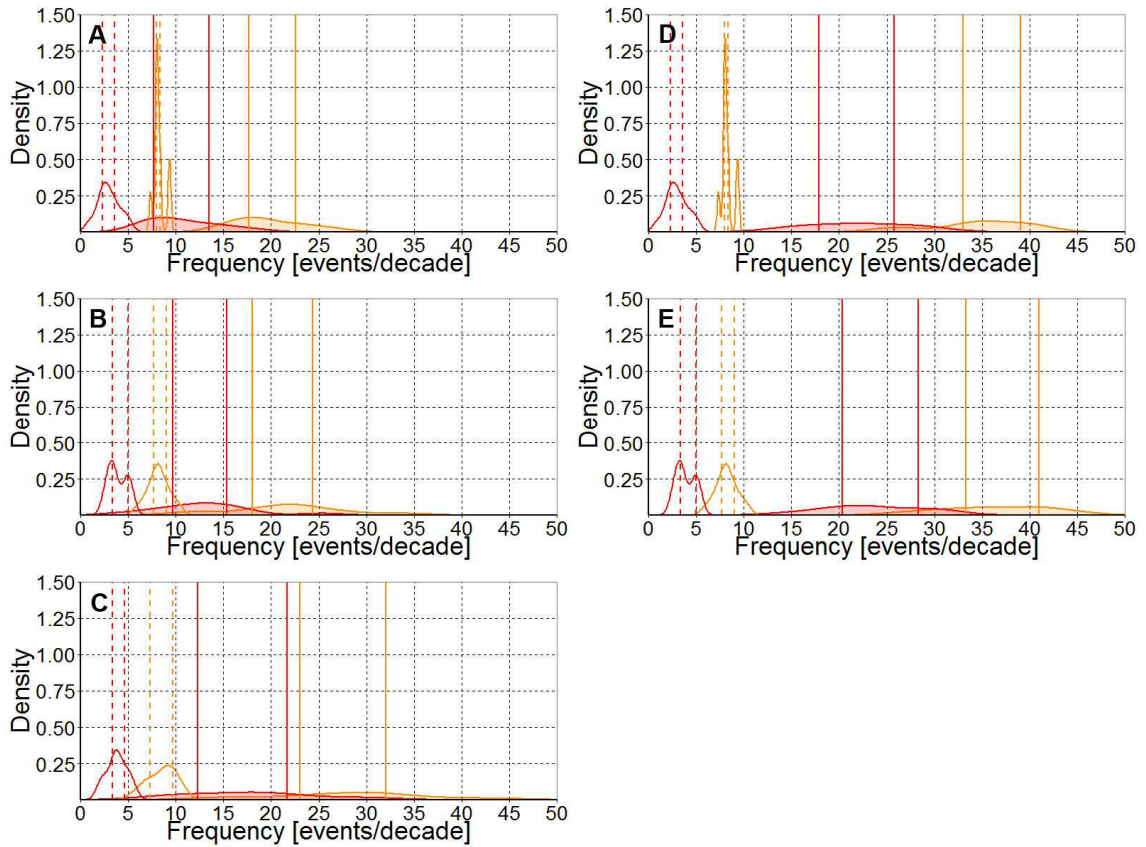


Figure 9.8. Same as Figure 9.6, but for the late 21<sup>st</sup> century. Note the different scale of the x-axis.

Table 9.6. Same as Table 2, but for the late 21<sup>st</sup> century. The bold underlined values are significant at the 1% significance level.

	MED	P90	%	L1	L2	L3	L4	L5	L6	L7	L8	L9	L10
COR11 – RCP 4.5	+1.9	+2.3	83	<b><u>+0.01</u></b>	+0.02	+0.03	+0.03	+0.03	+0.04	+0.03	+0.03	+0.03	+0.03
COR44 – RCP 4.5	+2.1	+2.7	78	+0.06	+0.04	+0.03	+0.03	+0.04	+0.03	<b><u>+0.03</u></b>	+0.03	<b><u>+0.04</u></b>	<b><u>+0.04</u></b>
COR11 – RCP 8.5	+3.8	+4.6	83	<b><u>+0.02</u></b>	<b><u>+0.03</u></b>	+0.03	+0.04	<b><u>+0.04</u></b>	<b><u>+0.04</u></b>	+0.04	+0.03	+0.03	+0.02
COR44 – RCP 8.5	+4.2	+5.6	75	<b><u>+0.07</u></b>	+0.05	+0.05	<b><u>+0.05</u></b>	<b><u>+0.06</u></b>	<b><u>+0.05</u></b>	<b><u>+0.05</u></b>	<b><u>+0.05</u></b>	<b><u>+0.06</u></b>	<b><u>+0.05</u></b>
ENS22 – SRES A1B	+3.5	+4.0	88	0.00	-0.01	-0.01	0.00	0.00	-0.01	-0.01	0.00	0.01	0.03

A similar pattern is found also when assessing the changes in severe heat wave frequencies. Under RCP 8.5, the frequency of severe heat waves is projected to be enhanced by a factor of 6–7 compared to the modelled historical period, which corresponds to more than two events per year. The severe heat waves are projected to occur regularly (at least once per year on average) also in the other scenarios. Nevertheless, a possible bias resulting from the overestimated severe heat wave frequencies in the historical simulations should be considered. For 2070–2099, an event with equal or higher magnitude than the observed 1994

heat wave is projected in a large majority (50 of 59) of model simulations. Moreover, in 30 model simulations such an event occurs at least once per decade, indicating a considerable increase compared to the near future. Alongside the substantial increase of heat wave frequencies, considerable uncertainties represented by wide IQRs and flat PDFs (Figure 9.8) must be taken into account. The width of the IQRs increased roughly by a factor of 2 compared to the near future, thus indicating a large variance among the individual model simulations.

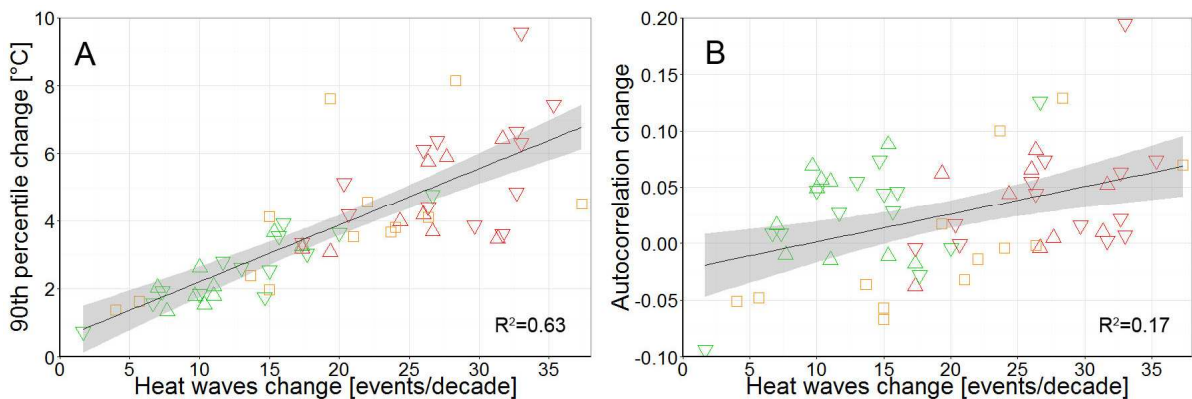


Figure 9.9. Same as Online Resource 1, but for the late 21<sup>st</sup> century. Note different scales of axes.

## 9.5 Discussion

### 9.5.1 Observed heat waves and selection of severe events

In the observed (E-OBS) data, 5 of 22 heat waves are regarded as ‘severe’ and may represent a type of events having particularly pronounced impacts on society and ecosystems. The 1994 heat wave is found to be the most distinctive during the 1970–1999 period, and it was associated with large excess mortality in the Czech Republic (Kyselý and Huth 2004), Poland (Kuchcik 2001) and other Central European countries. Lhotka and Kyselý (2015a) ranked this heat wave as the most severe in Central Europe over the whole 1950–2012 period. In addition to Central Europe, this event was extraordinary also in Western Ukraine (Shevchenko et al. 2014) where it was more pronounced than the well-known 2010 heat wave. Extreme weather conditions during the summer of 1994 were also present over Western Europe (Della-Marta et al. 2007). The 1976 heat wave was especially pronounced in Western Europe (Tomczyk and Bednorz 2016), and the other three severe heat waves (1971, 1974, and 1992) are well recognized in the Central European series of summer temperature (e.g. Kyselý

2002). The 1983 heat wave, which is characterized by the highest temperature amplitude, was not classified as ‘severe’ in our study due to its short length (3 days).

### 9.5.2 Historical simulations of heat waves

In the historical period, differences related to the model resolution are found. EURO-CORDEX models with the coarser 50 km grid substantially overestimated the frequency of severe heat waves, while this behaviour was improved when using their higher-resolution versions. This is in accordance with Vautard et al. (2013), who showed that the number of heat waves persisting more than a few days is overestimated in the EURO-CORDEX models but this feature is improved using the 12.5 km version of the RCMs. Vautard et al. (2013) supposed this characteristic to be linked to the simulation of precipitation, but this aspect was not analysed in their study. A possible mechanism may be related to a better representation of orography in COR11, which is important for proper function of convective schemes in the relatively complex terrain of Central Europe. Smoothed elevation in the coarser (50 km) grid in COR44 provides less occasions for orographic convection (Im et al. 2009) and may contribute to more frequent precipitation deficits that amplify a heat wave’s severity (e.g. Fischer et al. 2007). In addition, RCMs with the coarser grid have lower proportion of resolved precipitation compared to higher-resolution models (Rauscher et al. 2009) and thus more precipitable water is processed through their convective scheme and they are more prone to errors originating from these sub-grid processes.

Links between the magnitude of heat waves and precipitation in RCMs were studied by Lhotka and Kyselý (2015c). In general, models that overestimate total magnitude of heat waves exhibit drier conditions during these events compared to observed data and vice versa. An analogous mechanism might be present in our study, inasmuch as Kotlarski et al. (2014) demonstrated that a majority of EURO-CORDEX models with the 50 km grid exhibit drier summer conditions compared to their higher-resolution versions. Another possible mechanism contributing to the overestimated frequency of severe heat waves relates to atmospheric circulation. Plavcová and Kyselý (2016) concluded that overly persistent circulation in ENSEMBLES RCMs (driven by reanalysis) contributes to the overestimated frequency of long heat waves. The pronounced persistence of circulation patterns might be present also in our study, because the overestimated temporal autocorrelation of  $T_{\max}$  for lags of 5 days and longer was found in all model groups.

Although the historical simulations overestimated the frequency of severe heat waves, only few simulated such a severe event as occurred in 1994. Lhotka and Kyselý (2015c) showed that ENSEMBLES RCMs, driven by perfect boundary conditions, have difficulties to reproduce the 1994 heat wave, mainly due to unrealistic simulation of precipitation. Although this issue might have influenced our study, it is nevertheless necessary to consider to what extent such extreme events are typical for the recent climate and thus whether they should be simulated in RCMs driven by GCMs.

### 9.5.3 Scenarios of heat waves in the near future (2020–2049)

In the near future, EURO-CORDEX models forced by the ‘low’ RCP 4.5 concentration scenario exhibit the largest increase of heat waves frequency (especially simulations with the coarser 50 km grid), which relates to the largest change in the scale of the  $T_{\max}$  distribution and also enhanced temporal autocorrelation. Although the increment in median  $T_{\max}$  is comparable across all model groups, the location of the 90<sup>th</sup> percentile is particularly shifted in COR44 forced by RCP 4.5, and the largest increase of temporal autocorrelation was also found in this group. In general, the increased variance of the  $T_{\max}$  distribution might originate from changes in surface energy budget, soil moisture, and atmospheric circulation (Fischer and Schär 2009). It is possible that extreme temperatures might be enhanced in models forced by the RCP 4.5 scenario due to drier summer conditions and suppressed latent cooling, thus resulting in a longer upper tail of the  $T_{\max}$  distribution. The lowest increment of the heat wave frequency was present in ENSEMBLES simulations, which corresponds with generally negative changes in temporal autocorrelation of  $T_{\max}$  and only a small positive change of the scale parameter. This little change in spread of the  $T_{\max}$  distribution for the ENSEMBLES RCMs was found also by Fischer and Schär (2010), who showed only a small increase of standard deviation in the mid-21<sup>st</sup> century.

### 9.5.4 Scenarios of heat waves in the late 21<sup>st</sup> century (2070–2099)

The late 21<sup>st</sup> century is characterized by a substantial increase in heat wave frequencies, which is linked to ERF and is largest under the RCP 8.5 scenario. Analogous results were obtained by Jacob et al. (2014) using EURO-CORDEX models forced by both RCP 4.5 and 8.5 scenarios. The scale parameter is less important in this period compared to the near future, which corresponds to Ballester et al. (2010), who concluded that future changes in Central European heat waves are expected mostly to follow summer mean warming. Using

ENSEMBLES models forced by the SRES A1B concentration scenario, Fischer and Schär (2010) projected 13 heat waves per decade over Central Europe at the end of the 21<sup>st</sup> century. Because their definition of heat waves was based on six-day temporal criteria, this frequency is rather comparable to severe heat waves in our study and matches our results quite well.

## 9.6 Summary and conclusions

We analysed 62 regional climate model simulations from the ENSEMBLES and EURO-CORDEX projects in order to assess possible changes in Central European heat waves under climate change scenarios for the late 21<sup>st</sup> century along with related uncertainties. The main results can be summarised as follows:

- The RCMs simulate the frequency of heat waves relatively well in the historical period (1970–1999), but the frequency of severe heat waves is overestimated. The EURO-CORDEX RCMs with the 12.5 km grid perform better with respect to the simulation of severe heat waves compared to their low resolution (50 km grid) versions.
- In the near future (2020–2049) simulations, the frequency of heat waves is projected to be nearly twice higher compared to the historical period, while the frequency of severe heat waves increases by a factor of 2–3. The largest uncertainty originates from the selection of models. Differences between the concentration scenarios are small in this period, and the largest effective radiative forcing in RCP 8.5 is not associated with the highest frequency of heat waves.
- The largest increase of heat wave frequency in the CORDEX RCMs under the RCP 4.5 scenario in the near future is related to positive changes in temporal autocorrelation and relatively large change in the scale parameter of the  $T_{\max}$  distribution, while the smallest increment in the ENSEMBLES RCMs under SRES A1B is linked to negative changes in temporal autocorrelation of  $T_{\max}$  and only a small positive change in the scale parameter of the  $T_{\max}$  distribution.
- For the late 21<sup>st</sup> century (2070–2099), the largest uncertainty relates to the concentration scenario. Under RCP 8.5, 3–4 heat waves per summer are projected, compared to about two heat waves under RCP 4.5. Roughly two severe heat waves per summer are found on average for the RCP 8.5 simulations, and they are projected to become a regular phenomenon (once per summer on average) also under the other scenarios.



- The substantial increase of heat waves under RCP 8.5 is connected not only with the largest shift of the  $T_{\max}$  distribution but also with significant positive changes in temporal autocorrelation of  $T_{\max}$ , especially for lags of 5 days and more. Changes in the scale parameter of the  $T_{\max}$  distribution are less important than in the near future.
- Extraordinary heat waves such as the one that occurred in 1994 are projected to be still rather rare in the near future, but the large majority of RCMs simulate at least one event per decade in the late 21<sup>st</sup> century.

The enhanced occurrence of heat waves in a future climate is robust and was found under all concentration scenarios. This emphasizes an importance to implement suitable adaptation strategies, such as those recommended by the European Climate Adaptation Platform (<http://climate-adapt.eea.europa.eu>). Designing green spaces and corridors in urban areas, supporting urban farming and gardening, performing agro-forestry and crop diversification, improving water retention in agricultural areas, and establishing early warning systems would mitigate impacts of heat waves in a changing climate.

### **Acknowledgments**

The study was supported by the Czech Science Foundation, project 16-22000S, and the Charles University Grant Agency, student project no. 250215. The EURO-CORDEX simulations were carried out in several groups within the framework of the IMPACT2C FP7 project. The ENSEMBLES simulations were obtained from the ENSEMBLES project database funded within the EU-FP6. We also acknowledge the E-OBS data set from the same project, the data providers in the ECA&D project, and the National Sustainability Program I (NPU I), grant number LO1415 from the Ministry of Education, Youth and Sports of the Czech Republic.

### **References**

- Arnell NW, Livermore MJL, Kovats S, et al. (2004) Climate and socio-economic scenarios for global-scale climate change impacts assessments: Characterising the SRES storylines. *Glob Environ Chang* 14:3–20. doi: 10.1016/j.gloenvcha.2003.10.004
- Ballester J, Rodó X, Giorgi F (2010) Future changes in Central Europe heat waves expected to mostly follow summer mean warming. *Clim Dyn* 35:1191–1205. doi: 10.1007/s00382-009-0641-5

- Barriopedro D, Fischer EM, Luterbacher J, et al. (2011) The hot summer of 2010: redrawing the temperature record map of Europe. *Science* 332:220–224. doi: 10.1126/science.1201224
- Bastos A, Gouveia CM, Trigo RM, Running SW (2014) Analysing the spatio-temporal impacts of the 2003 and 2010 extreme heatwaves on plant productivity in Europe. *Biogeosciences* 11:3421–3435. doi: 10.5194/bg-11-3421-2014
- Beniston M, Stephenson DB, Christensen OB, et al. (2007) Future extreme events in European climate: an exploration of regional climate model projections. *Clim Change* 81:71–95. doi: 10.1007/s10584-006-9226-z
- Coumou D, Rahmstorf S (2012) A decade of weather extremes. *Nat Clim Chang* 2:491–496. doi: 10.1038/nclimate1452
- Davin EL, Stöckli R, Jaeger EB, et al. (2011) COSMO-CLM2: a new version of the COSMO-CLM model coupled to the Community Land Model. *Clim Dyn* 37:1889–1907. doi: 10.1007/s00382-011-1019-z
- Della-Marta PM, Haylock MR, Luterbacher J, Wanner H (2007) Doubled length of western European summer heat waves since 1880. *J Geophys Res* 112:D15103. doi: 10.1029/2007JD008510
- Déqué M, Somot S, Sanchez-Gomez E, et al. (2012) The spread amongst ENSEMBLES regional scenarios: regional climate models, driving general circulation models and interannual variability. *Clim Dyn* 38:951–964. doi: 10.1007/s00382-011-1053-x
- Deser C, Phillips A, Bourdette V, Teng H (2012) Uncertainty in climate change projections: The role of internal variability. *Clim Dyn* 38:527–546. doi: 10.1007/s00382-010-0977-x
- Deutscher Wetterdienst (DWD, 2015) 2015, August: Record temperature: 40.3°C in Kitzingen on 5 July and on 7 August 2015. Retrieved October 27, 2015. [http://www.dwd.de/EN/climate\\_environment/climatechange/climatechange\\_node.html](http://www.dwd.de/EN/climate_environment/climatechange/climatechange_node.html)
- Fink AH, Brücher T, Krüger A, et al. (2004) The 2003 European summer heatwaves and drought - synoptic diagnosis and impacts. *Weather* 59:209–216. doi: 10.1256/wea.73.04
- Fischer EM, Seneviratne SI, Lüthi D, Schär C (2007) Contribution of land-atmosphere coupling to recent European summer heat waves. *Geophys Res Lett* 34:L06707. doi: 10.1029/2006GL029068
- Fischer EM, Schär C (2009) Future changes in daily summer temperature variability: driving processes and role for temperature extremes. *Clim Dyn* 33:917–935. doi: 10.1007/s00382-008-0473-8
- Fischer EM, Schär C (2010) Consistent geographical patterns of changes in high-impact European heatwaves. *Nat Geosci* 3:398–403. doi: 10.1038/ngeo866

- Fischer EM, Knutti R. (2015) Anthropogenic contribution to global occurrence of heavy-precipitation and high-temperature extremes. *Nature Climate Change* 5: 560–565. doi:10.1038/NCLIMATE2617
- Hawkins E, Sutton R (2009) The potential to narrow uncertainty in regional climate predictions. *Bull Am Meteorol Soc* 90:1095–1107. doi: 10.1175/2009BAMS2607.1
- Haylock MR, Hofstra N, Klein Tank AMG, et al. (2008) A European daily high-resolution gridded data set of surface temperature and precipitation for 1950–2006. *J Geophys Res* 113:D20119. doi: 10.1029/2008JD010201
- Heinrich G, Gobiet A, Mendlik T (2014) Extended regional climate model projections for Europe until the mid-twentyfirst century: Combining ENSEMBLES and CMIP3. *Clim Dyn* 42:521–535. doi: 10.1007/s00382-013-1840-7
- Holtanová E, Valeriánová A, Crhová L, Racko S (2015) Heat wave of August 2012 in the Czech Republic: comparison of two approaches to assess high temperature event. *Stud Geophys Geod* 59:159–172. doi: 10.1007/s11200-014-0805-6
- Hurrell JW, Deser C (2010) North Atlantic climate variability: The role of the North Atlantic Oscillation. *J Mar Syst* 79:231–244. doi: 10.1016/j.jmarsys.2009.11.002
- Iglesias A, Quiroga S, Moneo M, Garrote L (2012) From climate change impacts to the development of adaptation strategies: Challenges for agriculture in Europe. *Clim Change* 112:143–168. doi: 10.1007/s10584-011-0344-x
- Im ES, Coppola E, Giorgi F, Bi X (2010) Validation of a high-resolution regional climate model for the alpine region and effects of a subgrid-scale topography and land use representation. *J Clim* 23:1854–1873. doi: 10.1175/2009JCLI3262.1
- Jacob D, Petersen J, Eggert B, et al. (2014) EURO-CORDEX: new high-resolution climate change projections for European impact research. *Reg Environ Chang* 14:563–578. doi: 10.1007/s10113-013-0499-2
- Kjellström E, Bärring L, Jacob D, et al. (2007) Modelling daily temperature extremes: recent climate and future changes over Europe. *Clim Change* 81:249–265. doi: 10.1007/s10584-006-9220-5
- Kjellström E, Boberg F, Castro M, et al. (2010) Daily and monthly temperature and precipitation statistics as performance indicators for regional climate models. *Clim Res* 44:135–150. doi: 10.3354/cr00932
- Konovalov IB, Beekmann M, Kuznetsova IN, et al. (2011) Atmospheric impacts of the 2010 Russian wildfires: Integrating modelling and measurements of an extreme air pollution episode in the Moscow region. *Atmos Chem Phys* 11:10031–10056. doi: 10.5194/acp-11-10031-2011
- Kotlarski S, Keuler K, Christensen OB, et al. (2014) Regional climate modeling on European scales: A joint standard evaluation of the EURO-CORDEX RCM ensemble. *Geosci Model Dev* 7:1297–1333. doi: 10.5194/gmd-7-1297-2014

- Kyselý J (2002) Temporal fluctuations in heat waves at Prague-Klementinum, the Czech Republic, from 1901-97, and their relationships to atmospheric circulation. *Int J Climatol* 22:33–50. doi: 10.1002/joc.720
- Kyselý J, Huth R (2004) Heat-related mortality in the Czech Republic examined through synoptic and “ traditional ” approaches. *Clim Res* 25:265–274.
- Kyselý J (2010) Recent severe heat waves in central Europe : how to view them in a long-term prospect? *Int J Climatol* 109:89–109. doi: 10.1002/joc1874
- Kuchcik M (2001) Mortality in Warsaw: is there any connection with weather and air pollution? *Geogr Pol* 74:29–45.
- Lau NC, Nath MJ (2014) Model simulation and projection of European heat waves in present-day and future climates. *J Clim* 27:3713–3730. doi: 10.1175/JCLI-D-13-00284.1
- Lemonsu A, Beaulant A, Somot S, Masson V (2014) Evolution of heat wave occurrence over the Paris basin (France) in the 21st century. *Clim Res* 61:75–91. doi:10.3354/cr01235
- Lhotka O, Kyselý J (2015a) Characterizing joint effects of spatial extent, temperature magnitude and duration of heat waves and cold spells over Central Europe. *Int J Climatol* 35:1232-1244. doi: 10.1002/joc.4050
- Lhotka O, Kyselý J (2015b) Hot Central-European summer of 2013 in a long-term context. *Int J Climatol* 35:4399-4407. doi: 10.1002/joc.4277
- Lhotka O, Kyselý J (2015c) Spatial and temporal characteristics of heat waves over Central Europe in an ensemble of regional climate model simulations. *Clim Dyn* 45: 2351-2366. doi: 10.1007/s00382-015-2475-7
- Meehl GA, Tebaldi C (2004) More intense, more frequent, and longer lasting heat waves in the 21st century. *Science* 305:994–997. doi: 10.1126/science.1098704
- Moss RH, Edmonds JA, Hibbard KA, et al. (2010) The next generation of scenarios for climate change research and assessment. *Nature* 463:747–56. doi: 10.1038/nature08823
- Nikulin G, Kjellström E, Hansson U, et al. (2011) Evaluation and future projections of temperature, precipitation and wind extremes over Europe in an ensemble of regional climate simulations. *Tellus A* 63A:41–55. doi: 10.1111/j.1600-0870.2010.00466.x
- Plavcová E, Kyselý J (2011) Evaluation of daily temperatures in Central Europe and their links to large-scale circulation in an ensemble of regional climate models. *Tellus A* 63A:763–781. doi: 10.1111/j.1600-0870.2011.00514.x
- Plavcová E, Kyselý J (2016) Overly persistent circulation in climate models contributes to overestimated frequency and duration of heat waves and cold spells. *Clim Dyn* 46:2805–2820. doi: 10.1007/s00382-015-2733-8

- Prather M, Flato G, Friedlingstein P, et al. (2013) Annex II: Climate System Scenario Tables. *Clim. Chang.* 2013 Phys. Sci. Basis. Contrib. Work. Gr. I to Fifth Assess. Rep. Intergov. Panel Clim. Chang.
- Rauscher SA, Coppola E, Piani C, Giorgi F (2010) Resolution effects on regional climate model simulations of seasonal precipitation over Europe. *Clim Dyn* 35:685–711. doi: 10.1007/s00382-009-0607-7
- Riahi K, Rao S, Krey V, et al. (2011) RCP 8.5-A scenario of comparatively high greenhouse gas emissions. *Clim Change* 109:33–57. doi: 10.1007/s10584-011-0149-y
- Robine J-M, Cheung SLK, Le Roy S, et al. (2008) Death toll exceeded 70,000 in Europe during the summer of 2003. *C R Biol* 331:171–178. doi: 10.1016/j.crv.2007.12.001
- Schneidereit A, Schubert S, Vargin P, et al. (2012) Large-Scale Flow and the Long-Lasting Blocking High over Russia: Summer 2010. *Mon Weather Rev* 140:2967–2981. doi: 10.1175/MWR-D-11-00249.1
- Shevchenko O, Lee H, Snizhko S, Mayer H (2014) Long-term analysis of heat waves in Ukraine. *Int J Climatol* 34:1642–1650. doi: 10.1002/joc.3792
- Strandberg G, Barring L, Hansson U, et al. (2014) CORDEX scenarios for Europe from the Rossby Centre regional climate model RCA4. Rep Meteorol Climatol. ISSN: 0347-2116
- Thomson AM, Calvin K V., Smith SJ, et al. (2011) RCP4.5: A pathway for stabilization of radiative forcing by 2100. *Clim Change* 109:77–94. doi: 10.1007/s10584-011-0151-4
- Tomczyk AM, Bednorz E (2016) Heat waves in Central Europe and their circulation conditions. *Int J Climatol* 36:770–782. doi: 10.1002/joc.4381
- van der Linden P, Mitchell JFB (2009) ENSEMBLES: Climate Change and its Impacts: Summary of research and results from the ENSEMBLES project. Met Office Hadley Centre, Exeter
- van Vuuren DP, Edmonds J, Kainuma M, et al. (2011) The representative concentration pathways: An overview. *Clim Change* 109:5–31. doi: 10.1007/s10584-011-0148-z
- Valeriánová A, Crhová L, Holtanová E, et al. (2015) High temperature extremes in the Czech Republic 1961–2010 and their synoptic variants. *Theor Appl Climatol*. doi: 10.1007/s00704-015-1614-8
- Vautard R, Gobiet A, Jacob D, et al. (2013) The simulation of European heat waves from an ensemble of regional climate models within the EURO-CORDEX project. *Clim Dyn* 41:2555–2575. doi: 10.1007/s00382-013-1714-z
- Zentralanstalt für Meteorologie und Geodynamik (ZAMG, 2013) New temperature record: 40.5°C in Bad Deutsch-Altenburg. Retrieved January 16, 2014. <http://www.zamg.ac.at/cms/de/klima/news/neuer-hitze-rekord-40-5deg-c-in-baddeutsch-altenburg>.

# 10 Article V: ‘Long-term variability of heat waves in Argentina and recurrence probability of the severe 2008 heat wave in Buenos Aires’

Matilde Rusticucci<sup>1</sup>; Jan Kysely<sup>2,4</sup>; Gustavo Almeida<sup>3</sup> and Ondřej Lhotka<sup>2,5</sup>

<sup>1</sup> Departamento de Ciencias de la Atmósfera y los Océanos – FCEN – Universidad de Buenos Aires, and Consejo Nacional de Investigaciones Científicas y Técnicas Argentina

<sup>2</sup> Institute of Atmospheric Physics AS CR, Prague, Czech Republic

<sup>3</sup> Instituto Nacional del Agua and Departamento de Ciencias de la Atmósfera y los Océanos – FCEN – Universidad de Buenos Aires, Buenos Aires, Argentina

<sup>4</sup> Global Change Research Centre AS CR, Brno, Czech Republic

<sup>5</sup> Faculty of Science, Charles University in Prague, Czech Republic

**Abstract:** Heat waves are one of the main concerns related to the impacts of climate change, because their frequency and severity are projected to increase in a future climate. The objective of this work is to study the long-term variability of heat waves over Argentina, and to estimate recurrence probability of the most severe 2008 heat wave in Buenos Aires. We used 3 definitions of heat waves that were based on (1) daily maximum temperature above the 90th percentile (MaxTHW), (2) daily minimum temperature above the 90th percentile (MinTHW), and (3) both maximum and minimum temperatures above the corresponding 90th percentiles (EHW). The minimum length of heat wave was 3 days and the analysis was performed over the October–March period. Decadal values of heat wave days in Buenos Aires experienced increases in all definitions, but at other stations, combinations of different trends and decadal variability resulted in some cases in a decrease of extreme heat waves. In the northwestern part of the country, a strong positive change in the last decade was found, mainly due to the increment in the persistence of MinTHW but also accompanied by increases in MaxTHW. In general, other stations show a clear positive trend in MinTHW and decadal variability in MaxTHW, with the largest EHW cases in the last decade. We also estimated recurrence probability of the longest and most severe heat wave in Buenos Aires (over 1909–2010, according to intensity measured by the cumulative excess of maximum daily temperature above the 90<sup>th</sup> percentile) that occurred from 3 to 14 November 2008, by means of simulations with a stochastic first-order autoregressive model. The recurrence probability of such long and severe heat wave is small in the present climate but it is likely to increase substantially in the near future even under a moderate warming trend.

**Keywords:** heat waves; long-term variability; climate extremes

## 10.1 Introduction

Impacts from recent climate-related extremes, such as heat waves, reveal significant vulnerability and exposure of some ecosystems and human society to current climate variability (Field et al. 2013). These impacts include enhanced morbidity and mortality

(Robine et al. 2008; Barriopedro et al. 2011), crop failures, forest fires, stress for livestock and wildlife, spreading of pests and increased energy demand for cooling (De Bono et al. 2004; Beniston et al. 2007).

On the global scale, there is only a medium confidence that the length and frequency of warm spells, including heat waves, have increased since the middle of the twentieth century (Hartmann et al. 2013). This uncertainty was mostly caused by the lack of data and studies over South America and Africa. However, models project near-term increases in the duration, intensity and spatial extent of heat waves and warm spells over most land regions (Kirtman et al. 2013).

Focusing on South America, Cerne and Vera (2011) showed that the majority of heat waves defined over a single station in Argentina are related to the progression of the South Atlantic convergence zone, which is regarded as an elongated convective band typically originating in the Amazon basin and protruding into the southeastern subtropical Atlantic Ocean (Carvalho et al. 2004). This large-scale synoptic pattern determines the warm meridional flow that drives high temperatures over the eastern subtropical coast of South America (e.g. Alessandro and de Garín 2003). A meridional transport of air masses over South America is the most intense over the entire Southern Hemisphere, mainly due to the presence of the mountain ridge of Andes (Rusticucci 2012).

The study of the occurrence of heat waves needs an extended quality-controlled data base containing daily data. Over Argentina, there have been studies related to the variability of extreme temperatures, but the spells were analysed during short periods because of incomplete data or their limited availability (Rusticucci and Vargas 1995, 2001). More recently and over a larger area, Alexander et al. (2006) considered one parameter related to warm spells, the Warm Spell Duration Index (WSDI). It is defined as the annual count of days with at least 6 consecutive days when maximum temperature exceeds the 90<sup>th</sup> percentile. This definition takes into account warm spells over the whole year, without consideration of the season, and it is restrictive about the number of missing data. The results over Argentina in the 1951–2003 period showed no significant linear trends, and these trends were both positive and negative over different regions. In an update of that paper, Donat et al. (2013) present HadEX2, which extended the number of stations and the period up to 1901–2010, and found the same sign and spatial inconsistency of the trends.

Without considering several days-long spells (only the number of days above or below some threshold individually), the number of warm nights (minimum temperature above the

90<sup>th</sup> percentile) has been increasing and the number of cold nights (minimum temperature below the 10<sup>th</sup> percentile) and days (maximum temperature below the 10<sup>th</sup> percentile) has been decreasing over Argentina, as well as over most land regions. However, the frequencies of warm days (maximum temperature above the 90<sup>th</sup> percentile) have been decreasing in some regions over Argentina (Rusticucci and Barrucand 2004; Alexander et al. 2006; Donat et al. 2013).

A definition of heat waves varies over literature but it is mainly related to the number of consecutive days that exceed a defined threshold. A relation between extreme temperature occurrence and their impacts on human health could provide useful thresholds for delimiting heat waves. As enhanced mortality in summer is related to temperature excesses of both minimum and maximum temperatures, so, we used these limits to define a heat wave. The analysis of this relationship is also useful for an installation of an operative alert system through the National Weather Service of Argentina ([www.smn.gov.ar](http://www.smn.gov.ar)) that could contribute to the population preparedness in order to avoid health impacts.

The first main objective of this work is to study the long-term variability in the occurrence of heat waves over Argentina, with focus on the warm period of the year and considering different heat wave definitions. The second main aim is to estimate recurrence probability of the most severe and longest heat wave in Buenos Aires by simulations with a stochastic time series model. These simulations were performed for the present climate as well as under several climate change scenarios.

The paper is structured as follows: a description of data, definition of a heat wave and information about stochastic time series model are given in Section 10.2. Results concerning long-term variability of heat waves over Argentina are shown in Section 10.3. Estimates of recurrence probability of the most severe and longest heat wave in Buenos Aires are presented in Section 10.4. Finally, discussion and conclusions follow in Section 10.5.

## **10.2 Data and methodology**

### 10.2.1 Data

The data were obtained from 58 stations located over Argentina north of 40° S (Figure 10.1). This is the most populated region, and it is prone to severe heat waves. We utilized all available stations with long-term daily maximum and minimum temperature series (with less than 2 % of missing data). Originally, the data were provided by the Argentine National



Weather Service and their quality was analysed through the European project CLARIS LPB, generating the open data base CLARIS LPB (Penalba et al. 2014). Table 10.1 shows all stations used for the analysis of long-term variability of heat waves, including their station ID, name, geographical coordinates and elevation. In this article, the term Buenos Aires represents the Autonomous City of Buenos Aires (Ciudad Autónoma de Buenos Aires).

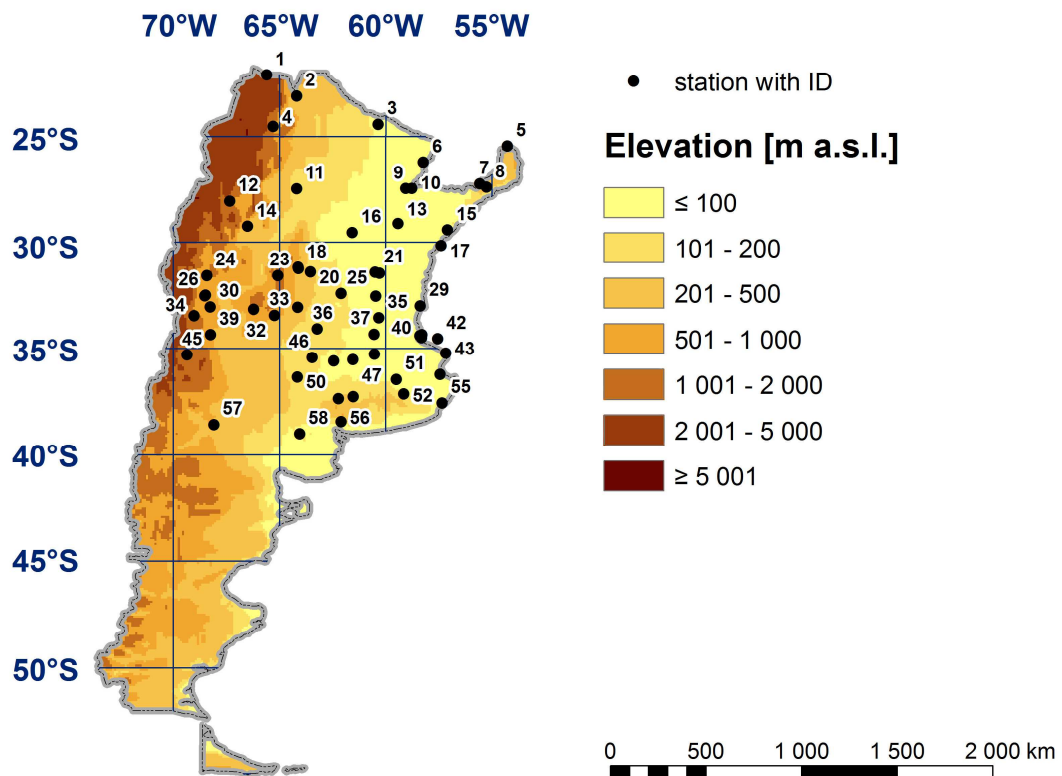


Figure 10.1. Locations of stations and the elevation model (ETOPO5) over the continental parts of Argentina.

Table 10.1. Stations utilized.

station ID	Name	Latitude (°S)	Longitude (°W)	Altitude (m)
1	LA QUIACA OBS.	22.10	65.60	3459
2	ORAN AERO	23.09	64.19	357
3	LAS LOMITAS	24.42	60.35	130
4	SALTA AERO	24.51	65.29	1221
5	IGUAZU AERO	25.44	54.28	270
6	FORMOSA AERO	26.20	58.23	64
7	POSADAS AERO	27.22	55.58	125
8	CERRO AZUL INTA	27.39	55.26	270
9	RESISTENCIA AERO	27.45	59.05	52
10	CORRIENTES AERO	27.45	58.77	60
11	SANTIAGO DEL ESTERO AERO	27.46	64.18	199
12	TINOGASTA	28.04	67.34	1201
13	RECONQUISTA AERO	29.11	59.42	53
14	LA RIOJA AERO	29.23	66.49	429
15	PASO DE LOS LIBRES AERO	29.41	57.09	70
16	CERES AERO	29.53	61.57	88
17	MONTE CASEROS AERO	30.16	57.39	54
18	CORDOBA AERO	31.19	64.13	474
19	CORDOBA OBSERVATORIO	31.24	64.11	425
20	PILAR OBS.	31.40	63.53	338
21	SAUCE VIEJO AERO	31.42	60.49	18
22	PARANA AERO	31.47	60.29	78
23	VILLA DOLORES AERO	31.57	65.08	569
24	SAN JUAN AERO	31.57	68.42	62
25	MARCOS JUAREZ AERO	32.42	62.09	114
26	MENDOZA AERO	32.5	68.47	704
27	MENDOZA OBSERVATORIO	32.53	68.51	827
28	ROSARIO AERO	32.55	60.47	25
29	GUALEGUAYCHU AERO	33.00	58.37	21
30	SAN MARTIN (MZA)	33.05	68.25	653
31	RIO CUARTO AERO	33.07	64.14	421
32	SAN LUIS AERO	33.16	66.21	713
33	VILLA REYNOLDS AERO	33.44	65.23	486
34	SAN CARLOS (MZA)	33.46	69.02	940
35	PERGAMINO INTA	33.56	60.33	65
36	LABOULAYE AERO	34.08	63.22	137
37	JUNIN AERO	34.33	60.55	81
38	BUENOS AIRES	34.35	58.29	25
39	SAN RAFAEL AERO	34.35	68.24	748
40	CASTELAR INTA	34.40	58.39	22
41	EZEIZA AERO	34.49	58.32	20
42	LA PLATA AERO	34.54	57.56	4
43	PUNTA INDIO B.A.	35.22	57.17	22
44	NUEVE DE JULIO	35.27	60.53	76
45	MALARGUE AERO	35.30	69.35	1425
46	GENERAL PICO AERO	35.42	63.45	145
47	PEHUAJO AERO	35.52	61.54	87
48	TRENQUE LAUQUEN	35.58	62.44	95
49	DOLORES AERO	36.21	57.44	9
50	SANTA ROSA AERO	36.34	64.16	191
51	AZUL AERO I	36.45	59.50	132
52	TANDIL AERO	37.14	59.15	175
53	CORONEL SUAREZ AERO	37.26	61.53	233
54	PIGUE AERO	37.36	62.23	304
55	MAR DEL PLATA AERO	37.56	57.35	21
56	BAHIA BLANCA AERO	38.44	62.10	83
57	NEUQUEN AERO	38.57	68.08	271
58	RIO COLORADO	39.01	64.05	79

### 10.2.2 Heat wave definition

Considering the impacts of heat waves on mortality in Buenos Aires, the extreme cases of excess mortality over the warm season (October–March) of the year are related to the occurrence of minimum temperature (MinT) above 20°C (where the curve changes its curvature) and maximum temperature (MaxT) above 32°C (Figure 10.2). These values correspond to the mean daily 90<sup>th</sup> percentile calculated over the warm season (October–March) of the year in the 1961–1990 period. Therefore, the 90<sup>th</sup> percentiles of both MinT and MaxT were taken to define a heat wave for the warm season of the year. To specify the minimum number of consecutive days that define a heat wave, their persistence was analysed.

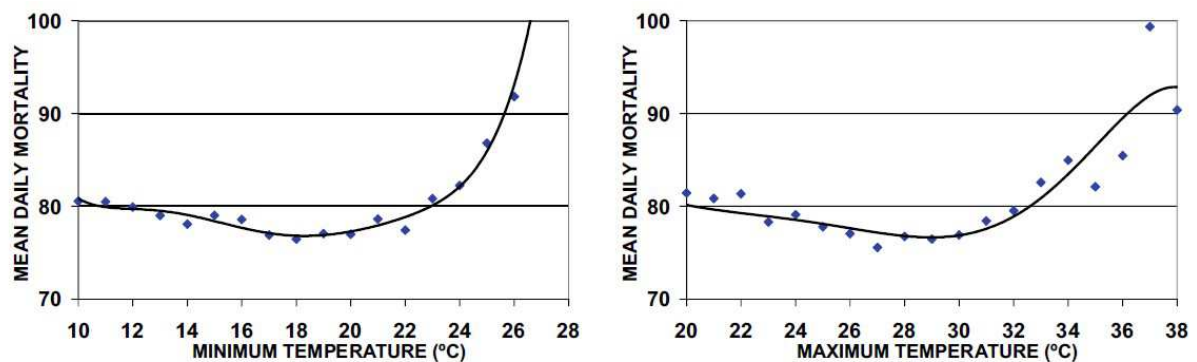


Figure 10.2. Minimum and maximum daily temperature vs. mean daily mortality in Buenos Aires (2011–2012) warm season.

In Buenos Aires, the analysis of persistence of days with MaxT above 32°C and simultaneously MinT above 20°C in the warm season (October to March) during the 1959–2010 period showed that 77% of the spells lasted 1 or 2 days, and the longest one persisted for 12 consecutive days. Based on this distribution, and because the objective was to analyse more persistent events, a heat wave was defined when temperature was above the threshold (the seasonally varying 90<sup>th</sup> percentile) for at least 3 consecutive days. The station-specific 90<sup>th</sup> percentiles of MinT and MaxT calculated over 1961–1990 were used to define and analyse heat waves over the complete data base (period 1961–2010). Using this limited 1961–1990 period allows updating the list of heat waves without recalculating the percentiles and provides a better comparison with other studies.

We use three different definitions of heat waves: spells of 3 or more consecutive days with (1) MinT above the daily 90<sup>th</sup> percentile of MinT (heat waves based on MinT: MinTHW), (2) Max T above the daily 90<sup>th</sup> percentile of MaxT (heat waves based on MaxT: MaxTHW) and

(3) the joint occurrence of MinT and MaxT above their 90<sup>th</sup> percentiles. These latter will be called extreme heat waves (EHW), due to the severity of the definition. In these three types of heat waves, we analyse long-term variability and decadal occurrence of the number of days in heat waves, the persistence and the intensity.

We considered the warm half of the year from October to March, in order to capture early and late heat wave occurrences, too. These cases, although not necessarily associated with extreme absolute temperatures, could have huge impacts on society as well. For example, Campetella and Rusticucci (1998) presented synoptic conditions during a strong heat wave in the last days of summer (end of March) with a pronounced impact on society, as schools in Buenos Aires were temporarily closed.

### 10.2.3 Stochastic time series model for daily temperatures

In order to estimate recurrence probability associated with the 2008 heat wave in Buenos Aires, we make use of long artificial time series of MaxT simulated by a first-order autoregressive model (AR(1)). The AR(1) model provides characteristics of heat waves and temperature threshold exceedances that are generally in good agreement with observations (e.g. Mearns et al. 1984; Macchiato et al. 1993; Colombo et al. 1999; Kysely 2010). Several variants of the AR(1) model exist; herein, we apply a model in which the seasonal cycle of MaxT is considered as a deterministic part and only deviations from this cycle are simulated as a stochastic component (Macchiato et al. 1993; Kysely and Kim 2009; Kysely 2010). For the present climate experiment, parameters of the model (mean, variance and the first-order autocorrelation coefficient) are estimated from MaxT data in Buenos Aires over 1961–2009; 100,000-year-long artificial time series of MaxT are then generated with the AR(1) model, from which recurrence probability of events analogous to (or exceeding) the 2008 heat wave is estimated. In a similar way, experiments for a climate warmer by 1, 2, and 4°C are carried out. Over Argentina, values of 2 to 3°C correspond to the projected 75<sup>th</sup> percentile of the distribution from the ensemble of CMIP5 models, for the RCP 4.5 scenario and the end of the 21<sup>st</sup> century (IPCC 2013), so the range from 1 to 4°C covers low- to high-climate change scenarios for Argentina and the late twenty-first century.

### 10.3 Long-term variability of heat waves in Argentina north of 40° S

Since the number of heat waves is small each year, we aggregated the number of days during heat waves (heat wave days) in decades, in order to analyse temporal changes in their occurrence. The first decade starts in the October 1960–March 1961 warm season.

The mean numbers of heat wave days per decade during the warm season for the whole 1961–2010 period, considering the three definitions MinTHW, MaxTHW and EHW, are shown in Figure 10.3. As an example, the city of Buenos Aires experienced, on average, 8 heat wave days per year for MinTHW, 6.5 heat wave days per year for MaxTHW and, if we consider MinT and MaxT simultaneously above their 90<sup>th</sup> percentiles, 2.5 heat wave days per year for the EHW definition. The most persistent extreme warm temperatures occurred over the north and north-eastern part of Argentina, for all three heat wave definitions.

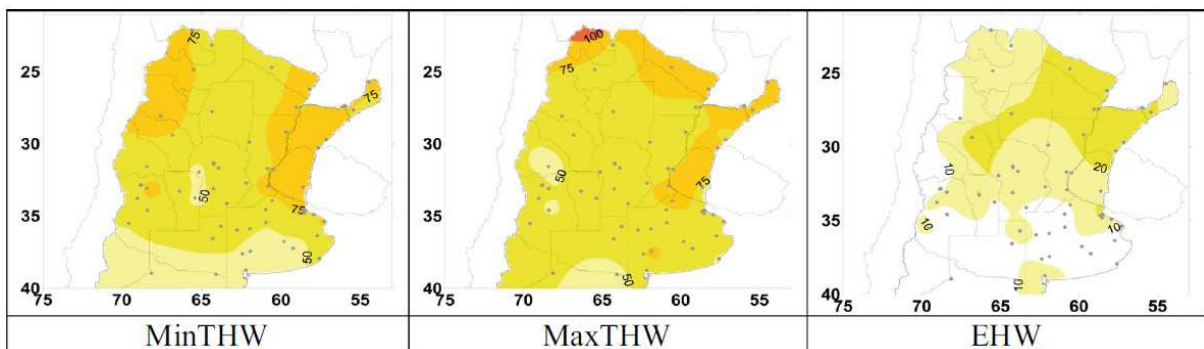


Figure 10.3. Mean number of days under a heat wave per decade, considering MinTHW, MaxTHW and EHW (summer)

Figure 10.4 shows the geographical distribution of the number of heat wave days for each decade. There is great variability among regions, but in general, the decade 2001–2010 was typical for the highest number of heat wave days according to all definitions. Although the occurrence of heat wave days by the MaxTHW definition decreased in some regions by the end of the twentieth century, the occurrence of MinTHW increased, and when combining both limits, EHW also showed the largest number of occurrences in the last decade, surpassing the 1981–1990 warm decade.

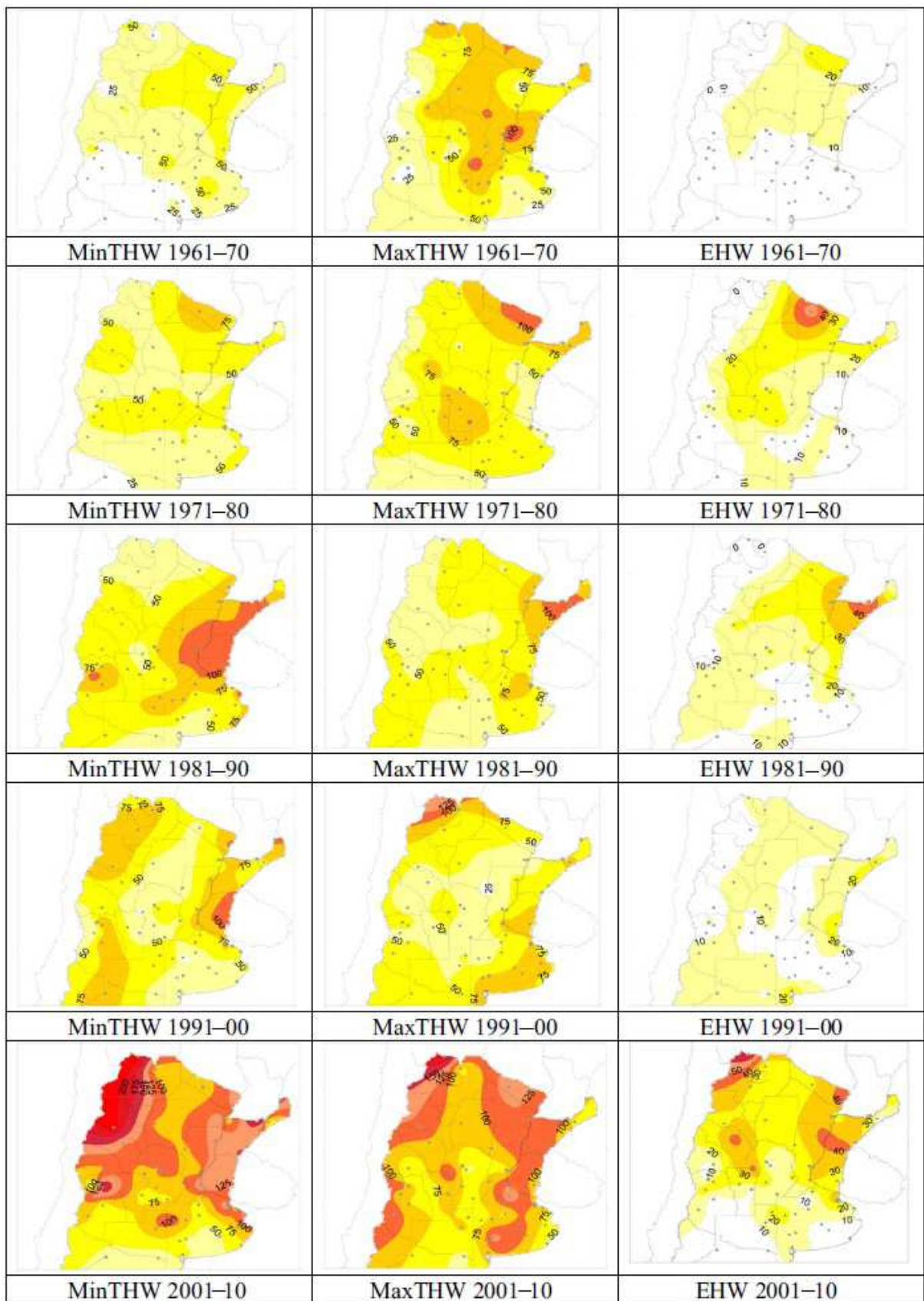


Figure 10.4. Number of days under a heat wave per decade, considering MinTHW, MaxTHW and EHW (summer).

Decadal frequency of heat waves (according to MinTHW, MaxTHW and EHW) at four typical stations is shown in Figure 10.5. Decadal values in Buenos Aires experienced clear increases in heat waves according to MinTHW and EHW, with the highest frequency for both in the 2001–2010 decade, while a less pronounced increase in heat waves according to MaxTHW. The combination of different trends and decadal variability at other stations resulted in some cases in the decrease of the extreme heat waves (EHW), as shown in Córdoba (Central Argentina). In the central-western part of the country, Mendoza shows an increment in the last decade, particularly for MinTHW. In the north-western part of the country, La Quiaca presents a huge increment in the last decade in EHW, mainly due to the increment in the persistence of MinTHW but also accompanied by increases in MaxTHW. Due to the sharp increase in the number of heat waves in the north-western region of Argentina (La Quiaca, Tinogasta), we checked again the data quality. The comparison with hourly data at other nearby stations in the 1991–2010 period confirmed the observed change in the last decade.

In general, most other stations over the analysed region show a clear positive trend in MinTHW, and decadal variability in MaxTHW, with the largest EHW cases in the last decade.

In order to analyse the variability of more frequent shorter heat waves, we separate the heat waves into two main groups according to their length, 3 to 5 days and longer. The difference in the number of short heat waves between the last (2001–2010) and the first (1961–1970) decades shows an increase in most of the country, for all three definitions (Figure 10.6). All stations present significant increasing trends for MinTHW (not shown).

Considering only these short heat waves, the north-western part of the country experienced from 10 to 30 more heat wave days for MinTHW in the last decade compared to the first decade, which is a substantial increase. All over the country, up to 5 more heat wave days for EHW occurred, with more than 10 heat wave days in the north-western region. The zero increment of heat wave days over central Argentina (according to MaxTHW) was related to the warm 1961–1970 decade in this region, as shown in Figure 10.4. A similar pattern but with generally insignificant linear trends was found for long heat waves.

To summarize this variability, all heat waves and stations are analysed together. The time series of the number of heat waves shows positive significant trend in all definitions, mainly driven by the short heat waves (Figure 10.7).



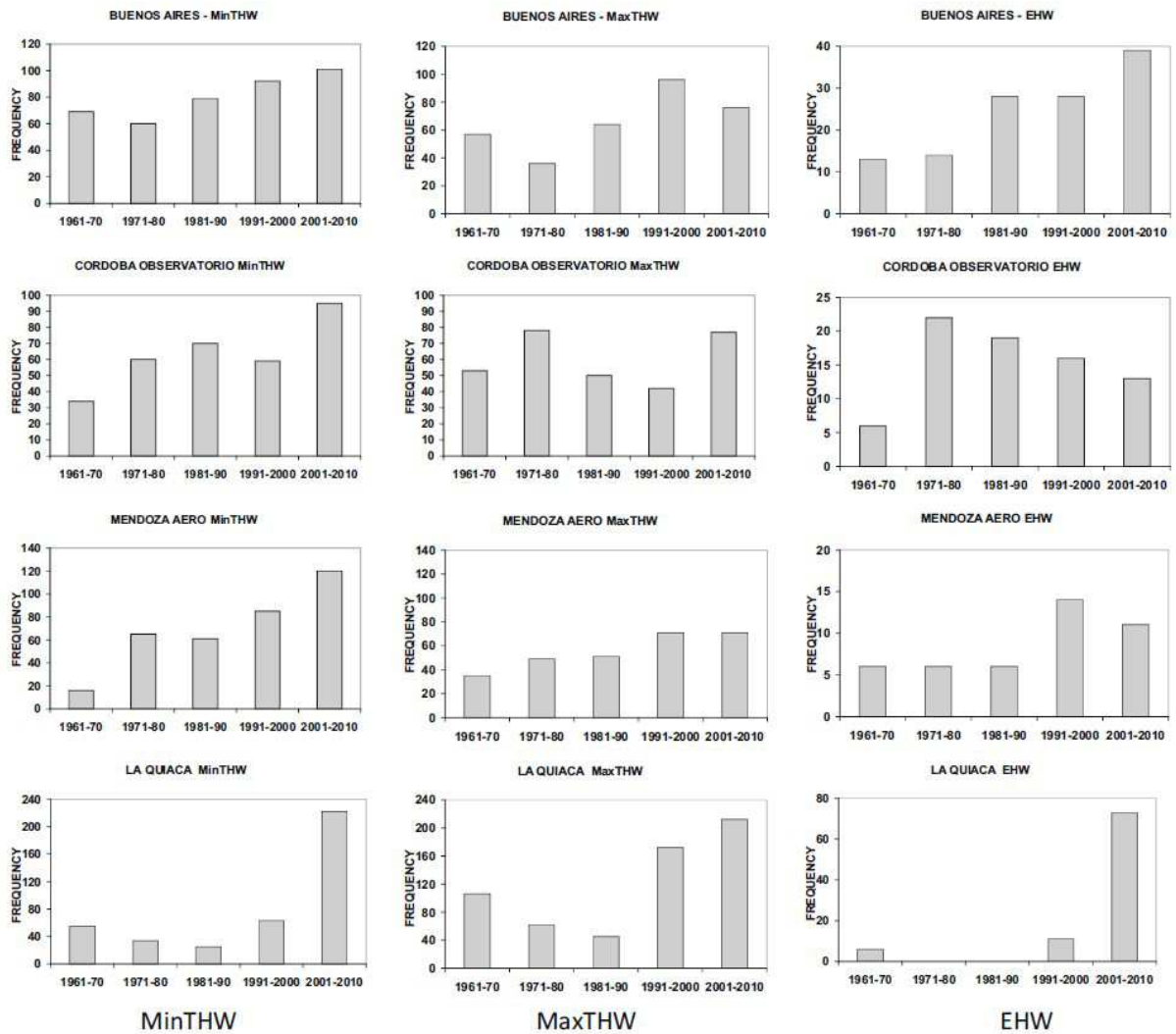


Figure 10.5. Number of MinTHW, MaxTHW and EHW over decades from 1961–70 to 2001–2010 at stations Buenos Aires, Cordoba Observatorio, Mendoza Aero and La Quiaca (from top to bottom).

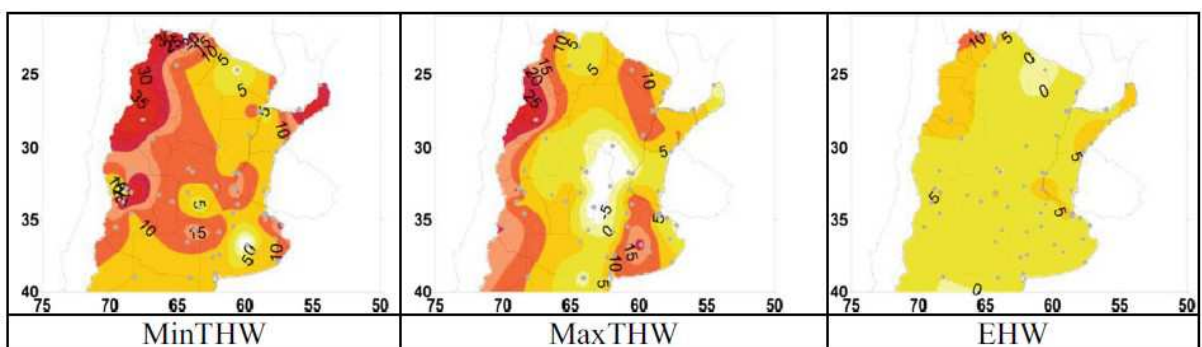


Figure 10.6. Differences in the number of short (3 to 5 days) heat waves between 2001–2010 and 1961–1970, considering MinTHW, MaxTHW and EHW.



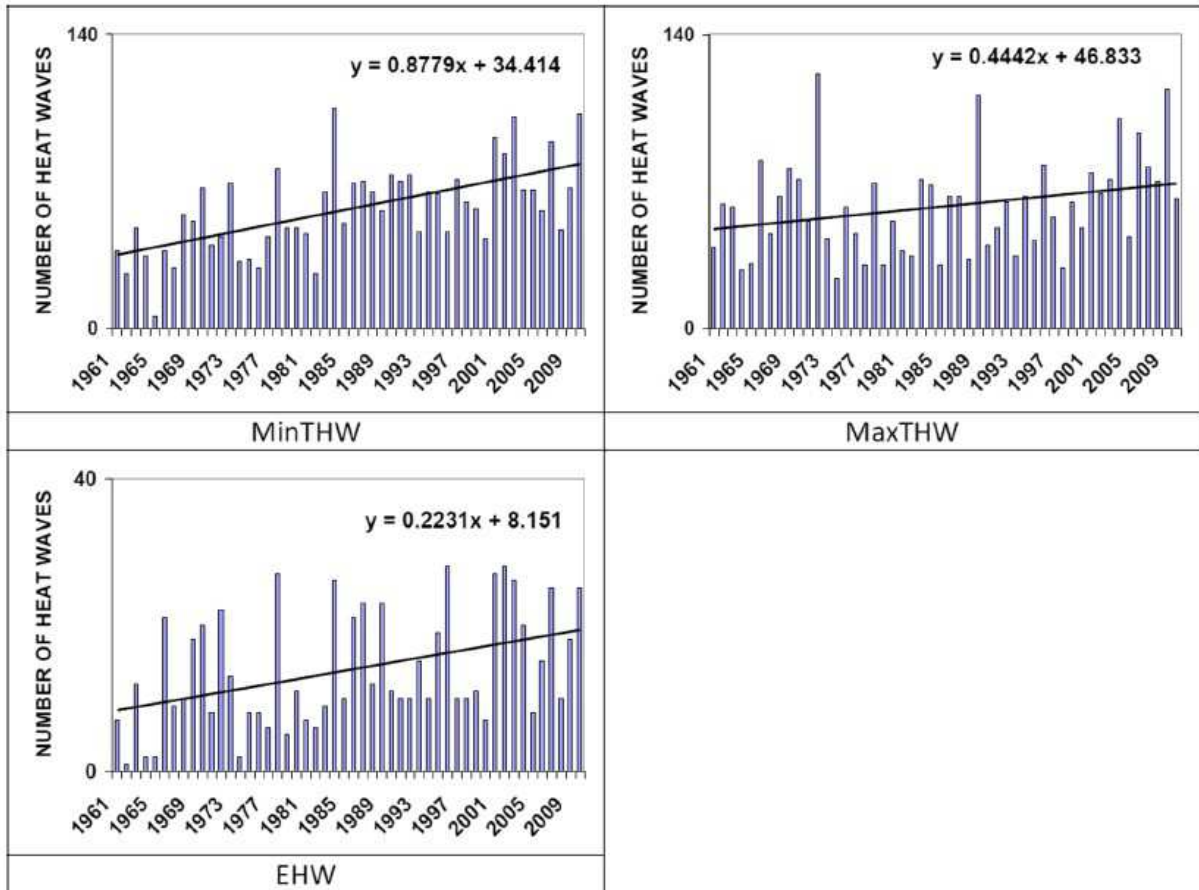


Figure 10.7. Time series of the number of heat waves, all lengths and stations over Argentina (1961–2010). Linear trend is fitted to the data.

Beside the duration, we considered the intensity of heat waves, measured by the sum of degrees C above the 90<sup>th</sup> percentile (cumulative excess of temperature). For comparison, the degree days were computed for each event, as the ratio between the intensity and length in each event. The degree days were accumulated for decades, and the differences in degrees C between two decades (2001–2010, 1961–1970) were computed. The short heat waves had the largest differences. A strong warming can be seen mainly over the northwest in MinTHW, while less warming or cooling in other regions (not shown).

#### 10.4 Recurrence probability of the extreme heat wave of November 2008 in BA

Since Buenos Aires is the location with the longest and most complete temperature record in Argentina, and also the area where most of the country’s total population lives, we focused on the most severe heat wave in Buenos Aires in more detail.

Over the whole period of available data (1909–2010), the November 2008 heat wave was the longest and most extreme one, mainly considering MaxT. It lasted for 12 days (from 3 to

14 November) and was associated with the cumulative MaxT excess above the 90<sup>th</sup> percentile of 32.6°C. The heat wave was rather exceptional as to its length and the cumulative MaxT excess compared to other heat waves in Buenos Aires, as the second most severe heat wave since 1909 (March 1952) had the cumulative MaxT excess of only 26 °C and lasted 11 days. This November 2008 heat wave was also exceptional in MinT and EHW, compared to the March 1952 heat wave, which lasted 11 days, the cumulative excess was 54 vs 16°C in EHW and 22 vs 4°C in MinT. Its spatial extent, considering persistence, covers a region in central-eastern Argentina (Figure 10.8).

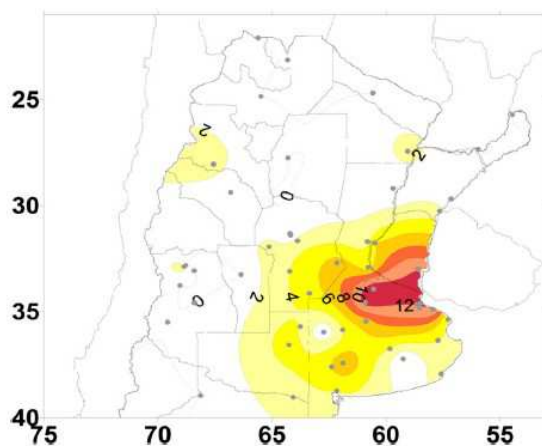


Figure 10.8. Number of days under 2008 November heat wave, considering MaxTHW.

Its recurrence probability was estimated from simulations of time series of MaxT by a first-order autoregressive (AR(1)) model (see Section 10.2.3). We generated 100,000-year-long series for the present climate (with parameters of the AR(1) model estimated over 1961–2009) in the first step and analogous series for a climate warmer by 1, 2 and 4°C, to represent possible climate change scenarios for the late twenty-first century.

We focused on three heat wave characteristics that define severity of the 2008 heat wave:

1. Cumulative MaxT excess above the 90<sup>th</sup> percentile  $\geq 32.6$  °C,
2. Length  $\geq 12$  days,
3. Both conditions 1 and 2 met.

Table 10.2 shows that the recurrence probability of a heat wave similar or exceeding the November 2008 heat wave in Buenos Aires is small in the present climate. The return periods

are estimated in the order of several hundreds to several thousands years, depending on the chosen characteristic. However, even a moderate warming substantially increases probability of such event: in a climate warmer by +1°C, the return periods decline by an order of magnitude, and in a climate warmer by +4°C, such heat waves are likely to occur regularly (once every 1–3 years).

Table 10.2. Return periods of the 2008 heat wave in Buenos Aires, estimated with the AR(1) model for the present climate and three climate change scenarios.

Return period [in years] of a heat wave with	Present climate (1961–2010)	+1°C warming	+2°C warming	+4°C warming
1) cumulative MaxT excess above the 90 <sup>th</sup> percentile (TS) $\geq$ 32.6°C	610	95	18	1.3
2) length $\geq$ 12 days	3700	380	55	3
3) TS $\geq$ 32.6°C and length $\geq$ 12 days	6250	670	80	3.5

### 10.5 Discussion and concluding remarks

The frequency of heat waves has been increasing in Argentina for all examined definitions over the 1961–2010 period. This finding brought more evidence for the IPCC statement that there is a worldwide increment of heat waves, since Hartmann et al. (2013) noted that the medium confidence is caused by a lack of studies, among others, over South America.

Generally, we found pronounced decadal variability, but the largest number of heat waves was observed in the last 2001–2010 decade, surpassing the warm 1981–1990 decade. The relatively cold 1991–2000 decade might be related to a lower activity of the South Atlantic Convergence Zone compared to the previous decade, as shown in Carvalho et al. (2004). However, Cerne and Vera (2011) demonstrated that heat waves over central Argentina occur even when the activity of the South Atlantic convergence zone is suppressed.

Focusing on individual stations, decadal values in Buenos Aires experienced increases in MinTHW and EHW, while the combination of different trends and decadal variability resulted in some cases (e.g. Córdoba and Las Lomitas) in the reduction of extreme heat waves in the last decade. The stations over the north-western part of the country (La Quiaca, Orán, Salta and Tinogasta) showed a strong positive change in the last decade, mainly due to increased persistence of MinTHW, but also accompanied by increases in MaxTHW.

In general, other stations showed a clear positive trend in heat waves in the light of MinTHW, and decadal variability in MaxTHW, with the most severe cases in the last decade when the simultaneous combination of MaxT and MinT excesses was most frequent. There

was a particularly strong increase in the intensity and number of heat waves of short lengths (3 to 5 days) in all three heat wave definitions.

Recurrence probability of the longest and most severe heat wave in Buenos Aires (over 1909–2010, according to intensity measured by cumulative excess of MaxT above the 90<sup>th</sup> percentile) that occurred in 2008 was estimated by simulations with a stochastic first-order autoregressive model that reproduces structure of the time series of daily temperatures. The results show that the recurrence probability of such long and severe heat wave is small in the present climate, but it is likely to increase substantially in the near future even under a moderate warming trend: by a factor of 6–10 with only a 1°C warming, by a factor of ~30–70 with a 2°C warming and by a factor of ~500–1000 with a 4°C warming. These results should be taken into account also in the design of adaptation and mitigation measures to protect society against adverse effects of extreme events in a changing climate.

### **Acknowledgments**

The study was supported by a joint project funded by the Ministerio de Ciencia, Tecnología e Innovación Productiva of Argentina (ARC/14/25) and the Czech Ministry of Education (7AMB15AR001), and by the UBA20020130100263BA and CONICET PIP0227 projects. The data were provided by the National Weather Service of Argentina.

### **References**

- Alexander L, Zhang X, Peterson TC, Caesar J, Gleason B, Klein Tank A, Haylock M, Collins D, Trewin B, Rahimzadeh F, Tagipour A, Ambenje P, Rupa Kumar K, Revadekar J, Griffiths G, Vincent L, Stephenson D, Burn J, Aguilar E, Brunet M, Taylor M, New M, Zhai P, Rusticucci M, Vazquez-Aguirre JL (2006) Global observed changes in daily climate extremes of temperature and precipitation. *J Geophys Res* 111:D05109.
- Alessandro AP, de Garín AB (2003) A study on predictability of human physiological strain in Buenos Aires City. *Meteorol Appl* 10:263–271. doi: 10.1017/S1350482703003062
- Barriopedro D, Fischer EM, Luterbacher J et al (2011) The hot summer of 2010: redrawing the temperature record map of Europe. *Science* 332:220–224. doi: 10.1126/science.1201224
- Beniston M, Stephenson DB, Christensen OB, et al. (2007) Future extreme events in European climate: an exploration of regional climate model projections. *Clim Change* 81:71–95. doi: 10.1007/s10584-006-9226-z
- Campetella C, Rusticucci M (1998) Synoptic analysis of an extreme heat wave over Argentina in March 1980. *Meteorol Appl* 5:217–226.

- Carvalho LMV, Jones C, Liebmann B (2004) The South Atlantic Convergence Zone : Intensity , Form , Persistence , and Relationships with Intraseasonal to Interannual Activity and Extreme Rainfall. *J Clim* 17:88–108.
- Cerne SB, Vera CS (2011) Influence of the intraseasonal variability on heat waves in subtropical South America. *Clim Dyn* 36:2265–2277. doi: 10.1007/s00382-010-0812-4
- Colombo AF, Etkin D, Karney BW (1999) Climate variability and the frequency of extreme temperature events for nine sites across Canada: Implications for power usage. *J Climate* 12:2490–2502.
- De Bono A, Giuliani G, Kluser S, Peduzzi P (2004) Impacts of summer 2003 heat wave in Europe. *UNEP/DEWA/GRID-Europe Environ Alert Bull* 2:1–4.
- Donat M, Alexander L, Yang H et al (2013) Updated analyses of temperature and precipitation extreme indices since the beginning of the twentieth century: The HadEX2 dataset. *J Geophys Res* 118:2098 – 2118. doi: 10.1002/jgrd.50150
- Field C, Barros V et al (2013) Summary for Policymakers. In: *Climate Change 2013: The Physical Science Basis. Contribution of Working Group I to the Fifth Assessment Report of the Intergovernmental Panel on Climate Change*, Cambridge University Press, Cambridge, United Kingdom and New York, NY, USA
- Hartmann DL, Klein Tank AMG, Rusticucci M et al (2013) Observations: Atmosphere and Surface. In: *Climate Change 2013: The Physical Science Basis. Contribution of Working Group I to the Fifth Assessment Report of the Intergovernmental Panel on Climate Change*, Cambridge University Press, Cambridge, United Kingdom and New York, NY, USA
- IPCC (2013) Annex I: Atlas of Global and Regional Climate Projections. In: *Climate Change 2013: The Physical Science Basis. Contribution of Working Group I to the Fifth Assessment Report of the Intergovernmental Panel on Climate Change*, Cambridge University Press, Cambridge, United Kingdom and New York, NY, USA
- Kirtman B, Power SB, Adedoyin JA et al (2013) Near-term Climate Change: Projections and Predictability. In: *Climate Change 2013: The Physical Science Basis. Contribution of Working Group I to the Fifth Assessment Report of the Intergovernmental Panel on Climate Change*. Cambridge University Press, Cambridge, United Kingdom and New York, NY, USA
- Kysely J, Kim J (2009) Mortality during heat waves in South Korea, 1991 to 2005: How exceptional was the 1994 heat wave? *Climate Res* 38(2):105–116.
- Kysely J (2010) Recent severe heat waves in central Europe: how to view them in a long-term prospect? *Int J Climatol* 30:89–109. doi 10.1002/joc.1874
- Macchiato M, Serio C, Lapenna V, LaRotonda L (1993) Parametric time series analysis of cold and hot spells in daily temperature: An application in southern Italy. *J Appl Meteor* 32:1270–1281.

- Mearns LO, Katz RW, Schneider SH (1984) Extreme high temperature events: changes in their probabilities with changes in mean temperature. *J Clim Appl Meteor* 23:1601–1608.
- Penalba OC, Rivera JA, Pántano VC (2014) The CLARIS LPB database: constructing a long-term daily hydro-meteorological dataset for La Plata Basin, Southern South America. *Geoscience Data Journal*. doi: 10.1002/gdj3.7
- Robine J-M, Cheung SLK, Le Roy S et al (2008) Death toll exceeded 70,000 in Europe during the summer of 2003. *C R Biol* 331:171–178. doi: 10.1016/j.crv.2007.12.001
- Rusticucci M, Barrucand M (2004) Observed trends and changes in Temperature Extremes over Argentina. *J. Climate* 17:4099–4107.
- Rusticucci M, Vargas W (1995) Synoptic Situations related to Spells of Extreme Temperatures over Argentina. *Meteorol Appl* 2:291–300.
- Rusticucci M, Vargas W (2001) Interannual variability of Temperature Spells over Argentina. *Atmósfera* 14:75–86.
- Rusticucci M (2012) Observed and simulated variability of extreme temperature events over South America. *Atmos Res* 106:1–17. doi: 10.1016/j.atmosres.2011.11.001

## 11 Conclusions and future perspectives

According to IPCC (2013), it is very likely that human influence has contributed to observed global scale changes in the frequency and intensity of daily temperature extremes since the mid-20<sup>th</sup> century. It is virtually certain that there will be more frequent hot and fewer cold temperature extremes over most land areas, and it is very likely that heat waves will occur with a higher frequency and duration in a possible future climate. The thesis aimed to strengthen the evidence from the observed data, critically evaluated the capability of climate models to simulate heat waves, and constructed climate change scenarios for heat waves over Central Europe. Principal outcomes of the doctoral dissertation are summarized as follows:

- The extremity index of heat waves (cold spells) was proposed and tested over Central Europe. This index is based on joint effects of temperature magnitude, duration, and spatial extent of individual events. Because it involves no ‘local’ settings, it may be applied also in other regions and data sets. The extremity index was found suitable for evaluating magnitude of heat waves in climate models and a similar index may be also used to assess severity of droughts, persistent rainfall, snowfall and other meteorological hazards.
- The list of severe heat waves and cold spells that occurred over Central Europe since 1950 was established. Spatial patterns of temperature anomalies for each event were visualized in maps, and heat waves (cold spells) were classified into four groups based on their characteristics. The methodology enables updating the list when a new version of the E-OBS data set is released. Enlisted events may be used as future analogues for comparison with simulated heat waves and cold spells in climate models and for other purposes. The list may also be broadened by including additional information about each event (observed losses, driving factors, etc.)
- Regional climate models driven by the reanalysis tend to underestimate the magnitude of the extraordinary 1994 heat wave. Those errors were linked to simulation of precipitation, because the largest underestimation was related to substantial overestimation of rainfall and vice versa. Inasmuch as extraordinary heat waves are expected to become one of the largest hazards of global climate change, their improper simulation is a serious deficiency of current climate models.

- Heat wave scenarios for a possible future Central European climate were constructed. In the near future (2020–2049), the mean projected frequency of heat waves is nearly twice higher (15 events/decade) compared to the historical period and this value is similar in all concentration scenarios. By contrast, the projected frequency of heat waves in the late 21<sup>st</sup> century (2–4 events/summer, 2070–2099) depends largely on concentration scenarios, so the climate change mitigation strategies are projected to be effective rather in the long term. However, it is possible to implement suitable adaptation strategies, such as those recommended by the European Climate Adaptation Platform (<http://climate-adapt.eea.europa.eu>), which would partially reduce impacts of heat waves in a changing climate.

There is still a need to improve climate models in order to obtain more credible simulation of heat waves in a possible future climate. Especially projections of persistent heat waves (such as those of 1994 and 2015) have to be interpreted with caution, because present climate models tend to underestimate such events. In addition to improving climate models, a focus should be given on broad collaboration within the geosciences community because many fundamental aspects of climate change extend beyond climate science. Estimating possible future socio-economic scenarios, population growth, ecosystem response, and climate change impacts on agriculture and forestry cannot be undertaken without widely ranging cooperation.



## **12 Acknowledgments**

The study was supported by the Charles University Grant Agency, student projects no. 532313 ‘Extremity index of heat waves and cold spells in Central Europe’ and 250215 ‘Climate change scenarios of heat wave characteristics in Central Europe – magnitude and uncertainties’. The work was undertaken also as part of national projects GAP209/10/2265 ‘Reproduction of links between atmospheric circulation and surface air temperature and precipitation distributions in climate models’ (2010–2014) and 16-22000S ‘Spatial and temporal characteristics of heat waves and cold spells in climate model simulations’ (2016–2018) funded by the Czech Science Foundation. The last research article was written under Czech–Argentinean bilateral project 7AMB15AR005 ‘Climate change effects on heat waves and their recurrence probabilities’, which was realized within the framework of the MOBILITY Activity funded by the Ministry of Education, Youth and Sports of the Czech Republic. I am grateful to my supervisor RNDr. Jan Kyselý, Ph.D., for his attentive scientific guidance during my doctoral studies. I would also like to thank my colleagues and friends for their valuable advice and comments on my work.

### 13 References (excluding chapters 6–10)

- Abreu JA, Beer J, Steinhilber F, et al. (2008) For how long will the current grand maximum of solar activity persist? *Geophys Res Lett* 35:L20109. doi: 10.1029/2008GL035442
- Altenhoff AM, Martius O, Croci-Maspoli M, et al. (2008) Linkage of atmospheric blocks and synoptic-scale Rossby waves: a climatological analysis. *Tellus A* 60:1053–1063. doi: 10.1111/j.1600-0870.2008.00354.x
- Ballester J, Rodó X, Giorgi F (2010) Future changes in Central Europe heat waves expected to mostly follow summer mean warming. *Clim Dyn* 35:1191–1205. doi: 10.1007/s00382-009-0641-5
- Barnett AG, Hajat S, Gasparrini A, Rocklöv J (2012) Cold and heat waves in the United States. *Environ Res* 112:218–224. doi: 10.1016/j.envres.2011.12.010
- Barriopedro D, Fischer EM, Luterbacher J, et al. (2011) The hot summer of 2010: redrawing the temperature record map of Europe. *Science* 332:220–224. doi: 10.1126/science.1201224
- Barriopedro D, García-Herrera R (2006) A Climatology of Northern Hemisphere Blocking. *J Clim* 19:1042–1063.
- Barriopedro D, García-Herrera R, Huth R (2008) Solar modulation of Northern Hemisphere winter blocking. *J Geophys Res* 113:D14118. doi: 10.1029/2008JD009789
- Bastos A, Gouveia CM, Trigo RM, Running SW (2014) Analysing the spatio-temporal impacts of the 2003 and 2010 extreme heatwaves on plant productivity in Europe. *Biogeosciences* 11:3421–3435. doi: 10.5194/bg-11-3421-2014
- Bednorz E (2011) Synoptic conditions of the occurrence of snow cover in central European lowlands. *Int J Climatol* 31:1108–1118. doi: 10.1002/joc.2130
- Beniston M (2013) Exploring the behaviour of atmospheric temperatures under dry conditions in Europe: evolution since the mid-20th century and projections for the end of the 21st century. *Int J Climatol* 33:457–462. doi: 10.1002/joc.3436
- Beniston M, Stephenson DB, Christensen OB, et al. (2007) Future extreme events in European climate: an exploration of regional climate model projections. *Clim Change* 81:71–95. doi: 10.1007/s10584-006-9226-z
- Black E, Blackburn M, Harrison G, et al. (2004) Factors contributing to the summer 2003 European heatwave. *Weather* 59:217–223. doi: 10.1256/wea.74.04
- Boé J, Terray L (2008) Uncertainties in summer evapotranspiration changes over Europe and implications for regional climate change. *Geophys Res Lett* 35:L05702. doi: 10.1029/2007GL032417

- Böhm R, Jones PD, Hiebl J, et al. (2010) The early instrumental warm-bias: a solution for long central European temperature series 1760–2007. *Clim Change* 101:41–67. doi: 10.1007/s10584-009-9649-4
- De Bono A, Giuliani G, Kluser S, Peduzzi P (2004) Impacts of summer 2003 heat wave in Europe. *UNEP/DEWA/GRID-Europe Environ Alert Bull* 2:1–4.
- Buehler T, Raible CC, Stocker TF (2011) The relationship of winter season North Atlantic blocking frequencies to extreme cold or dry spells in the ERA-40. *Tellus A* 63:212–222. doi: 10.1111/j.1600-0870.2010.00492.x
- Cassou C, Terray L, Phillips AS (2005) Tropical Atlantic Influence on European Heat Waves. *J Clim* 18:2805–2811.
- Cattiaux J, Hervé D, Peings Y (2013) European temperatures in CMIP5 : origins of present-day biases and future uncertainties. *Clim Dyn* 41:2889–2907. doi: 10.1007/s00382-013-1731-y
- Cattiaux J, Vautard R, Cassou C, et al. (2010) Winter 2010 in Europe: A cold extreme in a warming climate. *Geophys Res Lett* 37:L20704. doi: 10.1029/2010GL044613
- Cattiaux J, Yiou P, Vautard R (2012) Dynamics of future seasonal temperature trends and extremes in Europe: a multi-model analysis from CMIP3. *Clim Dyn* 38:1949–1964. doi: 10.1007/s00382-011-1211-1
- Colombo AF, Etkin D, Karney BW (1999) Climate Variability and the Frequency of Extreme Temperature Events for Nine Sites across Canada : Implications for Power Usage. *J Clim* 12:2490–2502.
- Croci-Maspoli M, Schwierz C, Davies HC (2007) A Multifaceted Climatology of Atmospheric Blocking and Its Recent Linear Trend. *J Clim* 20:633–649. doi: 10.1175/JCLI4029.1
- D’Ippoliti D, Michelozzi P, Marino C, et al. (2010) The impact of heat waves on mortality in 9 European cities: results from the EuroHEAT project. *Environ Health* 9:37. doi: 10.1186/1476-069X-9-37
- Dee DP, Uppala SM, Simmons AJ, et al. (2011) The ERA-Interim reanalysis: configuration and performance of the data assimilation system. *Q J R Meteorol Soc* 137:553–597. doi: 10.1002/qj.828
- Della-Marta PM, Haylock MR, Luterbacher J, Wanner H (2007a) Doubled length of western European summer heat waves since 1880. *J Geophys Res* 112:D15103. doi: 10.1029/2007JD008510
- Della-Marta PM, Luterbacher J, Weissenfluh H, et al. (2007b) Summer heat waves over western Europe 1880–2003, their relationship to large-scale forcings and predictability. *Clim Dyn* 29:251–275. doi: 10.1007/s00382-007-0233-1

- Dosio A, Paruolo P (2011) Bias correction of the ENSEMBLES high-resolution climate change projections for use by impact models: Evaluation on the present climate. *J Geophys Res* 116:D16106. doi: 10.1029/2011JD015934
- Fink AH, Brücher T, Krüger A, et al. (2004) The 2003 European summer heatwaves and drought - synoptic diagnosis and impacts. *Weather* 59:209–216. doi: 10.1256/wea.73.04
- Fischer EM, Seneviratne SI, Lüthi D, Schär C (2007) Contribution of land-atmosphere coupling to recent European summer heat waves. *Geophys Res Lett* 34:L06707. doi: 10.1029/2006GL029068
- Fischer EM, Schär C (2010) Consistent geographical patterns of changes in high-impact European heatwaves. *Nat Geosci* 3:398–403. doi: 10.1038/ngeo866
- Francis JA, Vavrus SJ (2012) Evidence linking Arctic amplification to extreme weather in mid-latitudes. *Geophys Res Lett* 39:L06801. doi: 10.1029/2012GL051000
- Gershunov A, Cayan DR, Iacobellis SF (2009) The Great 2006 Heat Wave over California and Nevada: Signal of an Increasing Trend. *J Clim* 22:6181–6203. doi: 10.1175/2009JCLI2465.1
- Ghosh S, Mujumdar PP (2008) Statistical downscaling of GCM simulations to streamflow using relevance vector machine. *Adv Water Resour* 31:132–146. doi: 10.1016/j.advwatres.2007.07.005
- Haarsma RJ, Selten F, Hurk BVD, et al. (2009) Drier Mediterranean soils due to greenhouse warming bring easterly winds over summertime central Europe. *Geophys Res Lett* 36:L04705. doi: 10.1029/2008GL036617
- Haylock MR, Cawley GC, Harpham C, et al. (2006) Downscaling heavy precipitation over the United Kingdom: A comparison of dynamical and statistical methods and their future scenarios. *Int J Climatol* 26:1397–1415. doi: 10.1002/joc.1318
- Haylock MR, Hofstra N, Klein Tank AMG, et al. (2008) A European daily high-resolution gridded data set of surface temperature and precipitation for 1950–2006. *J Geophys Res* 113:D20119. doi: 10.1029/2008JD010201
- Holtanová E, Valeriánová A, Crhová L, Racko S (2015) Heat wave of August 2012 in the Czech Republic: comparison of two approaches to assess high temperature events. *Stud Geophys Geod* 59:159–172. doi: 10.1007/s11200-014-0805-6
- Hurrell JW, Deser C (2010) North Atlantic climate variability: The role of the North Atlantic Oscillation. *J Mar Syst* 79:231–244. doi: 10.1016/j.jmarsys.2009.11.002
- Huth R, Kysely J, Bochníček J, Hejda P (2008) Solar activity affects the occurrence of synoptic types over Europe. *Ann Geophys* 26:1999–2004.
- International Panel on Climate Change (IPCC) (2013) *Climate Change 2013: The Physical Science Basis*. Cambridge University Press, Cambridge, UK, and New York, NY, USA

- Jacob D, Petersen J, Eggert B, et al. (2014) EURO-CORDEX: new high-resolution climate change projections for European impact research. *Reg Environ Chang* 14:563–578. doi: 10.1007/s10113-013-0499-2
- Jaeger EB, Seneviratne SI (2011) Impact of soil moisture–atmosphere coupling on European climate extremes and trends in a regional climate model. *Clim Dyn* 36:1919–1939. doi: 10.1007/s00382-010-0780-8
- Kalnay E, Kanamitsu M, Kistler R, et al. (1996) The NCEP/NCAR 40-year reanalysis project. *Bull Am Meteorol Soc* 77:437–471.
- Kjellström E, Bärring L, Jacob D, et al. (2007) Modelling daily temperature extremes: recent climate and future changes over Europe. *Clim Change* 81:249–265. doi: 10.1007/s10584-006-9220-5
- Kjellström E, Boberg F, Castro M, et al. (2010) Daily and monthly temperature and precipitation statistics as performance indicators for regional climate models. *Clim Res* 44:135–150. doi: 10.3354/cr00932
- Kjellström E, Nikulin G, Hansson U, et al. (2011) 21st century changes in the European climate: uncertainties derived from an ensemble of regional climate model simulations. *Tellus A* 63:24–40. doi: 10.1111/j.1600-0870.2010.00475.x
- Klein Tank AMG, Wijngaard JB, Konnen GP, et al. (2002) Daily dataset of 20th-century surface air temperature and precipitation series for the European Climate Assessment. *Int J Climatol* 22:1441–1453. doi: 10.1002/joc.773
- Knight JR, Alan RR, Folland CK, et al. (2005) A signature of persistent natural thermohaline circulation cycles in observed climate. *Geophys Res Lett* 32:2–5. doi: 10.1029/2005GL024233
- Konovalov IB, Beekmann M, Kuznetsova IN, et al. (2011) Atmospheric impacts of the 2010 Russian wildfires: Integrating modelling and measurements of an extreme air pollution episode in the Moscow region. *Atmos Chem Phys* 11:10031–10056. doi: 10.5194/acp-11-10031-2011
- Kotlarski S, Keuler K, Christensen OB, et al. (2014) Regional climate modeling on European scales: A joint standard evaluation of the EURO-CORDEX RCM ensemble. *Geosci Model Dev* 7:1297–1333. doi: 10.5194/gmd-7-1297-2014
- Kottek M, Grieser J, Beck C, et al. (2006) World Map of the Köppen-Geiger climate classification updated. *Meteorol Zeitschrift* 15:259–263. doi: 10.1127/0941-2948/2006/0130
- Kysely J (2010) Recent severe heat waves in central Europe: how to view them in a long-term prospect? *Int J Climatol* 109:89–109. doi: 10.1002/joc1874
- Kysely J (2008) Influence of the persistence of circulation patterns on warm and cold temperature anomalies in Europe: Analysis over the 20th century. *Glob Planet Change* 62:147–163. doi: 10.1016/j.gloplacha.2008.01.003

- Kysely J (2002) Temporal fluctuations in heat waves at Prague-Klementinum, the Czech Republic, from 1901-97, and their relationships to atmospheric circulation. *Int J Climatol* 22:33–50. doi: 10.1002/joc.720
- Lau NC, Nath MJ (2014) Model simulation and projection of European heat waves in present-day and future climates. *J Clim* 27:3713–3730. doi: 10.1175/JCLI-D-13-00284.1
- Luterbacher J, Dietrich D, Xoplaki E, et al. (2004) European Seasonal and Annual Temperature Variability, Trends and Extremes Since 1500. *Science* 303:1499–1503.
- Meehl GA, Tebaldi C (2004) More intense, more frequent, and longer lasting heat waves in the 21st century. *Science* 305:994–997. doi: 10.1126/science.1098704
- Müller M, Kaspar M (2014) Event-adjusted evaluation of weather and climate extremes. *Nat Hazards Earth Syst Sci* 14:473–483. doi: 10.5194/nhess-14-473-2014
- Nikulin G, Kjellström E, Hansson U, et al. (2011) Evaluation and future projections of temperature, precipitation and wind extremes over Europe in an ensemble of regional climate simulations. *Tellus A* 63A:41–55. doi: 10.1111/j.1600-0870.2010.00466.x
- Peings Y, Cattiaux J, Douville H (2013) Evaluation and response of winter cold spells over Western Europe in CMIP5 models. *Clim Dyn* 41:3025–3037. doi: 10.1007/s00382-012-1565-z
- Penalba OC, Rivera JA, Pántano VC (2014) The CLARIS LPB database : constructing a long-term daily hydro-meteorological dataset for La Plata Basin , Southern South America. *Geosci Data J* 1:20–29. doi: 10.1002/gdj3.7
- Perkins SE, Alexander L V. (2013) On the Measurement of Heat Waves. *J Clim* 26:4500–4517. doi: 10.1175/JCLI-D-12-00383.1
- Pfahl S, Wernli H (2012) Quantifying the relevance of atmospheric blocking for co-located temperature extremes in the Northern Hemisphere on (sub-)daily time scales. *Geophys Res Lett* 39:L12807. doi: 10.1029/2012GL052261
- Plavcová E, Kysely J (2016) Overly persistent circulation in climate models contributes to overestimated frequency and duration of heat waves and cold spells. *Clim Dyn* 46:2805–2820. doi: 10.1007/s00382-015-2733-8
- Plavcová E, Kysely J (2011) Evaluation of daily temperatures in Central Europe and their links to large-scale circulation in an ensemble of regional climate models. *Tellus A* 63A:763–781. doi: 10.1111/j.1600-0870.2011.00514.x
- Robine J-M, Cheung SLK, Le Roy S, et al. (2008) Death toll exceeded 70,000 in Europe during the summer of 2003. *C R Biol* 331:171–178. doi: 10.1016/j.crv.2007.12.001
- Rummukainen M, Rockel B, Bärring L, et al. (2015) 21st Century Challenges in Regional Climate Modeling. *Bull Am Meteorol Soc* 150331122920005. doi: 10.1175/BAMS-D-14-00214.1

- Russo S, Sillmann J, Fischer EM (2015) Top ten European heatwaves since 1950 and their occurrence in the coming decades. *Environ Res Lett* 10:124003. doi: 10.1088/1748-9326/10/12/124003
- Scaife AA, Folland CK, Alexander LV., et al. (2008) European Climate Extremes and the North Atlantic Oscillation. *J Clim* 21:72–83. doi: 10.1175/2007JCLI1631.1
- Scaife AA, Knight J, Vallis G, Folland C (2005) A stratospheric influence on the winter NAO and North Atlantic surface climate. *Geophys Res Lett* 32:L18715. doi: 10.1029/2005GL023226
- Scaife AA, Woollings T, Knight J, et al. (2010) Atmospheric Blocking and Mean Biases in Climate Models. *J Clim* 23:6143–6152. doi: 10.1175/2010JCLI3728.1
- Seneviratne SI, Lüthi D, Litschi D, Schär C (2006) Land–atmosphere coupling and climate change in Europe. *Nature* 443:205+209. doi: 10.1038/nature05095
- Shevchenko O, Lee H, Snizhko S, Mayer H (2014) Long-term analysis of heat waves in Ukraine. *Int J Climatol* 34:1642–1650. doi: 10.1002/joc.3792
- Schneidereit A, Schubert S, Vargin P, et al. (2012) Large-Scale Flow and the Long-Lasting Blocking High over Russia: Summer 2010. *Mon Weather Rev* 140:2967–2981. doi: 10.1175/MWR-D-11-00249.1
- Schubert S, Wang H, Suarez M (2011) Warm Season Subseasonal Variability and Climate Extremes in the Northern Hemisphere: The Role of Stationary Rossby Waves. *J Clim* 24:4773–4792. doi: 10.1175/JCLI-D-10-05035.1
- Simolo C, Brunetti M, Maugeri M, Nanni T (2014) Increasingly warm summers in the Euro–Mediterranean zone: mean temperatures and extremes. *Reg Environ Chang* 14:1825–1832. doi: 10.1007/s10113-012-0373-7
- Stefanon M, D’Andrea F, Drobinski P (2012) Heatwave classification over Europe and the Mediterranean region. *Environ Res Lett* 7:014023. doi: 10.1088/1748-9326/7/1/014023
- Sutton RT, Hodson DLR (2005) Atlantic Ocean Forcing of North American and European Summer Climate. *Science* 309:115–118.
- Tang Q, Leng G, Groisman PY (2012) European Hot Summers Associated with a Reduction of Cloudiness. *J Clim* 25:3637–3644. doi: 10.1175/JCLI-D-12-00040.1
- Taylor KE, Stouffer RJ, Meehl GA. (2012) An Overview of CMIP5 and the Experiment Design. *Bull Am Meteorol Soc* 93:485–498. doi: 10.1175/BAMS-D-11-00094.1
- Tomczyk AM, Bednorz E (2016) Heat waves in Central Europe and their circulation conditions. *Int J Climatol* 36:770–782. doi: 10.1002/joc.4381
- Unkašević M, Tošić I (2011) The maximum temperatures and heat waves in Serbia during the summer of 2007. *Clim Change* 108:207–223. doi: 10.1007/s10584-010-0006-4

- Vautard R, Gobiet A, Jacob D, et al. (2013) The simulation of European heat waves from an ensemble of regional climate models within the EURO-CORDEX project. *Clim Dyn* 41:2555–2575. doi: 10.1007/s00382-013-1714-z
- Vavrus S, Walsh JE, Chapman WL, Portis D (2006) The behavior of extreme cold air outbreaks under greenhouse warming. *Int J Climatol* 26:1133–1147. doi: 10.1002/joc.1301
- van der Linden P, Mitchell JFB (2009) ENSEMBLES: Climate Change and its Impacts: Summary of research and results from the ENSEMBLES project. Met Office Hadley Centre, Exeter
- van Vuuren DP, Edmonds J, Kainuma M, et al. (2011) The representative concentration pathways: An overview. *Clim Change* 109:5–31. doi: 10.1007/s10584-011-0148-z
- Walsh J, Phillips A (2001) Extreme cold outbreaks in the United States and Europe, 1948-99. *J Clim* 14:2642–2658.
- Werner PC, Gerstengarbe FV (2009) Katalog der grosswetterlagen Europas (1881-2009). Potsdam Institute for Climate Impact Research
- Wijngaard JB, Klein Tank AMG, Konnen GP (2003) Homogeneity of 20th century European daily temperature and precipitation series. *Int J Climatol* 23:679–692. doi: 10.1002/joc.906
- Wilby RL (2003) Past and projected trends in London's urban heat island. *Weather* 58:251–260.
- Winkler P (2009) Revision and necessary correction of the long-term temperature series of Hohenpeissenberg, 1781–2006. *Theor Appl Climatol* 98:259–268. doi: 10.1007/s00704-009-0108-y

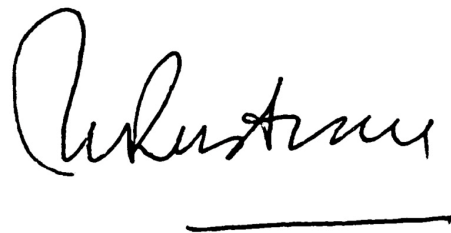


## 14 Appendices

**Subject:** Specification of the authorial share

As the leading author, I hereby declare that **Ondřej Lhotka** contributed to research article **‘Long-term variability of heat waves in Argentina and recurrence probability of the severe 2008 heat wave in Buenos Aires’** published in Theoretical and Applied Climatology as follows:

- performing literature review and assisting with writing of the introduction section
- visualizing meteorological stations into a map and helping with processing of figures
- computing recurrence probability of the extreme heat wave of November 2008 in Buenos Aires under present climate
- assisting with selection of climate change scenarios for computation of recurrence probability of the aforementioned heat wave in a future climate
- helping with interpretation of results and manuscripts’ proof-reading



Prof. Matilde Rusticucci  
University of Buenos Aires  
Department of Atmospheric and Ocean Sciences  
Buenos Aires, Argentina